NAWEA 2015 Symposium

Tuesday 09 June 2015 - Thursday 11 June 2015

Virginia Tech Campus

Goodwin Hall

Book of Abstracts

Table of contents

73

Wind Farm Layout Optimization Considering Turbine Selection and Hub Height Variation

Mr. ABDULRAHMAN, Mamdouh [1]; Prof. WOOD, David [2]

[1] The University Of Calgary

[2] The University of Calgary

Corresponding Author: maabdulr@ucalgary.ca

New aspects is added to the wind farm layout optimization problem. A variable hub height non-identical turbines wind farm design is presented. The manufacturers' technical data for 61 commercial horizontal axis wind turbine models is used in order to obtain more realistic results. Three objective functions are considered individually: (1) the total power production, (2) the farm capacity factor, and (3) the capital cost of output power index (based on nominal power and tower height). The results show that the flexibility of using non-identical turbines with different heights in the same wind farm can meet a wide range of preferences. By adapting the objective functions' weighting factors many preferred solutions can be obtained.

47

Graduate Education Programs in Wind Energy

Dr. ACKER, Tom [1]; Dr. MCGOWAN, Jon [2]; Prof. MANWELL, James [3]; Dr. SWIFT, Andrew [4]

[1] Northern Arizona University

[2] University of Massachusetts Amherst

[3] UMass Amherst

[4] Texas Tech University

Corresponding Author: tom.acker@nau.edu

The purpose of the North American Wind Energy Academy (NAWEA) is to facilitate the growth of wind power into a cost-effective, high-penetration, sustainable national energy source producing at least 10 times the 2012 electricity production levels. To meet this energy goal, the academy will expedite the creation of a critical new wind energy research and development agenda that bridges education, multiple disciplines, and diverse organizations, and fosters national and international collaborations. The overall goal of the NAWEA Educational Program is to expand the breadth and competence of the wind energy academic community throughout the region by working collaboratively to develop relevant curriculum, courses, degree programs, and/or certificates, with the ultimate objective of enabling the US to meet its wind energy goals.

The first steps taken by the NAWEA Education Committee in addressing its goals were to articulate a set of potential educational programs of interest to its members, focusing on university graduate and undergraduate programs, with an emphasis on graduate education. These programs were inspired by the discussions and presentations at the 2013 NAWEA Symposium in Boulder, Colorado, and include wind energy course and program certification, and a graduate certificate in wind energy.

Before proposing any new programs, however, it was decided that a thorough review of existing programs in the US and abroad was merited. This review showed that there are at least 45 four year educational institutions in the US that currently have wind energy engineering courses, with most offering a technical undergraduate course on the subject and with 20 offering graduate courses on the subject. Of the institutions offering graduate programs 40 have MS programs and 30 have programs that offer both MS and PhD programs. In addition, at least six schools offer a Graduate Certificate in Wind Engineering. Another area of interest here is the schools that have established wind energy centers, or renewable energy centers that include wind engineering. Fifty-seven such centers were identified. Expanding the scope of this outside of the US but within the footprint of NAWEA, 12 wind energy graduate programs were identified in Canada. In Mexico, the Mexican Center of Innovation in Wind Energy (Centro Mexicano de Innovaci6n en Energia E6lica, CEMIE-E6lico) was found to have 14 university participants out of its 32 founding members. In Europe, the wind energy education programs are somewhat more advanced than in North America. There are quite a number of wind energy education programs in Europe. The most notable of these are affiliated in some way with the European Master in Renewable Energy or the European Academy of Wind Energy (EAWE). With regards to EAWE, there are about 65 universities participants across Europe.

The purpose of this presentation will be to summarize the existing programs in wind energy, both in North America and Europe, and to describe the content of typical wind energy graduate programs. Discussion will then be directed at a proposal for a graduate certificate in wind energy that leverages the resources available at NAWEA member universities and partners, with the intent of collaborating on offering a robust and rigorous set of courses focused on wind energy, beginning with engineering but potentially spanning the range of applicable subject areas from business and policy to environment and engineering. The focus here is to enable training of graduate-level students that will be integral to advancing ideas, business, and engineering.

27

Benefits of vertically-staggered wind turbines from theoretical analysis and Large-Eddy Simulations

Cristina L. Archer, Shengbai Xie, and Niranjan Ghaisas
College of Earth, Ocean, and Environment
University of Delaware Newark,
Delaware, United States
and Charles
Meneveau
Department of Mechanical Engineering
Johns Hopkins University
Baltimore, Maryland, United States

Abstract for the 2015 Symposium of the North American Wind Energy Academy (NAWEA)
Blacksburg, VA, 9-11 June 2015
Session: Atmosphere/Turbine/Wake Interactions

Blade design, components, and materials in modern wind turbines have reached an unparalleled level of efficiency, to the point that no radical improvement in single-turbine efficiency is expected in the near future. More promising than single-turbine improvements are efficiency improvements at the wind farm level. For example, recent studies have focused on the horizontal layout of multiple wind turbines within a wind farm to improve overall efficiency, varying the horizontal spacing between turbines, the alignment between turbines in alternate rows (i.e., staggering), or the angles between rows and columns of turbines. This study is the first to address the benefits of staggering wind turbines in the vertical, rather than in the horizontal.

Two types of vertical staggering are considered. The first approach consists of adding smaller, vertical-axis wind turbines (VAWT) between the original, larger, horizontal-axis wind turbines (HAWT) to capture the lower but relatively undisturbed winds below the rotors. This approach is referred to as "multi-type" vertical staggering because different types of turbines are utilized. The second consists of lowering the height of selected rows within a wind farm, while keeping the same rotor area and turbine type, and it is referred to hereafter as "multi-height" vertical staggering, because the turbine type is the same in all rows and only the height of the turbine tower is varied.

Large-Eddy Simulations (LES) were conducted with two independent codes, the Wind Turbine and Turbulence Simulator (WiTTS) and the Software for Offshore/onshore Wind Farm Applications (SOWFA). WiTTS was used to simulate a multi-type case in which a large, HAWT (the REPower 5 MW with hub height Hh=87.6 m and diameter D=126 m) is surrounded by 20 VAWTs, each spanning an area of 20 m x 10 m and with center height H,=15 m (Figure la).
Periodic boundary conditions are used in all horizontal directions. Therefore, the computational domain is regarded as a fully-developed, infinite-large wind farm. The VAWTs are treated with a simplified approach using an actuator disk model with a thrust coefficient of 0.25 and the HAWT is resolved with actuator lines.

SOWFA was used to simulate the Lillgrund offshore wind farm in Sweden, which includes 48 HAWTs (Siemens 2.3 MW with Hh=63 m and D=93 m), but in which the turbines in every other row are lowered to Hh=53 m, i.e., 10 m lower than in the original layout. Also in SOWFA the HAWTs are treated as actuator lines.

For the multi-type vertical staggering, the following was found:

1) Energy extraction by the HAWT is similar with and without VAWTs because the wind speed near Hh is basically unaffected by the VAWTs (Figure la,b); however, the VAWTs generate additional electricity, therefore the proposed layout ultimately produces more electricity than the single HAWT alone.
2) The entire boundary layer is more turbulent with the VAWTs, as demonstrated by: higher values of turbulent kinetic energy (TKE) everywhere, including above the HAWT; an increased value of effective surface roughness; and a faster wake recovery due to enhanced turbulent mixing (Figure Ic,d);
3) A complex, multi-layer boundary forms, with alternating log and non-log regions (Figure lb), consistent with predictions obtained with a simple analytical top-down model in which the effect of a fully-developed wind farm is parameterized as either an increased eddy viscosity (in the non-log layers) or as a modified friction velocity and effective surface roughness (in the log layers);
4) The VAWTs have lower cut-in wind speed and are able to work in any wind direction without mechanical yawing, which enables the staggered wind farm to operate in a larger working range of wind speed and directions and has the potential to smooth out the variability of energy output;
5) Because VAWTs are less expensive to build, install, and maintain than HAWTs, multi-type vertical staggering appears to be a promising method to improve the energy generation of a wind farm.

For the multi-height vertical staggering case, the Lillgrund wind farm was simulated under the prevailing wind direction (from the southwest) and under neutral atmospheric stability. By lowering the heights of the turbines in the even rows, the overall energy generation in the multi- height vertically staggered wind farm remained basically the same as that of the original wind farm. Over an averaging time of 30 minutes, the original layout produced about 33.4 MW of power whereas the multi-height vertically-staggered layout produced 33.6 MW. However, the installation and material costs of building wind turbines that are 10-m shorter than the original design are lower than in the original layout. Although more analyses are needed, for example with additional wind directions and with smarter distribution of the lower wind turbines, these preliminary findings suggest that also multi-height vertical staggering can be an effective way to reduce costs without sacrificing energy production.

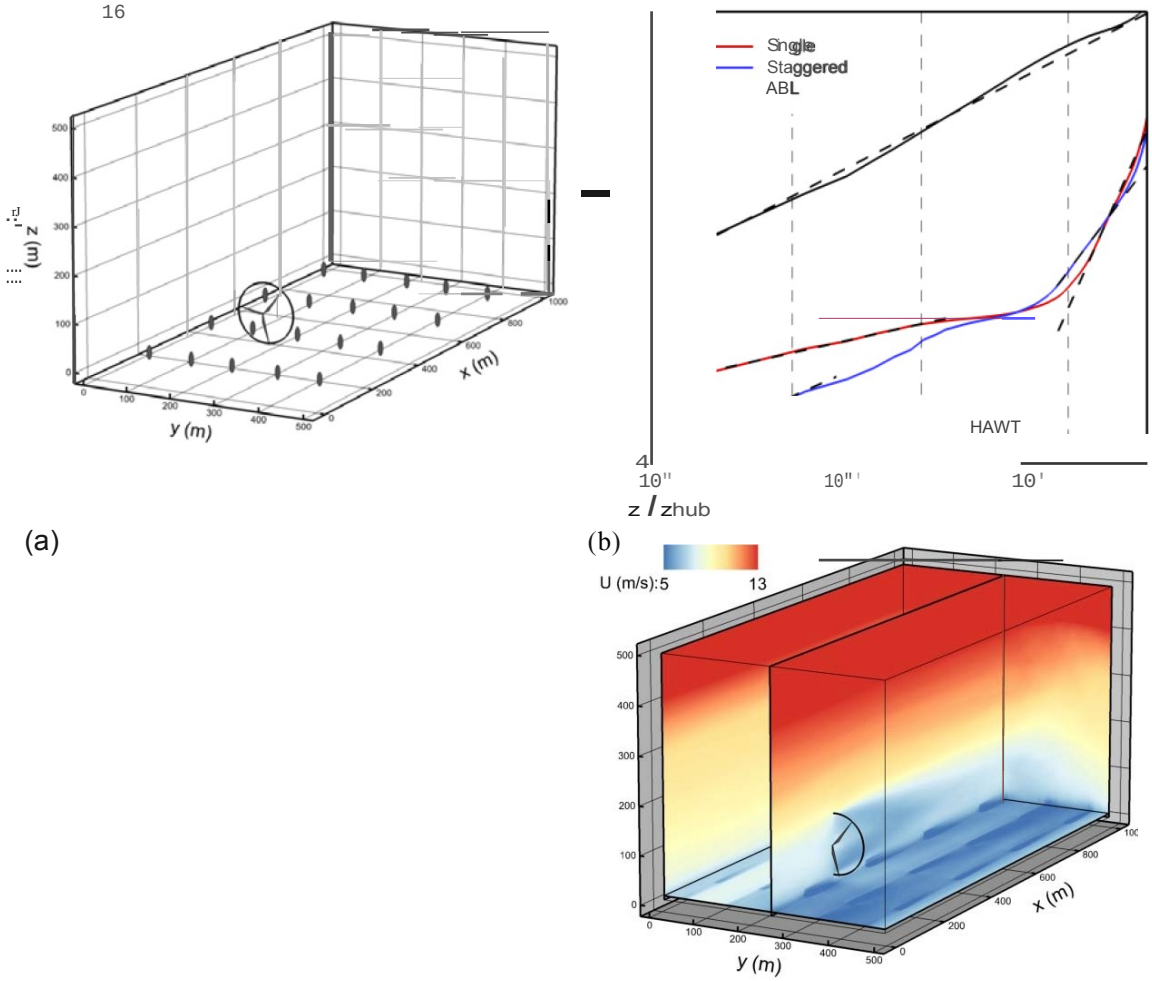
16
z (m)
y (m)
x (m)
Single
Staggered
ABL
HAWT
z / zhub
(a)
(b)
U (m/s):5
13
y (m)
x (m)

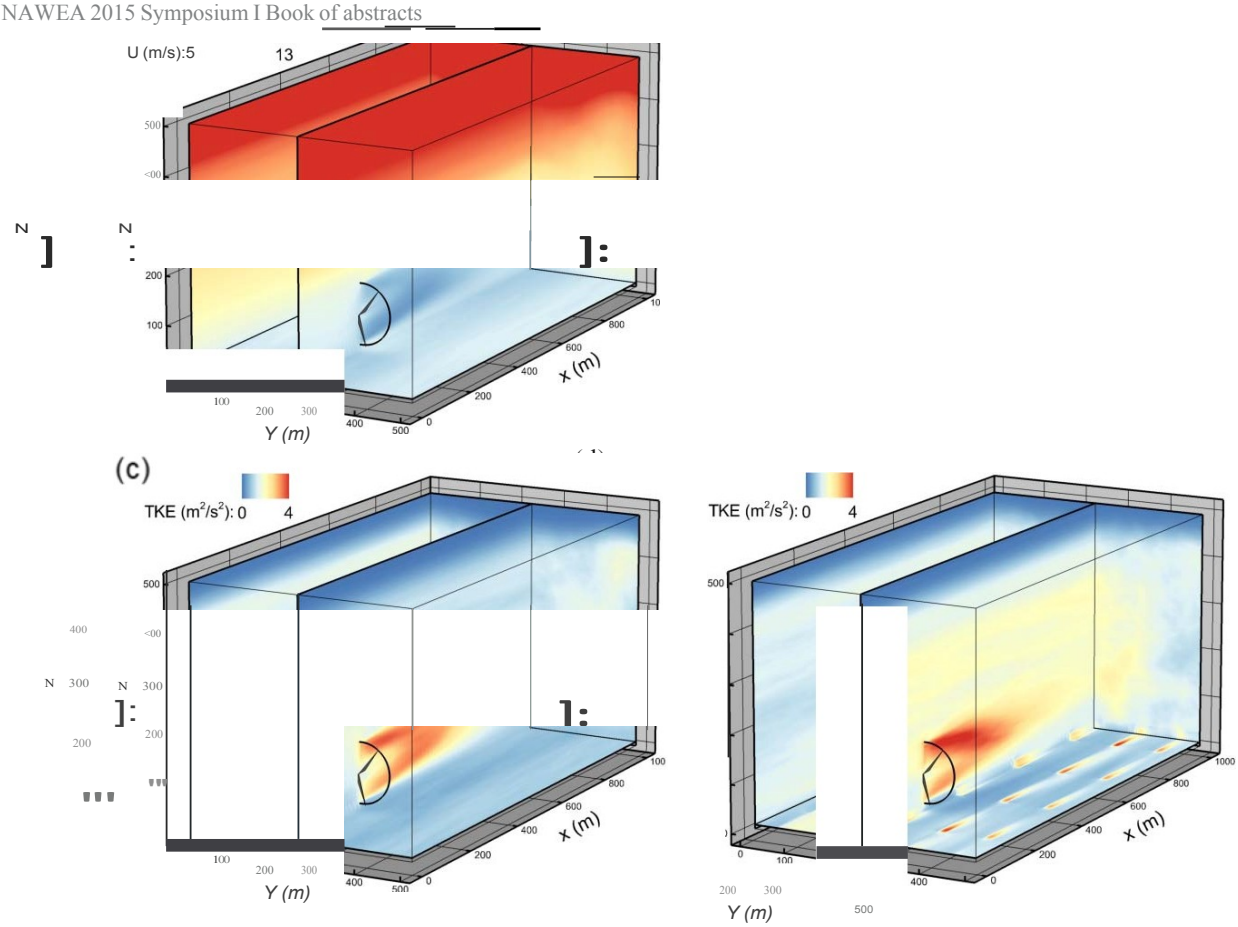

Figure 1The WiTTS model was used to simulate an infinitely-large, multi-type vertically-staggered wind farm, in which each horizontal-axis wind turbine is surrounded by 20 smaller vertical-axis wind turbines (top left). The resulting fully-developed boundary layer is complex, with alternating log and non-log layers (top right), following theoretical expectations.Cross-sections of mean velocity (U, mis) and turbulent kinetic energy (TKE, m2/sl) are compared for the original (a and c) and the multi-type vertically-staggered (b and d) layouts.

45

On the Effects of Directional Bin Size when Simulating Large Offshore Wind Farms with CFD

Dr. ARGYLE, Peter [1]; Prof. WATSON, Simon [1]
[1] Loughborough University

Corresponding Author: p.argyle@lboro.ac.uk

On the Effects of Directional Bin Size when Simulating Large Offshore Wind Farms with CFD

Peter Argyle, Simon Watson
CREST, Loughborough University, ENGLAND
p.argyle@lboro.ac.uk

Introduction

The most significant difference to an offshore wind farm resource assessment compared to onshore locations is the lower surface roughness values resulting from the lack of vegetation and terrain. As such, turbine wakes take longer to dissipate, and thus have a greater significance for the mean wind speeds and turbulence intensity encountered by turbines downstream. The greater influence of turbine wakes offshore, combined with the often regular turbine layouts of offshore farms, result in significant losses in power generation, and thus asset value, when the wind blows along a line of turbines. To reduce the risk to financial investment, computer simulations are often run to predict the expected wake losses of wind farms before they are built. As using Computational Fluid Dynamics (CFD) models to simulate numerous scenarios can be time consuming, it is important to use best practice to minimise the number of runs required to accurately capture the farm wake loss. This work investigates the number of simulations required to predict the production losses due to turbine wakes for a single scenario to an acceptable accuracy without compromising on the time required for such an investigation.

Method

For this work, CFD simulations are validated against production from the Nysted offshore wind farm in the Danish Baltic Sea. There are 72 turbines in a regular grid of 9 rows and 8 columns, with the columns offset such that the westerly 'down-the-line' direction investigated is 278° as shown below in figure 1. Production data are available from December 2006 through to February 2008 and are supplemented by meteorological data from MastM1. Although it is known that atmospheric stability significantly alters the turbine wake behaviour and is measurable using data from MastM1, there is no standard for defining the various stability categories and the required filtering process significantly reduces the quantity of available data. Therefore, this work will assume neutral atmospheric stability in both field data and simulations. To help focus on wake effects, only events where the hub height wind speed measured at MastM1 corresponds to the peak in the turbine thrust coefficient, 7.5±1m/s. In order to increase the number of validation data events, each row of 8 turbines within the farm are considered a subset, independent of the rest of the farm. Thus, if a turbine in the fourth row is undergoing maintenance, it is assumed this will not affect the productivity of turbines in other rows, although the whole fourth row of turbines are excluded from the analysis for the duration of the downtime. To prevent effects from the farm edges biasing the data, both the most northerly and southerly rows of turbines are ignored. The production values from the other 7 rows (minus any rows with data problems) are averaged together for each 10-minute event.

Figure 1 Layout of turbines and meteorological mast at the Nysted offshore wind farm. Turbines rows are separated by 5.9 rotor diameters (D) whilst the columns are separated by 10.4D.

It is known that the flow through a large offshore wind farm is not uniform in direction, i.e. variations occur due to the Coriolis effect, turbulent eddies and wake meandering. To account for this, it is common practice to investigate data from a narrow direction sector, called a direction bin. Wider bins result in a larger experimental data sample, although are more likely to suffer from incorporating events where the turbines which are expected to suffer wake losses are actually outside the wakes of the upstream turbines, creating

misleading results. Therefore, this work will consider the five directional bins shown in Table 1 below:

Table 1 List of direction bins used in this work

Case Name	Directions Included	Bin Size	Events
Case A	278±0.5°	1°	173
Case B	278±1.5°	3°	485
Case C	278±2.5°	5°	687
Case D	278±3.5°	7°	977
Case E	278±4.5°	9°	1238

Results

Figure 2, below, shows the power produced at each turbine position for each case study, normalised by the power generated by the free-stream turbine. Based on the results of previous studies [1] and indicated in Figure 3, simulations of Case A tend to significantly over-estimate the wake losses. With each subsequent case study, the wider bin size results in a lower simulated wake loss as the uniformly averaged collection of simulations becomes more biased towards flow directions further from the centre. The full paper will explore the use of non-uniform weighting (e.g. Gaussian) of simulations from different directions within a bin and compare with observations at the Nysted wind farm.

Figure 2 Average power generated by each turbine position, normalised by the production of the free-stream turbine

Figure 3 Average power simulated at each turbine position, normalised by the production of the free-stream turbine. For CaseC, multiple simulations have been uniformly averaged whilst CaseA shows the results from a single simulation.

Discussion

Since this study assumes neutral stability for the measured data, there are a significant number of measured events for each case study resulting in production power ratios for each case study that are statistically similar to each other, with the largest difference between CaseA and CaseC at turbine position 6. However, the simulation results for these two case examples shown in figure 3, deviate most in the first half of the farm, before converging their wake loss predictions by position 7. The separation in results early in the farm is likely to be a result of how the simulation averages are calculated, here given a uniform weighting, whereas Table 1 suggests a non-uniform distribution of measured wind flow directions. The full paper will explore the use of non-uniform weighting (e.g. Gaussian) of simulations from different directions within a bin and compare with observations at the Nysted wind farm.

Conclusion

Using CFD to simulate the wake losses of large offshore wind farms can be very time consuming. This is particularly true when large directional sector are considered. It is possible to reduce these time costs through the smarter use of fewer simulations and by analysing the variability of measured field data before simulations are made. However, these findings may be site specific, depending on the turbines and their layout within the offshore wind farm.

Works Cited

[1] P. Argyle, Computational Fluid Dynamics Modelling of Wind Turbine Wake Losses in Large Offshore Wind Farms, Incorporating Atmospheric Stability, Loughborough University, 2015.

70

A game-theoretic framework to investigate the conditions for cooperation between energy storage operators and wind power producers

S. Bhela, K.-S. Tam

Bradley Department of Electrical and Computer Engineering, Virginia Polytechnic Institute and State University, MC 0111, 1185 Perry St. / Room 302, Blacksburg, VA 24061, USA
E-mail: sidbhela@vt.edu, ktam@vt.edu

Abstract:

Energy storage, has widely been accepted as a means to provide capacity firming service to renewable sources of energy due to its capability to quickly start and shut down and its ability to have flexible ramping rates. Lithium Ion batteries in particular are of interest as their production cost is expected to significantly decrease over the next few years. In addition, Li-Ion batteries have high efficiency, high energy density and high cycling tolerance. These batteries are also used in electric vehicles whose penetration is expected to grow rapidly in the coming years.

The social benefit of energy storage to provide energy balancing service to renewable producers is evident, especially in the context of a micro-grid where deviations from distributed generation sources can be handled locally. However, co-operation with renewable producers may not be automatically guaranteed and would depend on the amount of revenue generated by balancing such deviations. Storage may derive more benefit from choosing to operate independently. Balancing wind deviations would take capacity away from providing other high value services to the micro-grid community such as arbitrage and regulation service.

The decision to enter the market and balance deviations for the wind producer is highly intertwined with the strategy adopted by the wind producer. Interactive problems in which the outcome of a rational agent's action depends on the actions of other rational players are best studied through the setup of a game-theoretic framework.

A case-study is presented here using wind and electricity market data for a site in west Texas. Historical data is used to calculate expected pay-offs for the month of January. The columns in the following table are the available strategies for the wind producer and the rows are the available strategies for the energy storage. There are four possible combination of strategies, which are discussed next:

WIND / **STORAGE**	**CO-OPERATION**	**NON-COOPERATION**
CO-OPERATION	**$ 707** **(Case 1)** **$6,988**	$195 (Case 2) $8,514
NON-COOPERATION	$2,108 (Case 4) $5,422	$195 (Case 3) $4,870

Table 1.1 – Payoff Table

The pay-off table provides the net revenues of the wind producer in the upper right corner and the net revenues of the energy storage in the lower left corner of each cell. Note that revenue from Production Tax Credits (PTC) is not included for the wind producer.

Case1:

In this case the wind producer and the energy storage play co-operative strategies to act as one entity and deliver the promised power output. The energy storage receives imbalance payments (fixed percentage of day-ahead market price) from the wind producer for giving priority to absorbing wind deviations – any remaining capacity is used for arbitrage, regulation service and absorbing load deviations and is paid by the utility. In addition to the imbalance payments to the energy storage, the wind producer may pay additional fines to the utility.

Case2:

In this case the wind producer chooses a non-cooperative strategy and pays hefty penalties (fixed percentage of day-ahead market price) to the utility. The energy storage indirectly co-operates by absorbing wind deviations through the utility, but gives preference to absorbing load deviations first - any remaining capacity is used for arbitrage and regulation service. Payment for imbalances (fixed percentage of day-ahead market price) is received through the utility instead of the wind producer. Penalty charged by the utility is assumed to be higher than the penalty charged by the energy storage entity.

Case3:

In this case both the wind producer and the energy storage choose non-cooperative strategies. The wind producer pays hefty penalties to the utility just like the previous case (Case 2). The energy storage chooses to operate independently by providing services to balance net deviations (load + wind deviations) - any remaining capacity is used for arbitrage and regulation service. Storage does not receive imbalance payments in this case.

Case4:

In this case the storage chooses to play a non-cooperative strategy by operating independently like the previous case (Case 3). The wind producer knowing that the storage will choose not to co-operate curtails its output when overproducing to reduce the imbalance on the system.

As evidenced from the pay-off table there is only one pure strategy Nash equilibrium (Case 1). The co-operative strategy for the wind producer strictly dominates its non-cooperative strategy. Similarly, the cooperative strategy for the energy storage strictly dominates its non-cooperative strategy. As both players would choose to play a co-operative strategy irrespective of the strategy chosen by the other player, the Nash equilibrium points to Case 1.

It is clear that in a market where penalties are imposed on any wind deviations both players would choose to co-operate with each other. Markets in which no imbalance penalties are charged shifts the equilibrium to a non-cooperative state. Therefore, imbalance penalties on both overproduction and underproduction is a necessary condition for co-operation between energy storage operators and wind producers.

8

Detection of Wake Impingement in Support of Wind Plant Control

C.L. Bottasso[1,2], S. Cacciola[1], J. Schreiber[1]

[1]Technische Universität München, München, Germany

[2]Politecnico di Milano, Milano, Italy

ABSTRACT

Objectives

Wind turbines operating in a wind plant may be affected by the wake of neighboring wind turbines. When this happens, the affected machine experiences reduced power output and increased fatigue loading. The implementation of any control strategy to address this problem, requires the ability to detect such an interference condition. For example, Fig. 1 depicts the case of wind plant control by wake deflection; in such a case, the detection of a wake interference condition may be used to yaw the affecting wind turbine until a clean condition on the affected machine is achieved.

This paper describes a methodology to detect on a wind turbine wake impingement by an upstream machine. The detection is based on the use of rotor loads. As rotor load sensors are becoming routinely available on modern wind turbines, for example to enable individual blade pitch control, no additional sensors or equipment is necessary for the implementation of the present method. The use of rotor loads for the detection of wind conditions is a technology that has been proposed and demonstrated in [1-5]. The present work extends the technology to the estimation of the wake state.

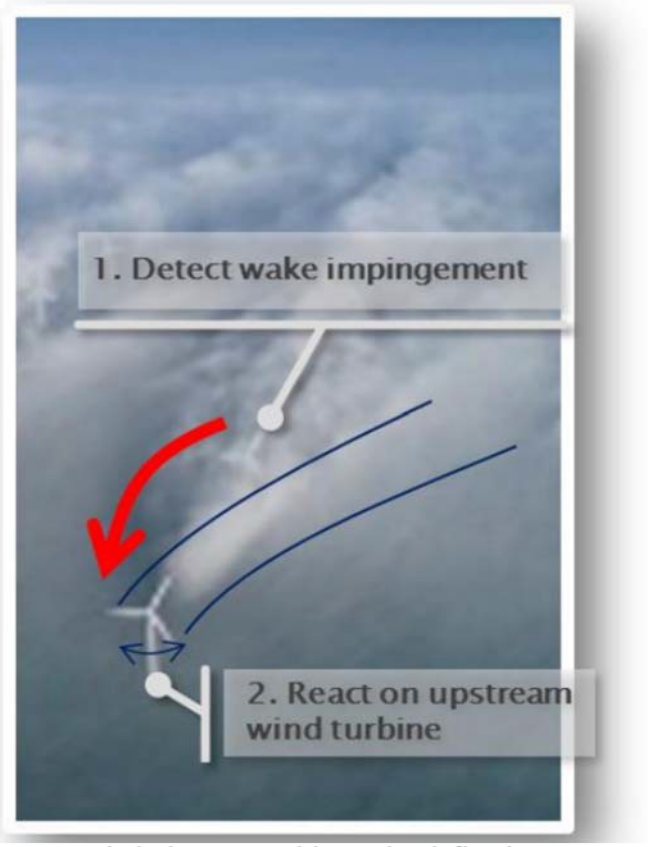

Figure 1. Wind plant control by wake deflection, supported by the detection of wake impingement.

Methods

At first, a new rotor-effective wind speed estimator is developed, based on the out-of-plane cone (i.e. averaged over the number of blades) bending rotor loads. From the cone loads measured at each time instant, an estimate of the rotor-effective wind speed may be obtained by the use of a Kalman filtering approach. Such a method delivers estimates of the wind speed and turbulence intensity of good accuracy and robustness with respect to the tuning parameters of the filter, as shown in Fig. 2.

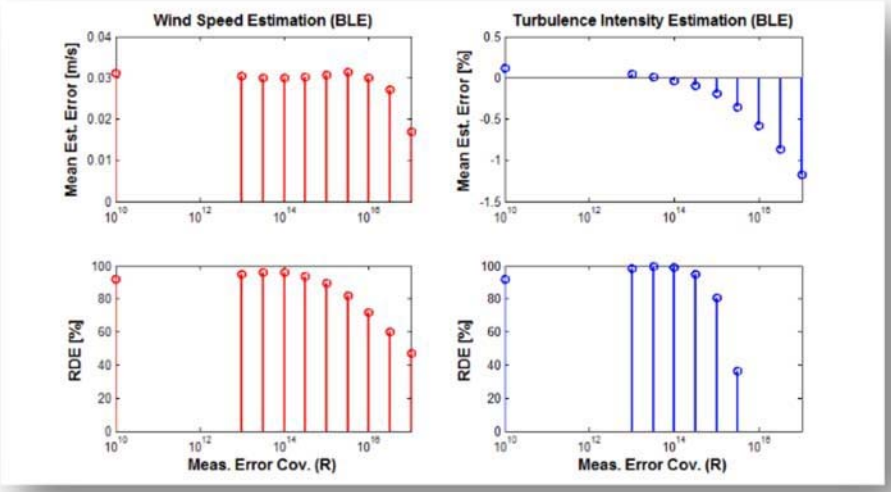

Figure 2. Estimation of rotor-effective wind speed (left) and turbulence intensity (right): mean estimation error (top), and relative degree of explanation (RDE) [6] (bottom).

Next, the method is specialized to the estimation of wind speed on sectors of the rotor disk. The concept is illustrated in Fig. 3, which shows how the passage of a blade over a disk sector can be used for estimating a sector-effective wind speed and turbulence intensity.

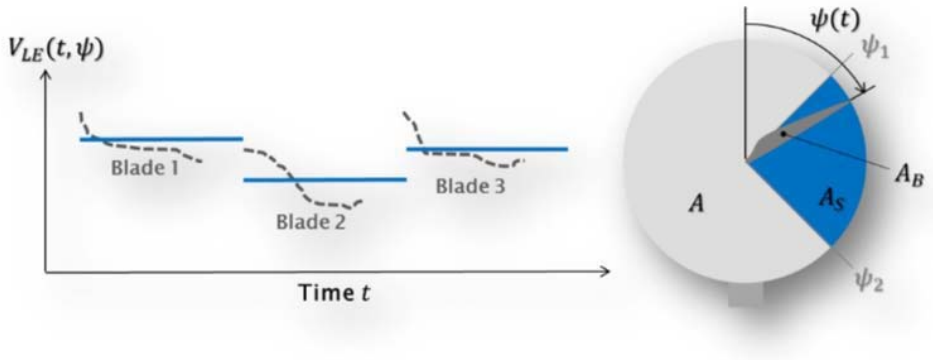

Figure 3. Estimation of local-effective wind speed and turbulence intensity, from the loads of a blade passing through a rotor disk sector.

Results

At first, the new method was tested using field test data on the NREL CART 3 wind turbine [7]. As no known wake interference condition of that machine with other wind turbines was available for this study, the local wind estimation method was used to estimate the different velocities in the top and bottom quadrants of the rotor, which gives an idea of the vertical wind shear. The comparison between estimated and measured values can only be qualitative, because only the values of the top and bottom met-mast anemometers is available, which are hardly comparable to the sector-effective wind speed estimates. Nonetheless, as shown in Fig. 4, the method follows reasonably well the trend of the met- mast anemometers and it is capable of consistently detecting a higher wind speed on the top than in the bottom quadrants.

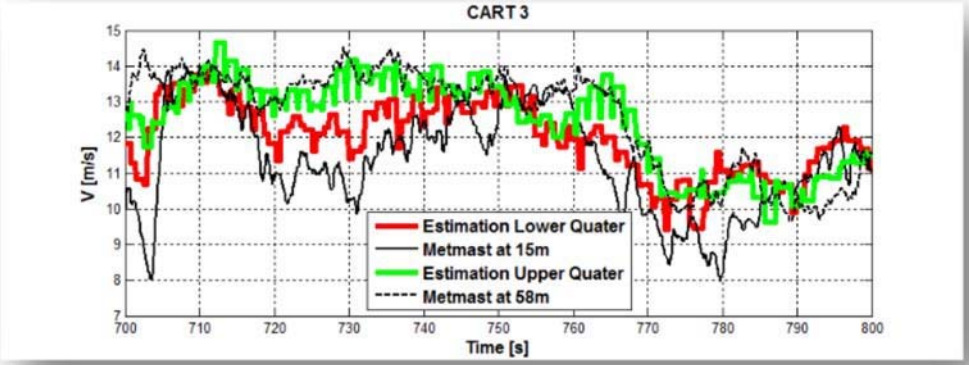

Figure 4. Estimation of top and bottom quadrant effective wind speeds, and comparison with met-mast data for the NREL CART 3 wind turbine.

Finally, the new method was used for estimating the local wind speed separately on the left and right parts of the rotor, thereby detecting the possible presence of an area of reduced speed and increased turbulence intensity, which may indicate the presence of a wake. As no experimental data was available for this case, a simulation study was conducted, by using a high-fidelity aeroservoelastic model [8] of a multi-MW wind turbine operating in different partial and full wake conditions. The results are summarized by Fig. 5, which shows the actual and estimated local wind speeds in two lateral quadrants of the rotor. Each subplot refers to a different overlap indicated by the lateral distance between the rotor and the wake center.

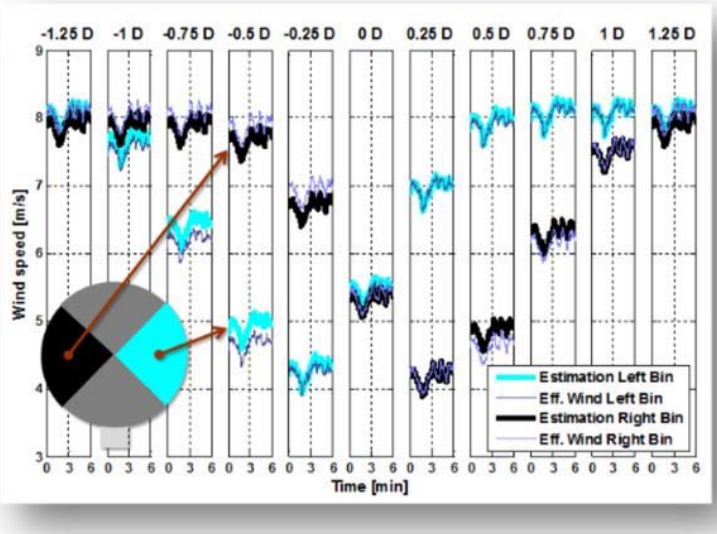

Figure 5. Estimation of local wind speed on two lateral rotor quadrants.

Conclusions

As well illustrated by the results shown here, the proposed method is capable of estimating with good accuracy the local wind speed and turbulence intensity, and in particular it is able to detect variations of these quantities on the two sides of the rotor that may be indicative of a wake interference condition. Similar results can be derived for various wind conditions, demonstrating the robustness of the local wind speed estimator. The new wake detector is currently being used for driving wake deflection strategies by active wind turbine yaw.

References

[1] C.L. Bottasso, C.E.D. Riboldi, "Validation of a Wind Misalignment Observer using Field Test Data", Renew Energ, 74:298-306, 2015.

[2] C.L. Bottasso, C.E.D. Riboldi, "Estimation of Wind Misalignment and Vertical Shear from Blade Loads", Renew Energ, 62:293-302, 2014.

[3] C.L. Bottasso, F. Campagnolo, V. Petrović, "Wind Tunnel Testing of Scaled Wind Turbine Models: beyond Aerodynamics", J Wind Eng Ind Aerod, 127:11-28, 2014.

[4] C.L. Bottasso, A. Croce, C.E.D. Riboldi, "Spatial Estimation of Wind States from the Aeroelastic Response of a Wind Turbine", TORQUE 2010, Heraklion, Greece.

[5] C.L. Bottasso, A. Croce, C.E.D. Riboldi, B. Sir, "Real-Time Estimation of Structural and Wind States for Wind Turbine Advanced Control", EWEC 2009, Marseille, France.

[6] M. Soltani, R. Wisniewsky, "Estimation of Rotor Effective Wind Speed: a Comparison", IEEE Trans. Contr. Syst. Technol., 21(4), 1155 1167, 2013.

[7] P.A. Fleming, D.J. Wright, F. Lindsay, J.W. van Wingerden, "Resonant Vibrations Resulting from the Re-Engineering of a Constant-Speed 2-Bladed Turbine to a Variable-Speed 3-Bladed Turbine", 49th AIAA Aerospace Sciences Meeting, Orlando, Florida, January 4-7, 2011.

[8] C.L. Bottasso, A. Croce, "Cp-Lambda – User's Manual", Politecnico di Milano, 2006-2015.

22

Sensitivity of Wind Turbine Airfoil Sections to Geometry Variations Inherent in Modular Blades

Mr. BROWN, Kenneth [1]; Mr. MOLINARO, Nick [1]; Mr. MEYERS, Tim [1]; Dr. BORGOLTZ, Aurelien [1]; Prof. DEVENPORT, William [1]; Mr. LUEDKE, Jonathan [2]; Mr. PESETSKY, David [2]

[1] Virginia Tech

[2] GE Power and Water

Corresponding Author: kenbrown@vt.edu

In the ongoing work to increase the efficiency of large-scale, horizontal-axis wind turbines, the modular blade concept has been proposed. The aerodynamic performance of modular blades, whose baseline profile remains unchanged from conventional blades but who are susceptible to a larger degree of variation in both manufacturing tolerances and fabrication materials, is yet unknown. This paper works towards quantifying the aerodynamic effects of variations to a baseline wind turbine section, specifically, examining the effects of offsets in the leading edge of the profile and the use of a tensioned fabric as a flow surface over the aft of the profile. Wind tunnel tests were performed on a modified DU91-W2-250 section with an offset in the leading edge and cavities in the aft that were alternatively fitted with fabric-covered panels and rigid aluminum panels. Measurements included lift, drag, airfoil surface pressures, and surface deflection of the fabric material. Preliminary results show the modifications have a noticeable impact on the aerodynamics of the ection, including altered surface pressure distributions and wake characteristics.

23

Exploiting the Characteristics of Kevlar-Wall Wind Tunnels for Conventional Aerodynamic Measurements with Implications for Testing of Wind Turbine Sections

Mr. BROWN, Kenneth [1]; Prof. DEVENPORT, William [1]; Dr. BORGOLTZ, Aurelien [1 1]
Virginia Tech

Corresponding Author: kenbrown@vt.edu

Currently regarded as a purely aeroacoustics tool with applications including the measurement of noise generation from wind turbine sections, the Kevlar-wall test section offers unique characteristics that may be leveraged to build upon conventional wind tunnel measurement methods. The use of Kevlar-wall test sections for aerodynamic as well as aeroacoustic measurements affords the wind turbine designer simultaneous measurement capability and thus significant savings in testing expenses. Towards validating the Kevlar-wall test section as an aerodynamic tool, this paper first examines two-dimensional wall interference corrections for Kevlar-wall test sections in comparison to those for traditional hard-wall test sections. Similarities and differences in the blockage and lift interference behavior of each test section are evaluated, as well as the agreement of corrected aerodynamic coefficients. This paper also addresses the accuracy of the panel method simulations of the Kevlar-wall boundary conditions, making comparisons of the wall pressure and wall deflection distributions between the simulation and measurement. Additionally, this paper explores how wall-mounted pressure taps in the Kevlar walls can be exploited to make measurements of lift.

50

Spatially Resolved Wind Tunnel Wake Measurements at High Angles of Attack and High Reynolds Numbers Using a Laser-Based Velocimeter

Daniel R. Cadel and K. Todd Lowe

A novel application of Doppler global velocimetry (DGV) has been developed for measuring wake profiles in wind tunnels at high Reynolds number flows and extreme angles of attack where aerodynamic loading is too high for standard pneumatic wake rakes. These cases are of particular importance to the wind energy community, as turbines regularly experience off-design conditions in the field; this data can aid in modeling and design tools. Wake rakes are limited in their operation such that the system cannot be implemented for very high angles of attack. At extreme angles of attack encompassing a full 360° of rotation, particularly where the airfoil is past stall, buffeting from large size scale vortices can cause high loadings. At these high angles of attack, blockage effects are also significant. Moreover, since Pitot probes cannot capture vorticity, measurements beyond stall do not yield worthwhile results [1]. To circumvent these issues at high angles, an "optical wake rake" system has been developed to provide velocity measurements through use of optical diagnostics, thus providing data at spatial resolutions finer than standard systems, without any flow disruption, and at any realizable angle of attack. A notional schematic of the configuration of the system is shown in Figure 1.

A laser diagnostic system known as cross-correlation Doppler global velocimetry (CC-DGV) [2,3] was used for the proof-of-concept measurements. The CC-DGV based optical wake rake consists of a beam of collimated laser light directed along the axis defined by linking the tips of the pressure probes of standard pneumatic rakes. Simultaneous imaging from three cameras provides three linearly independent velocity components, governed by the Doppler shift equation

$$Llv = \frac{(\hat{0} - \hat{i}) \cdot \vec{v}}{/l_0} \qquad (1)$$

where Ll is the measured Doppler frequency shift, /l is the incident laser wavelength, and $(\hat{o} - \hat{i})$ describes the vector difference between the Mie-scattered light direction (camera observation direction) and incident light direction, respectively [4]. The velocity measured by each camera is the component of the world-frame vector $\vec{V}$ in the $(\hat{o} - \hat{i})$ direction. An iodine vapor cell is placed in front of each camera; iodine vapor fluoresces, and thus modulates the incident light intensity, as a function of the cell length, temperature, vapor pressure, and the frequency of the light passing through [5]. As such, the Doppler frequency shift of scattered light can be determined by measuring the intensity relative to some reference state. CC-

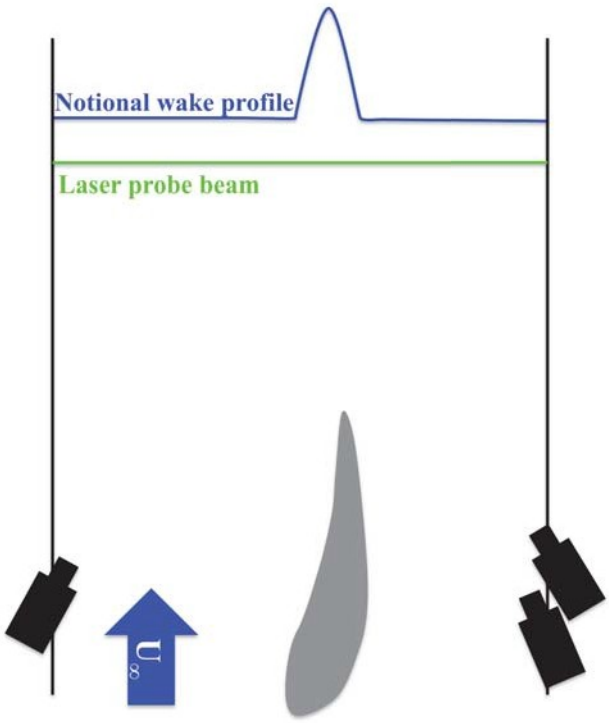

Fig. 1 Notional configuration of the laser probe beam and cameras in the Stability Wind Tunnel. The camera on the starboard side is located at approximately mid-span, while the two cameras on the port side are above and below the tunnel walls. The wake profile is measured at the position of the laser probe beam.

DGV determines the Doppler shift frequency by cross-correlating the time-history camera pixel signals with a reference signal as the incident laser light frequency is swept over a range of several GHz, corresponding to known features in the iodine vapor absorption spectrum. In this way, the offset between the pixel signal and a known reference can be found. A schematic of the CC-DGV data processing routine is shown in Figure 2. Uncertainties of 1.30 ms^{-1} for the streamwise component have been achieved in similar configurations.

Initial validation of the Optical Wake Rake was performed in the Virginia Tech Stability Wind Tunnel (SWT, Figure 3). The SWT is a closed-loop subsonic wind tunnel with a test section of cross-section 1.83 m by 1.83 m and length of 7.3 m. Turbulence levels are below 0.05%, and the maximum Reynolds number is 5 million per meter chord [6]. The airfoil model used for these measurements was an 800 mm chord length DU96-W-180 [7], with a span extending the width of the tunnel. A side-wall suction system was also used to increase flow uniformity [8]. Data was acquired for a full 360° angle-of-attack sweep at $20°$ increments and a Reynolds number of 10^6 as well as partial cross-sections at Reynolds numbers of $2x10^6$ and 3 $x10^6$. For the cross sections, the beam forming optics were mounted to the same traverse used for the pneumatic wake rake.

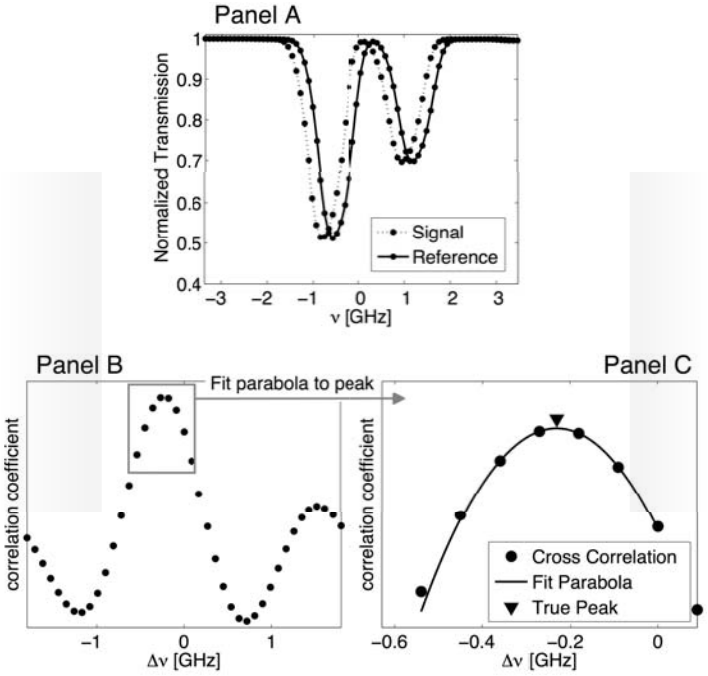

Fig. 2 Overview of cross-correlation and peak finding routines in CC-DGV. Panel A: measured spectra from scattered light and reference signals exhibit a Doppler shift between time series scans (shown for synthetic signals). Panel B: Result of scattered light and reference signal cross-correlation. Panel C: A parabolic peak-finding routine is employed to increase the precision of the peak shift location.

Fig. 3 Optical Wake Rake probe beam in the Stability Wind Tunnel downstream of the 0.800 meter DU96-W-180.

A Verdi V6 diode-pumped, solid state, Nd:YVO_4, continuous wave, 532 nm laser operating at 6 Watts output power was used to supply the beam. Three pco.edge sCMOS cameras with 5.5 megapixel resolution were positioned around the tunnel resulting in the nominal camera observation vectors listed in Table 1 (values are given to the camera image frame coordinate system origin, actual values in the beam path will vary slightly). DEHS seed oil was introduced through a slot in the test section in line with the laser beam, and allowed to recirculate through the tunnel. Results will be presented for the wake profile at several angles of attack at a chord-based Reynolds number of Re = 10^6, with validation data from the standard pneumatic rake. The data acquired is not for the full width of the tunnel due to restrictions from concurrent measurement campaigns; a portion roughly 1-2 feet in width across the tunnel was imaged, making drag integrals at high angles not feasible. Further validation of the system with wider camera fields of view and automated camera focusing and traversing is planned.

Table 1: Nominal geometry for Stability Wind Tunnel optical wake rake measurements

	X (streamwise)	Y (wall-normal)	Z (spanwise)
Camera 1 ô	-0.6865	0.4579	0.5648
Camera 2 ô	-0.6194	-0.7850	-0.0070
Camera 3 ô	-0.4731	0.3593	-0.8044
Laser î	0.0000	-1.0000	0.0000

Representative results are shown for previous work using CC-DGV in the Stability Wind Tunnel. For these measurements, boundary layer profiles were acquired at a chord position of 44% on the pressure side of a DU96-W-180 wind turbine airfoil. This model had a chord length of 0.457 meters (18 inches) across the full spanwise length of the tunnel test section. The angle of attack was -15°, corresponding to deep negative stall. Fiber optics were routed inside of the airfoil model and set to emit light outward from the surface through pressure taps, in a modified version of the "laser fence" technique of Meyers et al. [9]. Validation data was acquired using a custom fringe-type laser Doppler velocimeter. Profiles are shown in Figure 4 for Reynolds number cases of 1.5 million and 2 million. Root-mean-square (RMS) deviations from the LDV profiles were computed for each case; for $Re = 1.5\text{x}10^6$ and $Re = 2\text{x}10^6$, the RMS deviations were 2.77 ms^{-1} and 1.34 ms^{-1}, respectively.

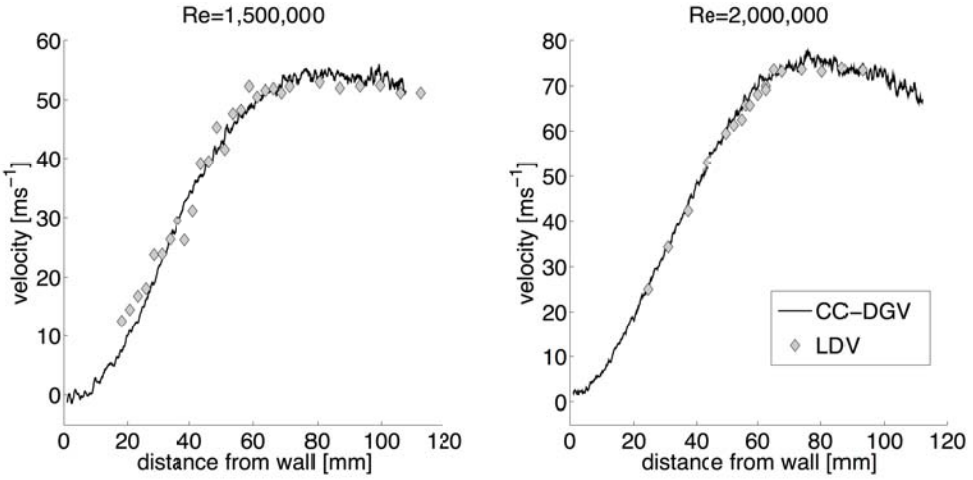

Fig. . Boundary layer profiles at 44% chord on the pressure side of an 18° chord DSA9 at 180 wind

turbine airfoil model at -15° angle of attack.

References

[1] Fauci R, Imperatore B. Design, realisation and performance evaluation of a high accuracy wake drag measurement device for CIRA transonic wind tunnel. Instrumentation in Aerospace Simulation Facilities, 2001 19th International Congress on ICIASF 2001 2001:438–47.

[2] Cadel DR, Ecker T, Lowe KT. Time-Domain Cross-Correlation Scan DGV (CCS-DGV) for Mean-Velocity Boundary Layer Measurements. 52nd Aerospace Sciences Meeting; 2014; AIAA-2014-1104.

[3] Cadel DR, Ecker T, Lowe KT. Volumetric Vector Velocity Measurements in a Hot Supersonic Jet. 17th International Symposium on Applications of Laser Techniques to Fluid Mechanics. Lisbon (Portugal); 2014;1.13.5.

[4] Charrett TOH, Nobes DS, Tatam RP. Investigation into the selection of viewing configurations for three-component planar Doppler velocimetry measurements. Appl Opt 2007;46:4102–16.

[5] Forkey JN, Lempert WR, Miles RB. Corrected and calibrated I_2 absorption model at frequency-doubled Nd:YAG laser wavelengths. Appl Opt 1997;36:6729–10.

[6] Remillieux M, Crede E, Camargo H, Burdisso R, Devenport W, Rasnick M, et al. Calibration and Demonstration of the New Virginia Tech Anechoic Wind Tunnel. 14th AIAA/CEAS Aeroacoustics Conference (29th AIAA Aeroacoustics Conference), Vancouver (British Columbia); 2008;AIAA-2008-2911

[7] Timmer WA, van Rooij RPJOM. Some aspects of high angle-of-attack flow on airfoils for wind turbine application. Delft University Wind Energy Research Institute 2001.

[8] Joseph LA. Transition Detection for Low Speed Wind Tunnel Testing Using Infrared Thermography. MS Thesis, Virginia Tech, 2014.

[9] Meyers JF, Lee JW, Cavone AA. Boundary layer measurements in a supersonic wind tunnel using Doppler global velocimetry. 15th International Symposium on Applications of Laser Techniques to Fluid Mechanics. Lisbon (Portugal); 2010:1.8.1.

Windtelligence: The Development of a Wind Farm Performance Management System

Todd Baert[1], Philip McKay[2], Rupp Carriveau[2*], David Ting[2], and Robert Kent[1]

[1]School of Computer Science, University of Windsor.
[2]Turbulence and Energy Laboratory, Ed Lumley Centre for Engineering Innovation, University of Windsor.
Corresponding Author: rupp@uwindsor.ca

ABSTRACT

The last decade has seen notable growth of wind energy in North America for the multi-megawatt class of turbines and farms [1]. While new development will continue, the attention of many developers is now turning to how to most cost effectively manage the operation and maintenance of their farms. Many of these capital-intensive assets are out of, or nearing the end, of their OEM service contracts. This leaves owners without a clear path forward of how to properly plan, budget, and act to maintain their farms. While manufacturer recommended maintenance intervals are useful, there is a strong interest in predictive maintenance. The analysis of historical production and maintenance data is most commonly used to assist in prognostic maintenance scheduling. Nearly all farms have comprehensive data monitoring built into their operations. For most operators however, the scope of the data available and the number of different sources it comes from, is overwhelming; and subsequently, little is done with it. Progressive owners that have developed their own performance monitoring practices are reluctant to share and forfeit competitive advantages. The industry is becoming aware of these challenges and has moved to develop standard measures of data harvesting. Efforts like IEC 61400-26, and IEA Task 33 are aimed at trying to address the standardization of language and data point tagging. These systems will help to further advance sector-wide initiatives like Sandia's Continuous Reliability Enhancement for Wind (CREW) that are aimed at benchmarking reliability for the entire US Fleet [2]. It's clear that there is a growing need for wind farms to begin to report basic reliability metrics both for the industry as a whole but also for their own operation. But in addition to meeting this minimum standard, a number of operations are interested in more advanced utilization of their own performance data. Estimates of remaining service life and its related influence on asset depreciation are valuable to owners and financiers. In addition to this, the prospect of proactive control to potentially reduce wake losses or increase the service life of expensive components has great appeal to progressive farms. To achieve these ends requires the collection of data from sources that are often beyond farm SCADA and may include OEM or third party structural health monitoring, ice monitoring sensors, etc. Now the operator is faced with the challenge of integrating these data streams that may not be congruent in duration or frequency. Further, the prospect of developing the proper queries to poll the correct data and perform the subsequent analysis and reporting becomes a formidable task.

In collaboration with the Wind Energy Institute of Canada and Kruger Energy, the University of Windsor is developing a flexible tool to empower wind farms to proactively optimize their performance. The web accessible database has been designed to facilitate the integration of data from a variety of sources. Queries can be developed graphically or through script. The objective of the system is to enable farms to meet minimum industry-wide reliability reporting standards, but also go beyond to competitively improve the operation of their farm. This could be through more comprehensive monitoring or advanced analyses enabled by the query tool built into the database. Figure 1 shows the results of a query for a wake loss scenario.

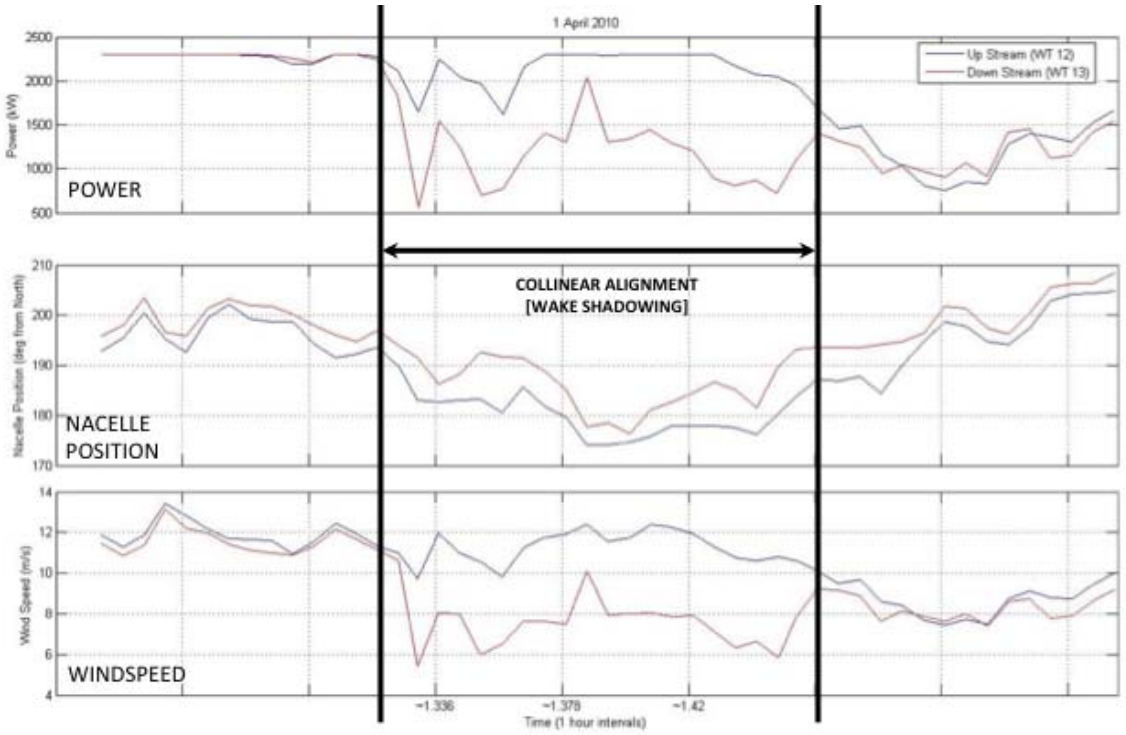

FIGURE 1. Wake Shadowing Scenario Revealed for Specific Query. Notable Power Losses Occur For a 10 Minute Period.

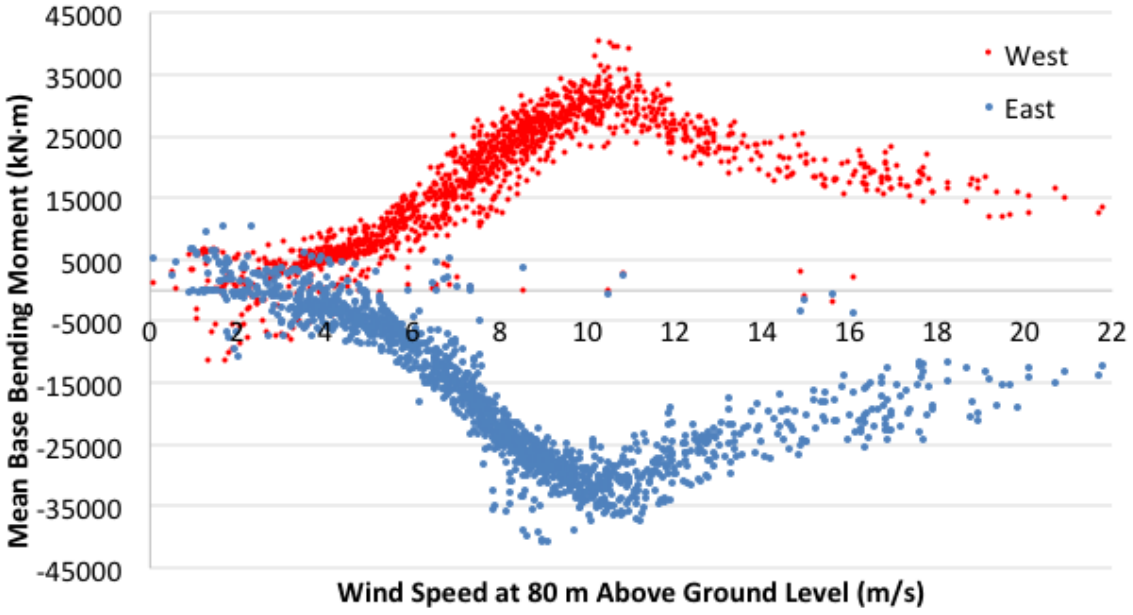

FIGURE 2. Mean Base Bending Moment Variation for Increasing Wind Speed (10 Minute Averaged Data).

Figure 1 shows measurable losses for Wind Turbine (WT) 12, which becomes directly downstream of WT13 once their nacelle positions reach roughly 195°. Figure 2 illustrates what is possible with the integration of a third party sensor to monitor bending at tower base. SCADA production data is correlated with strain values from two fibre-bragg gauges positioned at the tower base on the East and West faces of the tower. Mean base bending moment is seen to increase as wind speed increases. Beyond rated wind speeds, blade pitching begins to maintain nameplate power production. Figures 1 and 2 represent improved knowledge for a wind farm operator that is possible with the integration of resources. The Windtelligence database tool is being developed to assist wind farm owners in meeting minimum reliability reporting requirements and to enable them to enhance their competitiveness through improved wind farm intelligence. The tool can also be used by researchers to test the value of new analyses that could yield results advantageous for larger ongoing efforts like those of IEC and IEA.

REFERENCES

[1] Smith J., Carriveau R., S-K Ting. Inflow Parameter Effects on Wind Turbine Tower Cyclic Loading. *Wind Engineering*, 38(5), 2014, p.477–488.

[2] Peters V., Ogilvie A., Bond C. Continuous Reliability Enhancement for Wind (CREW) Database: Wind Plant Reliability Benchmark. *Sandia Report*, SAND2012-7328, September 2012.

16

Comparisons of Offshore Wind Turbine Reliability

Prof. CHRISTOU, Aristos [1]; Prof. MCCLUSKEY, Patrick [1]; Mr. LU, Yizshou [1]; Dr. DELORM, Tatiana [1]

[1] University of Maryland

Corresponding Author: christou@umd.edu

Abstract: The results of a comparative probabilistic reliability model applied to offshore wind turbine systems is presented. The model calculations are based on surrogate failure rate data from industrial onshore wind turbine technologies, related marine environment technologies and generic databases. Data are adjusted for the offshore marine environment and integrated with functional as well as reliability block diagrams. The developed models are applied to five generic horizontal-axis offshore wind turbine designs. Predicted subsystem failure rates and total system failure rates are reported and critical reliability limiting sub-assemblies are identified.

40

National Energy with Weather System (NEWS) simulator results

Dr. CLACK, Christopher [1]; Dr. MACDONALD, Alexander [2]; Ms. ALEXANDER, Anneliese [1]; Mr. DUNBAR, Adam [2]; Dr. WILCZAK, James [2]; Dr. XIE, Yuanfu [2]

[1] Cooperative Institute for Research in Environmental Sciences

[2] National Oceanic and Atmospheric Administration

Corresponding Author: christopher.clack@noaa.gov

The importance of weather-driven renewable energies for the United States energy portfolio is growing. The main perceived problems with weather-driven renewable energies are their intermittent nature, low power density, and high costs.

In 2009, we began a large-scale investigation into the characteristics of weather-driven renewables. The project utilized the best available weather data assimilation model to compute high spatial and temporal resolution power datasets for the renewable resources of wind and solar PV. The coincident time series of electrical load and weather data on a 13-km grid is used to investigate optimal designs of electric power systems over the contiguous US. In the past two years, the team have expanded the sophisticated mathematical optimization tool that is based upon linear programming (1) with an economic objective.

We performed a simplified test where the US electric system consisted of wind, solar PV, nuclear, hydroelectric and natural gas only with the addition of HVDC bulk transmission. The test shows that if the US meets its goals in price reduction of variable generation the US would only have dramatic reductions of carbon dioxide emissions that is cost effective with a national-scale interconnected system. The smaller the system the higher the carbon emissions and steeper the cost.

(1) C T M Clack, Y Fu, A E MacDonald, Linear programming techniques for developing an optimal electrical system including high-voltage direct-current transmission and storage, International Journal of Electric Power and Energy Systems 68, 103-114

37

Bio-Inspired Trailing Edge Noise Control

Mr. CLARK, Ian [1]; Prof. DEVENPORT, William [1]; Dr. ALEXANDER, W. Nathan [1]; GLEGG, Stewart [2]; Dr. JAWORSKI, Justin [3]; Dr. DALY, Conor [4]; Dr. PEAKE, Nigel [4]

[1] Virginia Tech

[2] Florida Atlantic University

[3] Lehigh University

[4] University of Cambridge

Corresponding Author: clarki91@vt.edu

Trailing edge noise remains a primary limiting factor in the widespread implementation of wind turbines, particularly near populated areas. Noise regulations commonly require acoustic de-rating of existing turbines, leading to reduced output and revenue. This presentation will describe an experimental study aimed at trailing edge noise control inspired by the unique features found on the wings of owls that use acoustic stealth while hunting prey. One of these features is a thin layer of fine hairs which grow from the exposed surfaces of the flight feathers. These hairs have been investigated and found to form a sort of canopy suspended above the surface of the owl's feathers. Previous wall-jet tunnel measurements have shown that high open-area canopies of similar characteristics can reduce surface pressure fluctuations on the underlying surface by as much as 30dB, and significantly attenuate roughness noise generated by that surface.

In the present work, treatments designed to replicate the effects of the canopy in a form suitable for application to an airfoil have been designed and tested in the Virginia Tech Stability Wind Tunnel. Over 20 variants of these designs have been tested by performing aeroacoustic wind tunnel measurements on a tripped DU96-W180 airfoil at chord Reynolds numbers up to 3 million. Exact details of the treatments are not given here since they are the subject of a current patent application, but the treatments will be described during the presentation. Variations include treatment thickness, density, length, position relative to the trailing edge and the effectiveness of treating only one side of the trailing edge. The treatments were placed over the center-half span of the airfoil in the trailing edge region. Measurements included far-field acoustic data from a 117-microphone phased array and mean surface pressure data from 80 pressure taps distributed over the airfoil profile. For some conditions a rake of Pitot and static probes was used to measure profiles through the airfoil wakes and infer the drag using a momentum balance approach.

Compared to the unmodified airfoil the treatments were found to be quite effective. Acoustic beamform maps and integrated spectra show up to 10dB of broadband attenuation of trailing edge noise in the vicinity of the treatment. The majority of the noise attenuation was observed in the frequency range above 1500Hz, but measurements below this frequency are inconclusive because of the large spot size of the phased array at these frequencies. The treatment remains effective throughout a wide parameter range and is not highly dependent on a particular geometry, but there appears to be strong potential for optimization. Treatments were found to be effective over an angle of attack range that extends over 10 degrees from zero lift. Compared to the unmodified airfoil, no additional noise was measured from the treated airfoil past this 10 degree range. The mean surface pressure data revealed that the presence of the treatment had little impact on the lift characteristics of the airfoil model. Drag rake results showed a small increase in drag proportional to the increase in wetted area resulting from the addition of the treatment to the unmodified airfoil.

32

The IMPOWR (Improving the Mapping and Prediction of Offshore Wind Resources) project: Evaluation of WRF PBL Schemes

Dr. COLLE, Brian [1]; SIENKIEWICZ, Matthew [1]; Dr. ARCHER, Cristina [2]; Dr. VERON, Dana [2]

[1] Stony Brook University

[2] University of Delaware

Corresponding Author: brian.colle@stonybrook.edu

Please see attached file.

I. Background and Motivation:

Mesoscale models are important for wind characterization and forecasting in the highly populated coastal marine environment of the Northeast U.S. (NEUS). However, this is an area with limited observations within the planetary boundary layer (PBL), with just a few buoys and short towers along the entire continental shelf. There are important diurnal circulations near the Northeast coast during the warm season, such as sea breezes and low-level jets. This presentation highlights the IMPOWR (Improving the Mapping and Prediction of Offshore Wind Resources) project, which focuses on the Nantucket Sound area and provides a rich dataset of observations within the PBL from a variety of sources: a Long-EZ aircraft that completed 18 flight missions in 2013-2014; a multi-level Cape Wind tower (to 60 m ASL) within Nantucket Sound available from 2003 to 2011 with additional measurements at 10 m during 2013-2014; LIDARs (since mid-2014) on the south shore of eastern Long Island and Block Island; as well as NDBC and ASOS surface stations (Fig. 1).

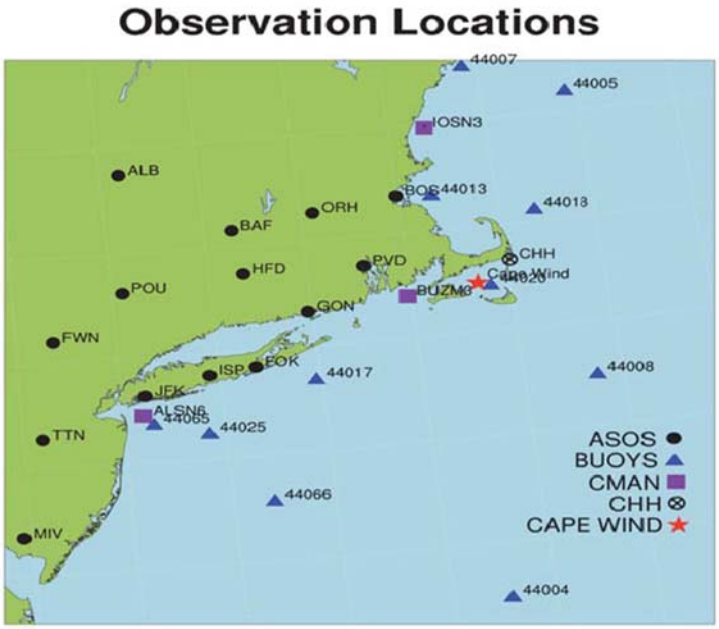

Figure 1. The observation locations for the IMPOWR field experiment. The Long-EZ aircraft took off from FOK over eastern Long Island.

Figure 2. Photo of the Long-EZ aircraft over the Cape Wind tower in Nantucket Bay.

The two goals of IMPOWR are: (1) to better understand some of the diurnal coastal flows in this region using a unique observational dataset, and (2) evaluate the performance of six planetary boundary layer (PBL) schemes in the Weather Research and Forecasting (WRF-ARW) model in the coastal marine environment down to 1.33-km grid spacing. Verification was completed for six WRF PBL schemes (two non-local, first-order schemes and four local, TKE-order schemes) that were run for 30-h for 90 randomly selected days between 2003 and 2011 using initial and boundary conditions from the North American Regional Reanalysis (NARR). Additional WRF simulations were completed for the IMPOWR case studies down to 1.33-km grid spacing.

II. Results:

Using the historical Cape Wind data, mean errors (MEs) for each WRF PBL scheme were calculated for day (1200 UTC through 2300 UTC) and night (0000 UTC through 1100 UTC) periods during the warm season (April to September; Fig. 3a) and cool season (October to March; Fig. 3b). This allows for a more in-depth investigation of the model wind speed biases as a function of the diurnal heating. During the warm season, wind speed biases for all schemes are largest at the 20-m level during the night and negative, with values between -0.50 and -0.80 m s^{-1}. The negative bias is smaller at the 41- and 60-m levels for both day and night, with the exception of the BouLac scheme, which shows negative biases increasing in magnitude from 20 m to 60 m. During the cool season, the nighttime biases are small, but the daytime biases are consistently negative in sign and increasing in magnitude with height. The largest cool season wind speed biases are found in the BouLac scheme, with a daytime value approaching -1.5 m s^{-1} at the 60-m level. MAE is very similar for all schemes at all times and levels, and fall between 1.65 and 2.15 m s^{-1} (Fig. 3.21-22). Excluding the BouLac scheme, there is little difference in wind speed bias or MAE between first-order (e.g, YSU, ACM2) or TKE-order closure (e.g, MYJ, MYNN2, BouLac, QNSE) schemes.

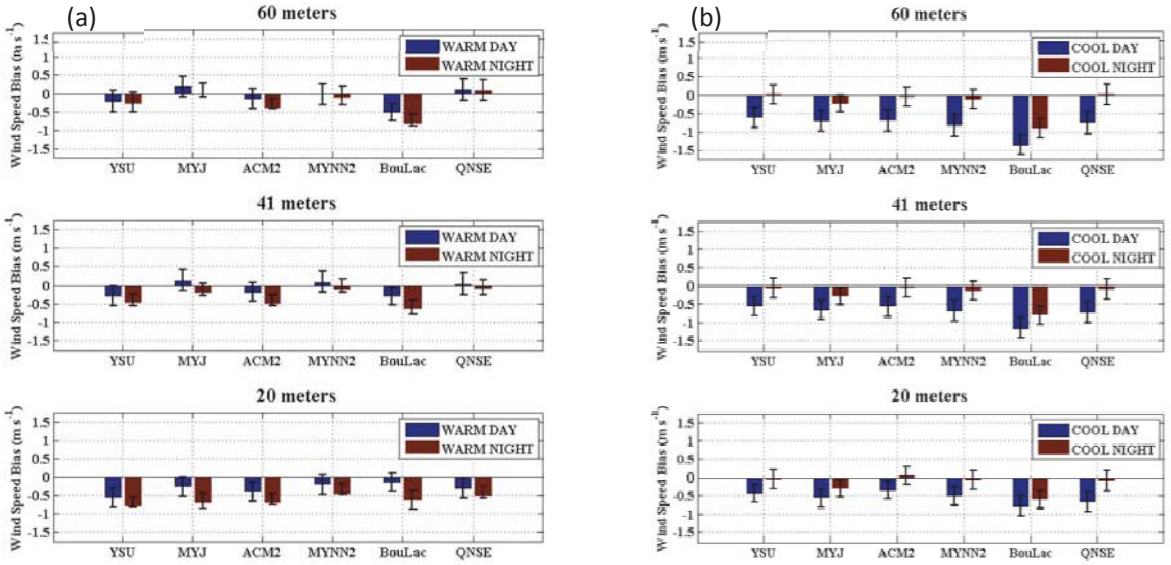

Figure 3: (a) Warm season (April to September) and (b) cool season (October to March) wind speed mean error in m s^{-1} for each of the six WRF PBL schemes at 60 m, 41 m, and 20 m. Daytime (1200 UTC to 2300 UTC) is in blue and nighttime (0000 UTC to 1100 UTC) is in red. Black bars represent the bootstrap 95% confidence intervals.

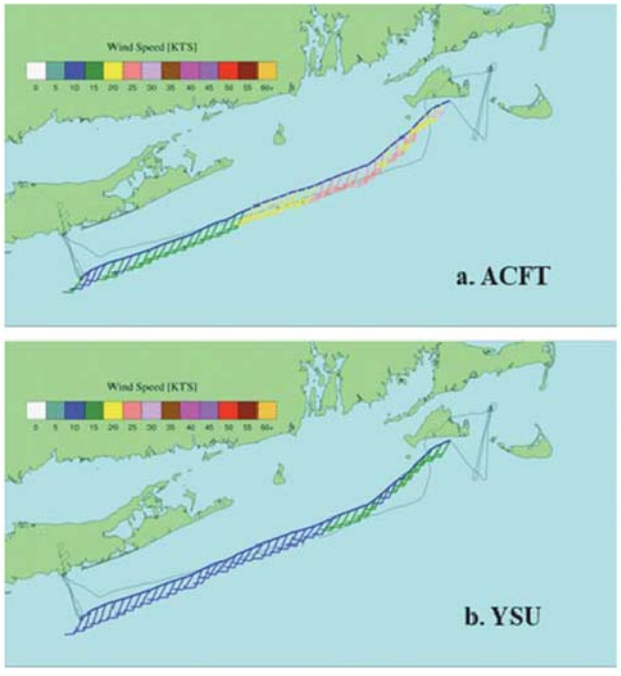

Figure 4. Winds (10 kts = 1 full barb) along the low-level flight track (20-60 m above surface) from 1802 – 1846 UTC 21 June 2013 for (a) aircraft observations and (b) the YSU PBL scheme.

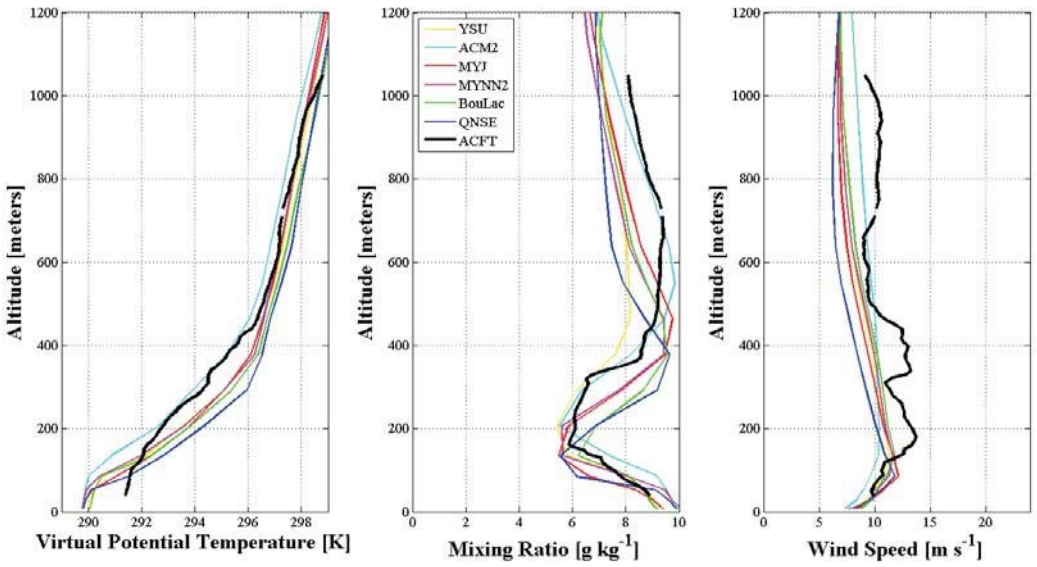

Figure 5. Modeled and observed profiles of (a) virtual potential temperature (K), (b) mixing ratio (g kg^{-1}) and (c) wind speed (m s^{-1}) for the aircraft spiral around the Cape Wind tower at ~1925 UTC 21 June 2013.

Additional model verification was performed from several Long-EZ aircraft flights during IMPOWR. In general, the WRF PBL schemes overestimated the height of the low-level coastal jet while underestimating the magnitude, as illustrated for a case on 21 June 2013 (Figs. 4 and 5). The aircraft measured 15–25 kt winds south of Block Island Sound and Long Island, while all PBL schemes showed only 5–15 kt winds. The observed jet was deeper than simulated (Fig. 5c) and the model also was too cool and stable at low-levels as compared to the aircraft spirals over Cape Wind (Fig. 5a). Other cases will be shown and summarized that illustrate these issues as well.

In order to explore some of the reasons for the model errors, additional simulations were completed using variety of different initial conditions (different NCEP model analyses) and sea- surface temperature (SST) perturbations. We also completed relatively long simulations (72 hours) to test whether there were any spinup issues of the marine boundary layer. The model SSTs tend to be 1-2 ^{o}C too cool during the warm season on average, so we hypothesized that this may be contributing to the model errors. The results were more sensitive to the atmospheric initial and boundary conditions than the PBL schemes and SST. There is also evidence to suggest that some of the errors observed around Cape Wind in Nantucket Bay may not be representative of other locations outside the Bay given the strong diurnal variations in the Bay and surrounding island geometries.

III. Conclusions:

The IMPOWR project collected a unique dataset for model validation and a better understanding of the diurnal coastal flows in this region (e.g., New York Bight Jet), which will be highlighted in this presentation. The main conclusions of the modeling validation part of this study include:

- Mean errors in wind speed, temperature and dew point temperature are highly variable in the coastal and offshore regions, varying by season, diurnal period, latitude and distance from the coast. All PBL schemes generally have similar ME values, with the exception of the BouLac scheme, which shows warmer surface temperatures during the cool season and stronger (weaker) winds over the land (water).
- Model verification results at the Cape Wind tower in Nantucket Sound show that wind speed biases are negative for all schemes, diurnal periods, and seasons. Biases are largest at the 20-m level during the warm season (except for the BouLac scheme) most likely due to prevailing warm southerly flow over a colder SST field in the model leading to increased stability and less mixing of momentum down to the surface.
- During the cool season the flow regime is mostly offshore, resulting in cold continental air flowing over warm water and the development of a neutral to unstable PBL. Cool season wind speed biases are largest at 60 m, likely due to enhanced mixing resulting from warmer model SST fields and resultant sensible heat fluxes.
- During the warm season perturbations to the SST field result in changes to the PBL structure. Specifically a warmer SST field was shown to improve the profiles of wind speed, moisture and temperature throughout the shallow PBL. Minimal changes were observed above the PBL due to the presence of a strong stable layer.
- Different analyses used as initial and lateral boundary conditions led to larger variations in atmospheric structure throughout the PBL and free atmosphere than different PBL schemes alone.

Application of Fast Pressure-Sensitive Paint to an Oscillating Wind Turbine Airfoil

Kevin J. Disotell
disotell.1@osu.edu
Graduate Research Fellow
The Ohio State University
Columbus, OH, USA

Pourya Nikoueeyan
pnikouee@uwyo.edu
Graduate Research Assistant
University of Wyoming
Laramie, WY, USA

Jonathan W. Naughton
naughton@uwyo.edu
Professor
University of Wyoming
Laramie, WY, USA

James W. Gregory
gregory.234@osu.edu
Associate Professor
The Ohio State University
Columbus, OH, USA

2015 North American Wind Energy Academy (NAWEA) Symposium Abstract

BACKGROUND

In the unsteady flow environment experienced by wind turbine blades, large excursions in local angle of attack and significant three-dimensional flows arise that complicate the prediction of stall onset and unsteady loading. Accurate predictions of the dynamic loads are critical to the pursuit of lightweight, reliable structures to lower the cost of wind energy (Ref. 1). To this end, diagnostic measurement tools capable of fine spatial resolution and high frequency response are important for better understanding unsteady aerodynamic effects on blade pressure distribution.

The sparseness of conventional pressure transducers has historically provided motivation for the development of pressure-sensitive paint (PSP), an optical surface pressure measurement technique with inherently fine spatial resolution. Within the last decade, the bandwidth of certain paint formulations has been significantly increased to resolve unsteady flows; a flat frequency response on the order of several kHz is now readily achievable (Ref. 2). PSP consists of luminescent molecules adhered to the test surface by a thin binder layer, typically on the order of 10 microns. The luminophore responds to the local partial pressure of oxygen, which is directly proportional to absolute air pressure. An illumination source such as a light-emitting diode or expanded laser beam excites the luminophore, and the emitted light intensity captured by a scientific-grade camera is converted to absolute pressure via calibration. Each point on the painted surface thus responds as a molecular-sized transducer, with spatial resolution limited by the camera pixel size.

Recent advancements in unsteady PSP data acquisition and processing techniques have been developed for rotating blades to account for errors caused by model movement and deformation in nonuniform illumination fields. The single-shot lifetime technique (Ref. 3) and motion capturing technique (Ref. 4) are two methods which have arisen. Due to its straightforward procedure and commonality of required hardware, the single-shot technique has been used across a range of small test facilities (Ref. 5, 6) and large-scale wind tunnels (Ref. 7).

PSP measurements have been historically limited to the compressible flow regime to achieve sufficient signal-to-noise ratio in the data images (Ref. 8, 9). Recent wind tunnel testing with unsteady PSP has been geared toward helicopter applications (Ref. 10, 11), although temperature error due to compressibility effects has been noted. Under isothermal conditions or with an accurate temperature correction available, laser-based excitation and highly reflective paints can enable instantaneous PSP measurements at Mach numbers near $M \approx 0.15$, corresponding to dynamic pressures of approximately 1.5 kPa (Ref. 6, 12). Unsteady aerodynamic effects can result in even larger pressure differences, considering that peak suction levels on oscillating airfoils can reach factors of the free stream dynamic pressure (Ref. 13). With the present availability of suitable paints, the above considerations present an opportunity for PSP to be deployed as a measurement tool for resolving the global pressure distribution on wind turbine blades.

DESCRIPTION OF WORK

The work to be discussed has the objective of demonstrating PSP as a viable tool for measuring global surface pressure on wind turbine blades. To our knowledge, this work represents the first application of PSP to a low-speed airfoil undergoing pitch oscillation used to mimic unsteady changes in incidence angle. While much of the dynamic stall literature has focused on relatively thin airfoils for helicopter applications, the current effort will use the single-shot PSP technique to investigate the unsteady stalling behavior of a thick airfoil section (Delft DU97-W-300) representative of wind turbine blades. In the talk, aspects of the data collection method will be presented along with

sample results demonstrating the capabilities of the measurement technique. Results to be presented will consist of global pressure maps obtained during dynamic stall development, including a controlled case with vortex generator tabs applied.

SUMMARY OF RESULTS

PSP experiments were performed in the University of Wyoming subsonic wind tunnel, an open-circuit facility. Flow conditions were Mach number M=0.13, chord Reynolds number Re=224,000, and reduced frequency k=0.106 based on semichord. The pitch schedule was given by $\alpha=15.7°+11.2°\sin(93.5t)$, with the measured lift hysteresis loop shown in Figure 1.

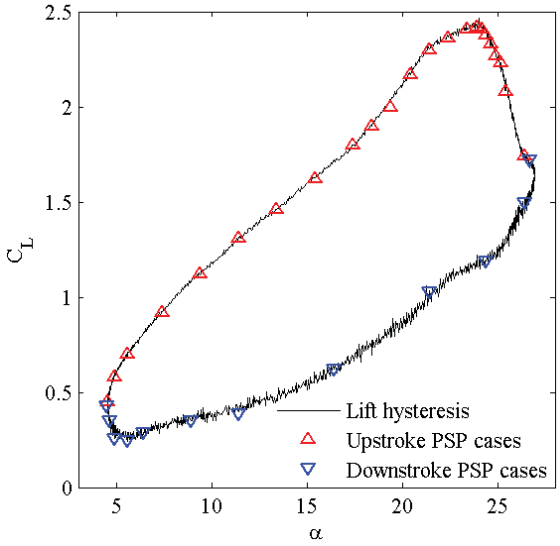

Figure 1: Phase positions for unsteady PSP data collection (k=0.106, M=0.13, Re=224,000).

The static lift curve of the DU-97-W-300 airfoil was measured with and without PSP applied to the wing. The middle third of the airfoil span was painted with porous polymer/ceramic PSP basecoat doped with platinum tetra(pentafluorophenyl) porphyrin (PtTFPP) luminophore. Typical pressure sensitivity for this paint formulation is up to 0.6% per kPa at atmospheric pressure, and bandwidth up to 6 kHz – more than sufficient to capture the fundamental airfoil oscillation frequency of 15 Hz. An *in-situ* pressure calibration of the paint signal was performed with a set of 12 pressure taps situated near midspan on the upper airfoil surface. Phase-locking of the PSP system to a shaft encoder allowed the instantaneous surface pressure to be captured over a sweep of phase angles, as denoted on the lift coefficient (C_L) hysteresis loop in Figure 1. PSP data were acquired approximately once every fourth oscillation cycle, which was a limitation of the camera frame rate (Cooke Corp. PCO.1600).

In Figure 2, phase-averaged surface pressure maps measured by PSP (average of 64 cycles) are shown for selected phases of the oscillation in terms of pressure coefficient (C_p). The data were spatially filtered using a 13×13 pixel (4.2% chord) median filter to attenuate shot noise effects. At α=6.2° rising (Figure 2a), the flow is reattaching and three-dimensionality in the spanwise direction is apparent. Trailing-edge stall progresses as the angle of attack increases (Figure 2b-e). Leading-edge suction ($C_p \sim -5$) begins to collapse at the lift stall angle, which occurs near α=24° (Figure 2f). PSP indicates a complex breakdown of the flow in Figure 2f, with an isolated zone of increased suction developing on the aft part of the airfoil. Just beyond lift stall, the primary separation vortex grows stronger in Figure 2g-h, an observation also noted from the planar velocity field measurements of Ref. 13. The pressure signature of the vortex appears to show a mild degree of three-dimensionality. In the post-stall flow, the leading-edge suction zone entirely collapses and the aft region shows a flat pressure profile representing a fully stalled condition (Figure 2j-l). Surface maps such as these can provide powerful complementary insight to the flow field measurements of Ref. 13 which were previously conducted with the same test article.

A controlled case featuring several vortex generator (VG) tabs applied to half of the painted region was acquired to demonstrate detection of 3-D patterns on the oscillating airfoil using PSP. The particular way in which VGs interact with the flow is extremely challenging to glean from a sparse set of pressure transducers. Therefore, this was a desirable case to demonstrate wherein PSP measurements could be used for direct validation of computational models desired by industry. A sample result of the measured flow pattern is shown in Figure 3, with the location of VGs labeled. The VG design was not optimized for the boundary layer flow in the test; this appears to be evident in the region of stagnant flow behind the tabs and the higher C_p levels ahead of them at the leading edge compared to the other side of midspan (y/b = 0).

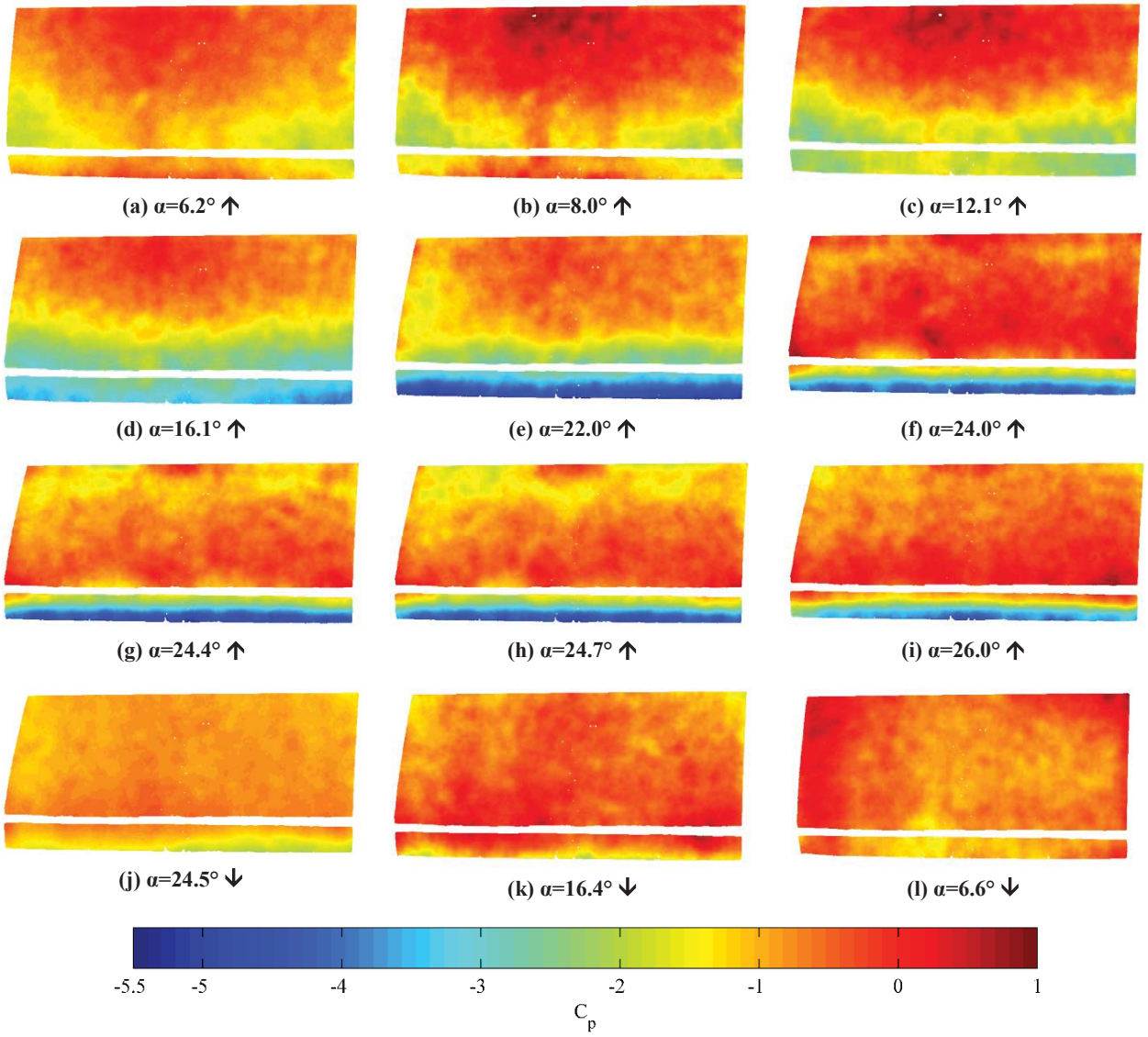

Figure 2: Phase-averaged PSP images of oscillating DU97-W-300 airfoil at selected phase positions. Flow is from bottom to top in each image; arrows indicate upstroke/downstroke directions.

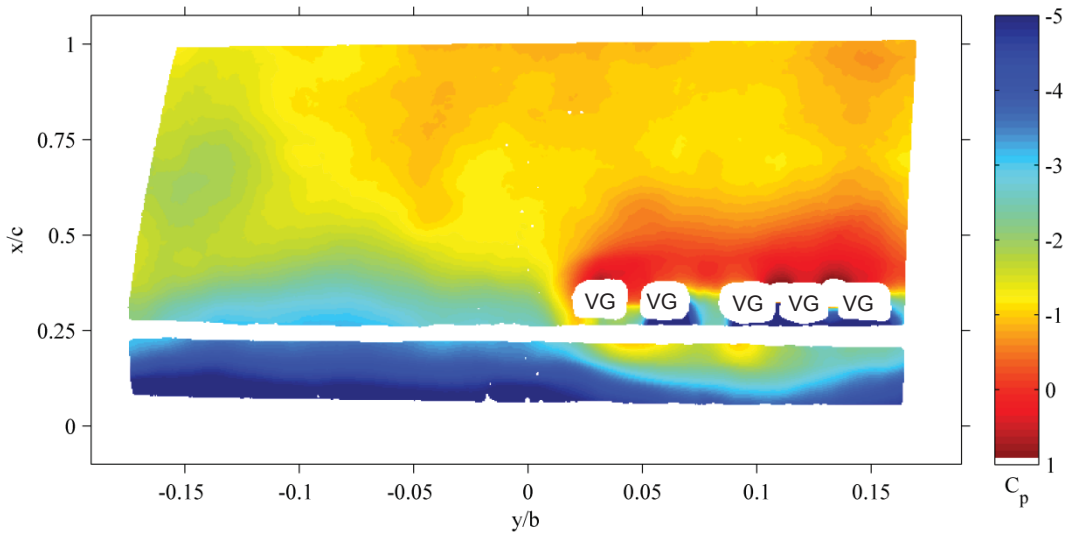

Figure 3: PSP image of flow pattern on oscillating airfoil with vortex generators installed (α=22.1°, upstroke).

CONCLUSIONS

The PSP tests were viewed as successfully demonstrating application of the technique to a low-speed flow with unsteady surface motion, a test condition historically outside the capabilities of conventional PSP systems. Pressure fields were obtained with strong signal-to-noise ratio by minimizing the effect of temperature error through test procedure, and the single-shot lifetime method cancelled the effects of surface movement and nonuniform illumination which otherwise introduce significant error to the measurement. Moreover, the fast frequency response of the paint appeared to capture unsteady pressure topologies tracking with oscillation phase.

ACKNOWLEDGMENTS

The authors gratefully acknowledge a Career Development Grant to K. Disotell from The Ohio State University, partial support from the U.S. Department of Energy (DESC0001261, Timothy J. Fitzsimmons), and additional support through a gift to the University of Wyoming from BP Alternative Energy North America, Inc.

REFERENCES

1. Cohen, J., Schweizer, T., Laxson, A., Butterfield, S., Schreck, S., Fingersh, L., Veers, P., and Ashwill, T., "Technology Improvement Opportunities for Low Wind Speed Turbines and Implications for Cost of Energy Reduction: July 9, 2005 - July 8, 2006," National Renewable Energy Laboratory, NREL TP-500-41036, 2008.
2. Gregory, J.W., Sakaue, H., Liu, T., and Sullivan, J.P., "Fast Pressure-Sensitive Paint for Flow and Acoustic Diagnostics," *Annual Review of Fluid Mechanics,* Vol. 56, 2014, pp. 303-330. doi: 10.1146/annurev-fluid-010313-141304.
3. Juliano, T.J., Kumar, P., Peng, D., Gregory, J.W., Crafton, J., and Fonov, S., "Single-Shot, Lifetime-Based Pressure-Sensitive Paint for Rotating Blades," *Measurement Science and Technology,* Vol. 22, (8), 2011, pp. 085403. doi: 10.1088/0957-0233/22/8/085403.
4. Sakaue, H., Miyamoto, K., and Miyazaki, T., "A Motion-Capturing Pressure-Sensitive Paint Method," *Journal of Applied Physics,* Vol. 113, (8), 2013, pp. 084901. doi: 10.1063/1.4792761.
5. Juliano, T.J., Disotell, K.J., Gregory, J.W., Crafton, J.W., and Fonov, S.D., "Motion-Deblurred, Fast-Response Pressure-Sensitive Paint on a Rotor in Forward Flight," *Measurement Science and Technology,* Vol. 23, (4), 2012, pp. 045303. doi: 10.1088/0957-0233/23/4/045303.

6. Disotell, K.J., Peng, D., Juliano, T.J., Gregory, J.W., Crafton, J.W., and Komerath, N.M., "Single-Shot Temperature- and Pressure-Sensitive Paint Measurements on an Unsteady Helicopter Blade," *Experiments in Fluids,* Vol. 55, (2), 2014, pp. 1671. doi: 10.1007/s00348-014-1671-2.
7. Wong, O.D., Watkins, A.N., Goodman, K.Z., Crafton, J.W., Forlines, A., Goss, L., Gregory, J.W., and Juliano, T.J., "Blade Tip Pressure Measurements using Pressure Sensitive Paint," AHS 2012-000233, American Helicopter Society 68th Annual Forum and Technology Display, Fort Worth, TX, May 1-3, 2012.
8. Mendoza, D.R., "Limiting Mach Number for Quantitative Pressure-Sensitive Paint Measurements," *AIAA Journal,* Vol. 35, (7), 1997, pp. 1240-1241. doi: 10.2514/2.228.
9. Bell, J.H., "Applications of Pressure-Sensitive Paint to Testing at very Low Flow Speeds," AIAA 2004-0878, AIAA 42nd Aerospace Sciences Meeting and Exhibit, Reno, NV, January 5-8, 2004.
10. Gardner, A.D., Klein, C., Sachs, W.E., Henne, U., Mai, H., and Richter, K., "Investigation of Three-Dimensional Dynamic Stall on an Airfoil using Fast-Response Pressure-Sensitive Paint," *Experiments in Fluids,* Vol. 55, (9), 2014, pp. 1807. doi: 10.1007/s00348-014-1807-4.
11. Juliano, T.J., Peng, D., Jensen, C.D., Gregory, J.W., Liu, T., Montefort, J., Palluconi, S., Crafton, J., and Fonov, S., "PSP Measurements on an Oscillating NACA 0012 Airfoil in Compressible Flow," AIAA 2011-3728, 41st AIAA Fluid Dynamics Conference and Exhibit, Honolulu, HI, 2011.
12. Disotell, K.J., and Gregory, J.W., "Measurement of Transient Acoustic Fields using a Single-Shot Pressure-Sensitive Paint System," *Review of Scientific Instruments,* Vol. 82, (7), 2011, pp. 075112. doi: 10.1063/1.3609866.
13. Naughton, J.W., Strike, J., Hind, M., Magstadt, A., and Babbitt, A., "Measurements of Dynamic Stall on the DU Wind Turbine Airfoil Series," American Helicopter Society 69th Annual Forum, Phoenix, AZ, May 21-23, 2013.
14. Timmer, W.A., and van Rooij, R.P.J.O.M., "Summary of the Delft University Wind Turbine Dedicated Airfoils," *Journal of Solar Energy Engineering,* Vol. 125, (4), 2003, pp. 488-496. doi: 10.2514/2.228.

28

Utilizing Radar Measured Velocity Fields to Forecast Turbine Wind Speeds

James B. Duncan Jr.[1], Brian D., Hirth[1], John L. Schroeder[2]

[1]*National Wind Institute, Texas Tech University, Lubbock, TX, USA*
[2]*Department of Geosciences, Texas Tech University, Lubbock, TX, USA*

Wind turbines almost exclusively operate in a reactive state. In most cases, a parcel of air may entirely pass through the rotor sweep before the turbine's control system even attempts to adapt. Given a wind turbine typically has no knowledge of the upstream flow conditions, a snapshot of the approaching wind field could provide for improved turbine performance through a reduction of structural loads and increased energy capture. Although information of the near-upstream flow conditions has been examined through the use of nacelle mounted LIDAR (Light detection and ranging) systems (e.g. Bossanyi et al. 2014; Mikkelsen et al. 2013; Schlipf et al. 2011), employing three-dimensional wind field maps derived from scanning instruments to provide an extended wind speed forecast for individual turbine locations has never been investigated.

Utilizing Texas Tech University's Ka-band Doppler radar systems, researchers have demonstrated the ability to derive three-dimensional wind field maps of the complex flows and wake structures surrounding an individual turbine (Hirth and Schroeder 2013) as well as within wind plants (Hirth et al. 2015). While only the radial component of the wind may be derived from a single radar (or LIDAR) system, a dual-Doppler scanning strategy allows for the extraction of the full horizontal velocity vector and construction of horizontal wind field map as shown in Figure 1.

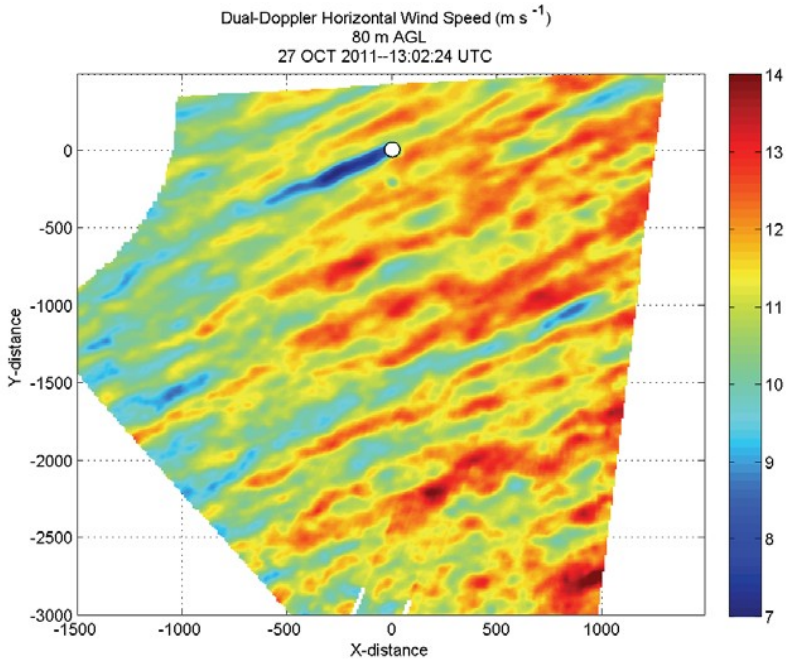

Figure 1. Dual-Doppler horizontal wind speed (m/s) synthesis at 80 m AGL for a single volume ending at 13:02:24 UTC on 27 October 2011.

Whereas nacelle mounted LIDAR systems predominantly sample wind speeds in the near-upstream region of the turbine, radars have the ability to provide wind speed and direction measurements over a much larger domain with the temporal resolution necessary to resolve and track wind features relevant to wind turbine controls. The acquired information allows for the attempted prediction of turbine inflow wind speed and direction one minute or more in advance. The acquired measurements adjacent to a farm also provide an opportunity to identify and track regional scaled weather phenomena (e.g. fronts, outflow boundaries, etc.) before they arrive onsite.

The data used for this investigation were collected surrounding a single utility scale turbine on 27 October 2011. Details of the deployment, radar scanning strategies employed and analysis domain used can be found in Hirth and Schroeder (2013). Dual-Doppler volumes over a three dimensional grid with 10-m horizontal and vertical grid spacing were constructed approximately every 45 s. In order to forecast wind speeds to the turbine's position, the following methods were applied. Given a radar volume, a governing wind direction was calculated at 1D upstream of the turbine. This governing wind direction was an average of the wind directions across the rotor swept area and was calculated at 1D upstream to mitigate the effects of ground clutter associated with the turbine rotor on the adjacent wind field. Conventional wisdom might lead one to use this governing wind direction to project the upstream flow field from the turbine's location to obtain a preview of the incoming wind. However, in order to minimize the error in forecasted wind speed estimates, this wind direction alone cannot be the only consideration.

Organized coherent structures are embedded within the turbulent flow-fields of the atmospheric boundary layer. One structure type, referred to as near-surface streaks, are elongated areas of enhanced/reduced wind speeds (Traumner et al. 2015), and have been shown using full-scale radar measurements to be skewed to the left of the wind direction (e.g. Lorsolo et al. 2008; Marathe 2014). While generally aligned with the prevailing wind direction, these streak features do not passively advect with the mean flow field. To examine the variation between projected and actual streak motion, a four-minute period of wind speed data was analyzed. Beginning with an initial radar volume scan, two streak features of enhanced wind speed were isolated. To derive the projected advection, an area average wind direction and speed representative of the features were calculated. Using this vector and the amount of time until the completion of the volume scan, a forecasted position of the feature was generated. For this initial work, the advection of the features was based upon visual inspection of the wind field map at the end of each volume. Shown in Figure 2, the true advection of the feature lagged the forecasted position and was several degrees to the left of the projected advection according to the governing wind speed and direction from the prior volume scan. For this four-minute span, variation in advection ranged from 2.6° - 8.3° to the left of projected motion.

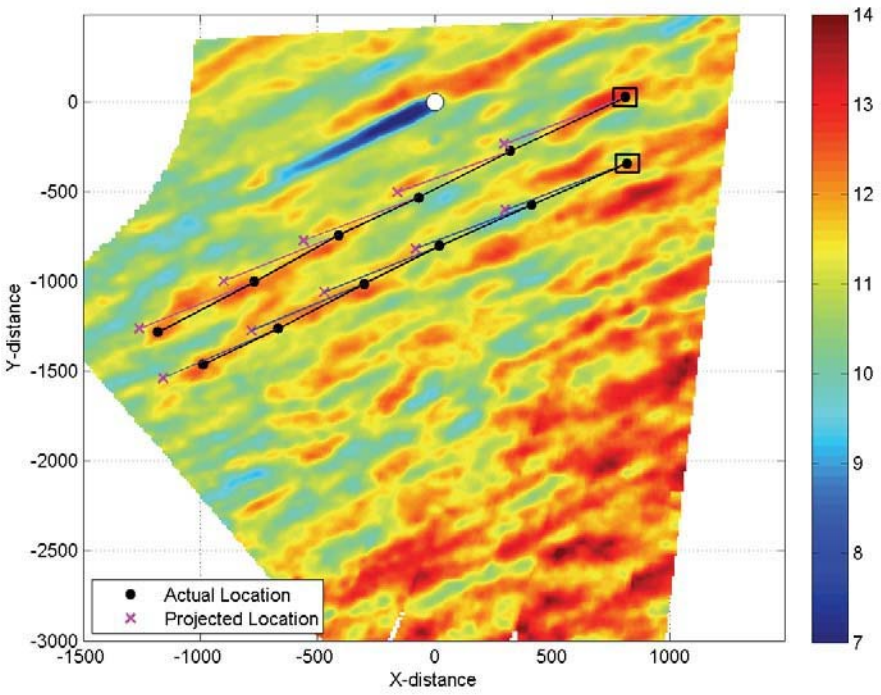

Figure 2. Dual-Doppler horizontal wind speed (m/s) synthesis at 80 m AGL for a single volume ending at 12:59:26 on 27 October 2011 demonstrating actual streak motion (circle) versus projected motion (cross) based upon the governing wind speed and direction determined using five consecutive dual-Doppler volume scans between 12:55:31 – 12:59:26 UTC.

With knowledge regarding the advection of near-surface streaks, a directional offset was applied to the upstream look-angle to obtain the best estimate of the future-forecasted wind speeds at the turbine location. To generate a future-forecasted time series, wind speeds at hub height were analyzed at distances between 1-10 D upstream of the turbine at intervals of approximately 10.5 m. Given the wind speed associated with each feature, a time offset was derived denoted as the time it would take for that feature to reach the turbine. Assuming that the wind speed magnitude of the feature did not vary with time, a forecasted wind velocity time series may be generated based upon a future time of arrival.

To verify these estimates, projected wind speeds are compared to data from the nacelle mounted 3-cup anemometer. The performance of the radar derived future-forecasted wind speeds for one sample volume scan are displayed in Figure 3. Analysis of the sample horizontal wind field map allows for the projection of wind speeds, which averaged on a 3-second time scale for the duration of 44 seconds, yields a RMSE value of 0.199 m/s. When expanding to a 10-second averaging window, the RMSE value decreases to 0.124 m/s.

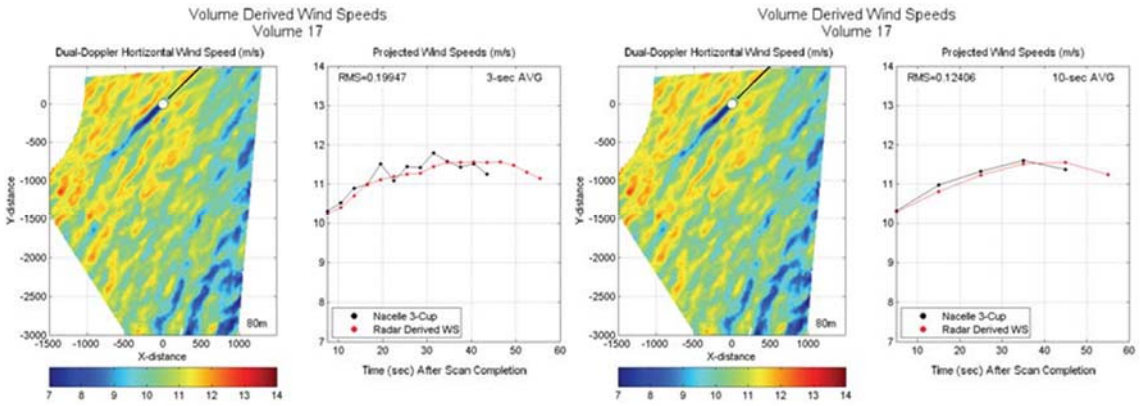

Figure 3. Comparison of nacelle mounted 3-cup anemometer (black) to future-forecasted radar derived wind speeds (red) according to 3-sec (left) and 10-sec (right) averaging times.

Preliminary results demonstrate the ability to predict future conditions at the turbine leveraging radar-derived dual-Doppler horizontal wind field maps. Unique to employing this method is the ability to accurately forecast wind speeds upwards of a minute or more in advance from the turbine. If sub-minute radar volume revisits are available, as they were in this case, another snapshot preview of the wind field can be collected and further integrated into the real-time prediction system. The coordinated deployment of multiple specialized Doppler radar systems and associated dual-Doppler synthesis techniques can provide the foundational information to construct proactively responding turbine control systems yielding a reduction in structural loads and an increase in power output. Elevating the radars to hub height could reduce the time to collect hub height information by an order of magnitude and further enhance the method.

ACKNOWELDGEMENTS:
The use of radar technology to document wind plant complex flows occurred with support from the United States Department of Energy Congressionally Directed Project: Great Plains Wind Power Test Facility (DE-FG-06-GO86092). This specific research is funded through support from the National Science Foundation: Building the Foundation for Smart Wind Farms through First-Order Controls Opportunities based on Real-Time Observations of Complex Flows (CBET-1336935).

REFERENCES:

Bossanyi, E. A., A. Kumar, and O. Hugues-Salas, 2014: Wind turbine control applications of turbine-mounted LIDAR. *J. Phys.: Conf. Ser.*, **555**, 012011.

Hirth, B. D. and J. L. Schroeder, 2013: Documenting wind speed and power deficits behind a utility-scale wind turbine. *J. Appl. Meteor. Climatol.,* **52**, 39-46.

Hirth, B. D., J. L. Schroeder, W. S. Gunter, and J. G. Guynes, 2015: Coupling Doppler radar-derived wind maps with operational turbine data to document wind farm complex flows. *Wind Energy*, **18**, 529-540.

Lorsolo, S., J. L. Schroeder, P. Dodge, and F. Marks, 2008: An observational study of hurricane boundary layer small-scale coherent structures. *Mon. Wea. Rev.*, **136**, 2871-2893.

Marathe, N. 2014: Investigation of power performances and wakes of wind turbines under yawed flow. Dissertation, Texas Tech University, 141 pp.

Mikkelsen, T., N. and Couauthors, 2013: A spinner-integrated wind lidar for enhanced wind turbine control. *Wind Energy*, **16**, 625-643.

Schlipf, D., J. Anger, S. Kapp, O. Bischoff, M. Hofsäß, A. Rettenmeier, and M. Kühn, 2011: Prospects of optimization of energy production by lidar assisted control of wind turbines. *Proc. European Wind Energy Conference and Exhibition*, EWEA, Brussels, 14-17 2011.

Träumner, K., T. Damian, C. Stawiarski, and A. Wieser, 2015: Turbulent structures and coherence in the atmospheric surface layer. *Bound.-Layer Meteor.*, **154**, 1-25.

44

Structural modelling of blades for small wind turbines

Mr. EVANS, Samuel [1]; Mr. BRADNEY, David [1]; Prof. CLAUSEN, Philip [1]

[1] The University of Newcastle, Australia

Corresponding Author: c3038433@uon.edu.au

Small wind turbines are defined as having a power output and rotor diameter less than 50 kW and 16 m respectively. Turbines of this class are typically used to provide off-grid generation and can be sited in locations which experience comparatively high wind turbulence due to obstacles such as dwellings, vegetation, and unfavourable topography. These wind regimes can be detrimental to both power output and component fatigue life. Small wind turbines have several significant design and operational differences compared to large commercial scale wind turbines. In order to maintain an ideal tip speed ratio, small wind turbines usually operate at higher rotor speeds (-200-600 rpm) compared to commercial scale wind turbines (-10-30 rpm), therefore increasing both the centrifugal loading and number of fatigue cycles experienced during a blades design life. The rotor is usually aligned passively to the inlet wind direction via the means of a tail fin. This method of yaw control can result in complex load cases acting on the blades due to both gyroscopic forces and rotor yaw error. Key differences in blade design of small wind turbines include; relatively small masses (where mass has been shown to approximate a cubic relationship to blade radius), the lack of an internal spar member, relatively high stiffness (particularly in the lead-lag direction), and the lack of a circular blade root transition region and pitch control mechanism.

When considering blade development for small wind turbines, design tools such as computational fluid dynamics (CFD), and aeroelastic modelling software packages are not frequently used due to limited budgets and time constraints. In this study we compare several different methods used to model the structural behaviour of a 5 kW Aerogenesis small wind turbine blade (2.5 m in length). These include a finite element (FE) model incorporating the layup properties of the fibreglass composite, a simple isotropic plate FE model, and a simple beam model. Aerodynamic loads will be determined via the unsteady blade element momentum method (BEM) where algorithms to account for effects such as dynamic inflow, dynamic stall, yaw error, and wind shear are included. Metrics including blade deflection, blade stress, and computation time will be compared for a range of aerodynamic load cases appropriate for small wind turbine operation (i.e. high rotor speeds, large yaw errors, etc.). The structural models will then be compared according to solution accuracy and computational time. The results of this study are expected to aid the design of small wind turbine blades in an accurate and time effective manner. Particular applications may include the prediction of lifetime fatigue loading, and blade design via iterative genetic algorithms whereby computational time is paramount.

35

The Role of Damping in Offshore Wind Turbine Dynamics

Ms. FONTANA, Casey [1]; Ms. CARSWELL, Wystan [2]; Dr. ARWADE, Sanjay [2]; Dr. DEGROOT, Don [3]

[1] University of Massachusetss Amherst

[2] University of Massachusetts Amherst

[3] University of Massachusetts

Corresponding Author: cfontana@umass.edu

To reach the goal of generating 353 of electricity from wind by 2035, the U.S. must turn to offshore wind farms. The development of offshore wind turbines (OWTs) presents new challenges for the support structure not faced in onshore wind turbine development. Although offshore winds are more consistent than onshore winds, they also produce a greater random environmental load demand. These increased offshore wind speeds result in a much greater demand on monopile support structures, as resonance generated by stochastic wind, wave, and mechanical loading causes them to fall subject to accelerated cyclic fatigue. These resonance concerns increase monopile OWT stiffness requirements, thereby increasing material costs; approximately 20-303 of the capital cost for OWTs is specifically for the support structure.

As a result, it is important to determine the contribution each damping source (aerodynamic damping, hydrodynamic damping, structural damping, soil damping, and sometimes tuned mass dampers) on these types of loading. The least is known about soil damping, which is more aptly referred to as foundation damping (as it is inherently a function of hysteretic soil-foundation interaction). Even though literature suggests that foundation damping can contribute up to 1.53 critical damping to structural response, current design guidelines do not provide a method for estimating it and it is often conservatively neglected in structural design.

The purpose of this parameter study was to determine how foundation damping affects structural demands over a variety of wind, wave, and operating conditions. OWT behavior was analyzed using the National Renewable Energy Laboratory's (NREL) open-source wind turbine simulation software (FAST), which can model both stochastic environmental loading and mechanical load effects from turbine operation. The NREL 5MW turbine was used for the OWT model due to its prevalence in this field of research, and the effect of foundation damping was broadly modeled through structural damping of the OWT tower for damping ratios ranging from 03 to 53. Turbulent wind speeds of 3 m/s (cut-in), 11.4 m/s (rated), and 25 m/s (cut-out) were used for the operating cases, and wind speeds greater than 25 m/s were used for the parked and feathered cases. Examining the sensitivity of structural loading to damping may allow foundation damping to be advantageously incorporated into design guidelines, potentially leading to a more efficient OWT design and reduction in the large cost of the support structure.

Given that fatigue analysis is important for ensuring the design life of OWTs, the effective contribution of damping on fatigue damage accumulation was also estimated. Fatigue life of the OWT was analyzed using another open source NREL software called MLife, a Matlab-based program that calculates fatigue life and statistics for one or more time series. With this software, a similar parameter study was performed to evaluate the effect of foundation damping on short-term damage-equivalent loads (DELs), damage rates based on single time-series, and lifetime DEL results that are based on the entire set of time-series data. This influence of foundation damping on the accumulated lifetime damage and the time until failure will allow for a better estimation of OWT design life.

34

Modeling dynamic stall for a free vortex wake model of a floating offshore wind turbine

Mr. GAERTNER, Evan [1]

[1] University of Massachusetts, Amherst

Corresponding Author: evan.gaertner@gmail.com

Floating offshore wind turbines in deep waters offer significant advantages to onshore and near-shore wind turbines. However, due to the motion of floating platforms in response to wind and wave loading, the aerodynamics are substantially more complex. Traditional aerodynamic models and design codes do not adequately account for the floating platform dynamics. Turbines must therefore be over designed due to loading uncertainty and are not fully optimized for their operating conditions. Previous research at the University of Massachusetts, Amherst developed the Wake Induced Dynamics Simulator, or WInDS, a free vortex wake model of wind turbines that explicitly includes the velocity components from platform motion. WInDS rigorously accounts for the unsteady interactions between the wind turbine rotor and its wake, however, as a potential flow model, the unsteady viscous response in the blade boundary layer is neglected. This work addressed this concern through the integration of a Leishman-Beddoes dynamic stall model into WInDS. The stand-alone dynamic stall model was validated against two-dimensional unsteady data from the OSU pitch oscillation experiments and the coupled WInDS model was validated against three-dimensional data from NREL's UAE Phase VI campaign. WInDS with dynamic stall shows substantial improvements in load predictions for both steady and unsteady conditions. WInDS with the dynamic stall model should provide the necessary aerodynamic model fidelity for future research and design work on floating offshore wind turbines.

Model development and validation will be presented, along with several thrusts of ongoing work. The addition of the dynamic stall model allows more insight into the prevalence and severity of dynamic stall in response to unsteady floating platform motion. Full characterization of these transient loads is an important consideration due to the high reliability necessitated by the offshore environment. Collaborative work is also ongoing to couple WInDS with NREL's computer-aided engineering tool FAST, fully coupled with FAST's existing submodules for controls, hydrodynamic, and structural dynamics. Finally, preliminary work on the use of the coupled FAST and WInDS models for design optimization will be presented. The goal of this research is to further optimize the turbine rotor to specifically account for the unsteady aerodynamic loading brought on by floating platform motion.

30

The Impact of Offshore Wind Turbines on Underwater Ambient Noise Levels

GLEGG, Stewart [1]

[1] Florida Atlantic University

Corresponding Author: sglegg@fau.edu

The underwater sound levels generated by offshore wind turbine farms is a concern because of the possible environmental impact on marine mammals. This paper will consider how sound generated by a wind turbine is transmitted into a shallow water channel. It is shown that the underwater sound levels can be calculated for a typical offshore wind turbine by using the theory of Chapman and Ward (1990) combined with aeroacoustic models of trailing edge noise on the wind turbine blades. A procedure is given for estimating the underwater sound levels from a wind turbine whose airborne noise levels are known. The results indicate that the sound levels are strongly modulated at the blade passing frequency, which leads to infrasound that is more easily detected than a continuous sound source of the same level.

10

Optimizing building geometry to increase the energy yield in built environments.

Ms. GRAYSON, Malika [1]

[1] Cornell University

Corresponding Author: graysonmalika@gmail.com

A crucial element in the use of wind as a source of energy in the built environment, is finding ways to maximize its flow. As flow approaches the windward fa<ade of a building's structure, it accelerates causing an increase in velocity both at the roof's edge and above the separation bubble. Devices such as small scale wind turbines are usually placed in this flow region for energy harvesting purposes. The present research aims to further investigate the accelerated flow by modifying the building's structure to be a concentrator of the wind, maximizing the available wind energy. Using Computational Fluid Dynamics (CFD), preliminary investigations explored sloped facades at four arbitrary angles. Simulations show that at an angle of 30 degrees, there is a velocity amplification of more than 1003 at the separation point directly above the roof (Figure 1). In addition, there is little to no reversed flow in the decreased separation bubble minimizing turbulence intensity. Conducted wind tunnel experiments simulating flow behavior over the models support the findings presented and show that with a simple fa<ade change, the flow characteristics are greatly affected.

Using the 30-degree slope as a guide angle, elliptical facades were also investigated. Two-dimensional CFD optimizations were used to find angles that gave the highest power density directly above the rooftop. Results show that at higher angles, when the elliptical fa<ade is steeper, there is further velocity amplification. The optimized elliptical fa<ade will provide a base for a three dimensional structure where both optimization tests and eventual wind tunnel testing will be done to support the findings.

75

Assessing the Structural Impact of Low Level]ets over Wind Turbines

Dr. BASU, Sukanta [1]; Dr. RUIZ-COLUMBIE, Arquimedes [2]; Dr. TUTKUN, Murat [3]; Dr. CASTILLO, Luciano [4]; GUTIERREZ, Walter [5]; Dr. ARAYA, Guillermo [5]; KILIYANPILAKKIL, Praju [6]

[1] 3Department of Marine, Earth, and Atmospheric Sciences; North Carolina State University

[2] National Wind Institute, Texas Tech University

[3] Institute for Energy Technology (IFE), Kjeller, Norway

[4] department of Mechanical Engineering, Texas Tech University

[5] Department of Mechanical Engineering, Texas Tech University

[6] of Marine, Earth, and Atmospheric Sciences; North Carolina State University

Corresponding Author: walter.gutierrez@ttu.edu

Low Level Jets (LLJs) are defined as regions of relatively strong winds in the lower part of the atmosphere. They are a common feature over the Great Plains in the United States. It has been reported that 75 3 of LLJs in the Great Plains occur at night and with seasonal patterns, affecting significantly the wind energy production. Present results have corroborated some of the LLJ's known characteristics. LLJs develop due to the formation of stable stratification in the lower atmosphere. This paper is focused on the determination of the static/dynamic impact that real LLJs produced in West Texas have over wind turbines. High-frequency (50Hz) observational data from the 200-m tower data (Reese, Texas) have been input as inflow conditions into the NREL FAST code in order to evaluate the structural impacts of LLJ's on a typical wind turbine. Due to the higher levels of wind speed, the potential for power increase proportional to the cube of the velocity. It has been observed that during an LLJ event the level of turbulence intensities and TKE are significantly much lower than those during unstable conditions; as a result, cyclical aerodynamic loads on turbine blades are different. Low-frequency oscillations prevail in stable conditions with formation of LLJ, as opposed to high-frequency oscillations more prevalent in unstable conditions. The turbulent kinetic energy is lower in LLJ but the energy concentrates in particular frequencies that can stress the turbine. From the point of view of the wind turbine loads/stresses, we have detected frequencies that can be correlated with those from the incoming wind.

25

Engineering model of unsteady aerodynamics of Horizontal axis wind turbines

Mr. HAMMAM, Mohamed [1]

[1] PhD candidates, Department of Mechanical and Manufacturing Engineering, University of Calgary, Canada.

Corresponding Author: mmahamma@ucalgary.ca

Small wind turbines use MPPT (Maximum power point Tracking) algorithm that depends on the performance relation developed using a steady BEM [Blade Element Momentum] code. However, small wind turbines work under harsh unsteady environment that is subjected to large fluctuation in wind and rotor speeds.This will lead to unsteady power generated that differ significantly from the one predicted using steady codes. In this work,a semi-empirical model is developed that correlates an unsteady physical variable,like the unsteady stream line length, to a measurable variable in unsteady operation, like tip speed ratio.This model use the unsteady Euler equation supplied with a measured data of power coefficient and wind speed of a 5 kW wind turbine.The analysis shows that the stream line length shows some correlation with tip speed ratio. Further data analysis is currently underway to investigate this correlation and further results will be reported in the final presentation.

76

NCAR's Recent Advances in Wind Power Forecasting

Dr. HAUPT, Sue [1]

[1] National Center for Atmospheric Research

Corresponding Author: devenport@vt.edu

The National Center for Atmospheric Research (NCAR) has been developing and enhancing a Wind Power Forecasting System in partnership with Xcel Energy that integrates high resolution and publically available modeling capabilities with artificial intelligence methods. This forecasting system has recently been updated to include specific technologies for uncertainty quantification, short-term detection of wind power ramps by blending the Variational Doppler Radar Analysis System with an Expert System, enhanced wind-to-power conversion techniques, and prediction of icing and snow conditions.

The system ingests external, publically available weather model data and observations. In order to provide information specific to Xcel Energy's region, high resolution numerical weather prediction (NWP) simulations assimilate specific local weather observations. The weather observations range from routine meteorological surface and upper air data to data from the wind farms, including wind speed data from the Nacelles. Finally, to optimize estimates of short-term changes in wind power requires nowcasting technologies such as the Variational Doppler Radar Analysis System (VDRAS) that is blended with an observation-based Expert System.

The strength of the wind power forecasting system lies in blending the various components to produce a power forecast that can be used by Xcel Energy grid operators and energy traders. That blending is accomplished with the Dynamical Integrated Forecast (DICast) System. The wind speeds predicted by DICast must then be translated into power using NCAR's empirical power conversion algorithms. A quantile approach is used to quality control the observations. The uncertainty of these predictions can then be quantified using an Analog Ensemble (AnEn) approach. Finally, warnings of potential icing and heavy snow are provided.

11

Combining economic and fluid dynamic models to determine the optimal spacing in very large wind-farms

Richard J. A. M. Stevens[1,2], Benjamin F. Hobbs[3,*], Andrés Ramos[4] and Charles Meneveau[1]

[1]Department of Mechanical Engineering & Center for Environmental and Applied Fluid Mechanics, Johns Hopkins University, Baltimore, Maryland 21218, USA

[2]Department of Physics, Mesa+ Institute, and J. M. Burgers Centre for Fluid Dynamics, University of Twente, 7500 AE Enschede, The Netherlands

[3]Department of Geography & Environmental Engineering and E[2]SHI, Johns Hopkins University, Baltimore, Maryland 21218, USA

[4] Institute for Research in Technology (IIT), ICAI School of Engineering, Comillas Pontifical University, C/Sta. Cruz de Marcenado 26, 28015 Madrid, Spain

* Presenter

Now that wind-farms are becoming increasingly larger, the economics and physics of wind farms become intrinsically coupled and important when designing large wind farms. It is important to develop wind farm models in which economic considerations can be combined with physical considerations in a transparent and intuitive way. For smaller wind-farms the majority of the turbines can be placed such that physical wake effects are relatively limited and thus physical effects may be less important. However, for large wind farms (e.g. with hundreds or thousands of turbines) it is important to consider the influence of wake effects on the optimal turbine spacing. For the design of wind-farms the industry uses site-specific, detailed optimization calculations for wind-turbine placement based on wake models (1; 2; 3; 4; 5; 6). Such calculations aim to place the turbines such that wake effects are limited with respect to the prevailing incoming wind-directions at the site under consideration. There are also academic studies that use wake models to optimize turbine placement using Monte Carlo simulations (7), genetic algorithms (8), or evolutionary algorithms (9; 10). In this work we will combine economic and fluid dynamic models to determine the main parameters that are important for the design of very large wind-farms.

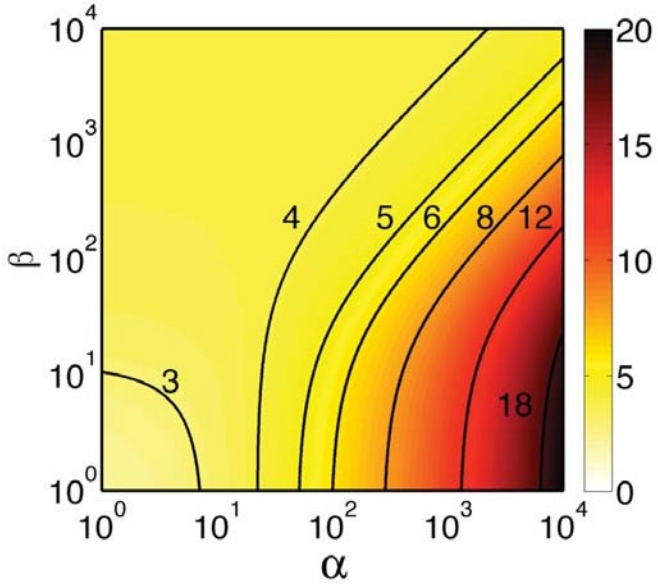

Figure 1: Optimal spacing as function of dimensionless turbine cost (a) and dimensionless cable cost (β), see equation (2). The optimal spacing increases with increasing a or decreasing β.

It is known that wake models do not capture the effect of the interaction between the atmosphere and very large wind-farms correctly (11). These effects are described by "top-down" single-column type models which are based on momentum analysis and horizontal averaging. These models give a vertical profile of the average velocity profile by assuming the existence of two logarithmic regions, one above the turbine hub-height and the other below (12; 13; 14; 15; 16; 17; 18; 19). The mean velocity at hub-height is used to predict the wind-farm performance as

function of the main design parameters. Meyers & Meneveau (20) showed, by accounting for the turbine and land costs, that the optimal spacing in the limit of very large wind-farms can be found analytically using "top-down" models. For typical land costs (e.g. Texas) they found an optimal spacing of 12 – 15 turbine diameters, which is

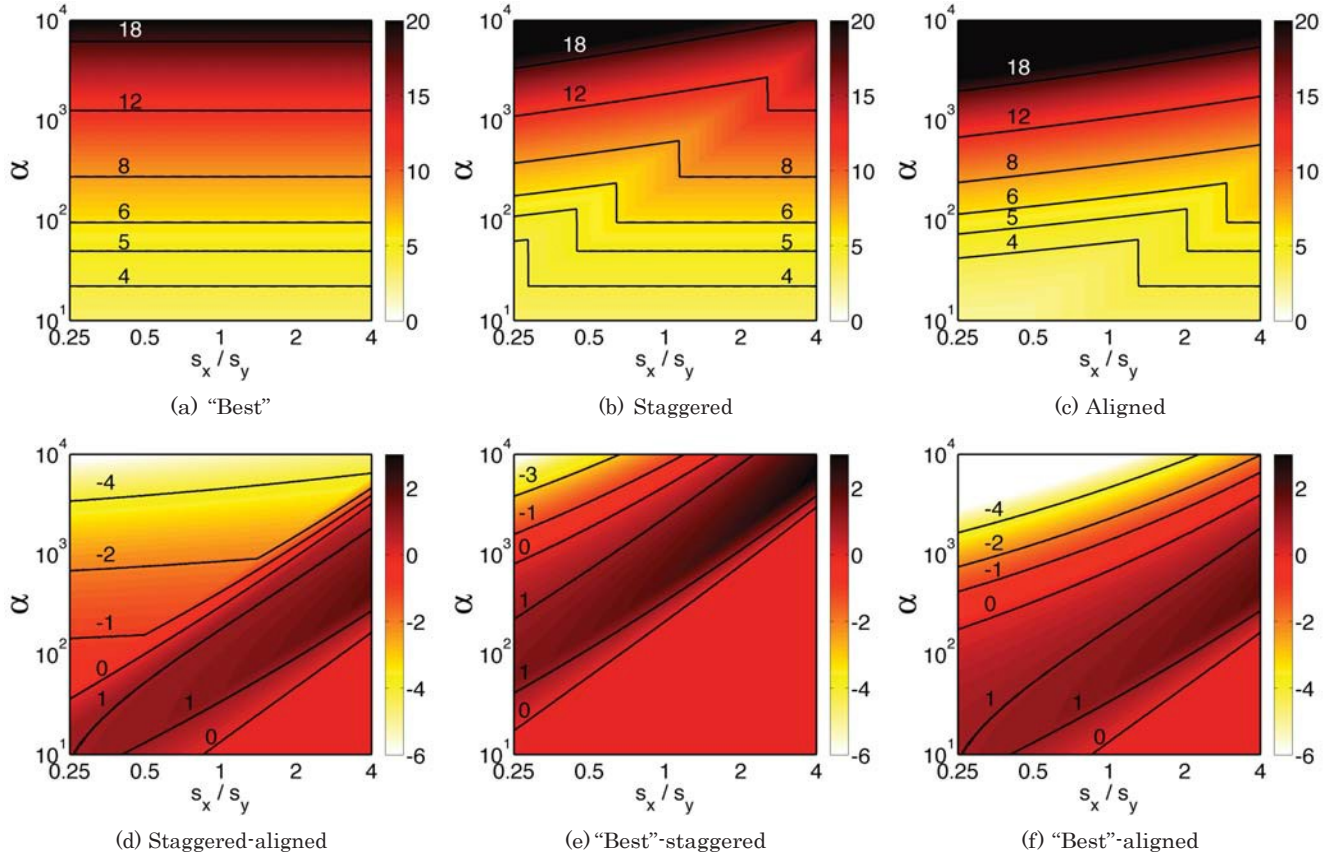

Figure 2: Optimal turbine spacing based on the normalized power per unit cost for different wind-farm layouts as function of the ratio s_x/s_y and a, for $\beta = 0$. (a) "best" layout in which the power production is limited by the vertical kinetic energy flux that can be obtained for a given turbine density, and a (b) staggered and an (c) aligned layout in which the area is not necessarily used optimally. Panels (d-f) give the differences between the results shown in panels (a-c) in different ways. Positive values indicate that turbines in an aligned (or staggered) wind-farm should be placed closer together than using the "best" (or staggered) configuration.

significantly larger than the value found in actual wind-farms (6 – 10 turbine diameters). However, their approach did not take into account cable costs, specific turbine placements, profit considerations and maintenance costs. In this paper, we generalize the framework to include these considerations.

Here we expand the method used by Meyers and Meneveau (20) to determine the optimal turbine spacing in a very large wind-farm. The influence of several additional aspects, such as cable costs, maintenance costs, the wind-farm layout, and the effect of optimizing net revenue instead of normalized power per unit cost, are addressed. This abstract summarizes a selection of these results, addressing the effect of cable costs and wind-farm layout. Here we consider the difference between several wind-farm layouts. For very large wind-farms the turbine power production for a given turbine density is limited by the vertical kinetic energy flux that can be obtained on that land area when the distance between turbines placed directly in each others wakes is maximized (11). This limit we call the "best" layout, which we will compare with the aligned and staggered layouts.

Following Meyers and Meneveau (20) a simple cost function that includes the turbine, land, and cable cost, is formulated as follows:

$$\text{Cost} = \text{Cost}_{\text{turb}} + (sD)\text{Cost}_{\text{cable}} + (sD)^2\text{Cost}_{\text{land}}. \tag{1}$$

The objective is to minimize the levelized cost per unit output (\$/MWh) or to maximize its reciprocal (power per unit cost). Here a and β are two non-dimensional parameters, representing turbine and cable costs, compared to land costs, respectively. They are defined as:

$$a = \frac{\text{Cost}_{\text{turb}}/(\frac{1}{4}\pi D^2)}{\text{Cost}_{\text{land}}}, \qquad \beta = \frac{\text{Cost}_{\text{cable}}/D}{\text{Cost}_{\text{land}}}. \tag{2}$$

These dimensionless cost ratios are used to define the normalized power per unit cost as

$$P^* = \frac{P_\infty(s_x, s_y, \text{layout}, \ldots)}{s} \frac{\text{Cost}_{\text{land}}}{\text{Cost}_{\text{turb}}/(\text{sD})^2 + \text{Cost}_{\text{cable}}/(\text{sD}) + \text{Cost}_{\text{land}}} = \frac{P_\infty(s_x, s_y, \text{layout}, \ldots)}{s} \frac{4s^2/\pi}{a + 4\beta s/\pi + 4s^2/\pi}, \quad (3)$$

where $P_\infty(s_x, s_y, \text{layout}, \ldots)$ indicates the normalized predicted power output for the turbines in the wind-farm. The coupled wake boundary layer (CWBL) model is used to evaluate the wind-farm performance as a function of the spacing between the turbines in the streamwise s_x and spanwise s_y direction, the wind-farm layout, the size of the wind-farm (19), etc.. It has been shown that the CWBL model agrees well with results from large eddy simulations (LES) and field measurements in Horns Rev and Nysted (11; 21).

In agreement with the results of Meyers and Meneveau (20), figure 1 shows that without cable costs ($\beta = 0$) the optimal turbine spacing strongly depends on the turbine to land cost ratio a. However, when cable costs are included the obtained optimal spacing can be significantly smaller.

To assess the influence of the wind-farm layout we evaluated the optimal spacing for aligned, staggered, and "best" layout in figure 2 as function of a and the ratio between the streamwise and spanwise turbine spacing s_x/s_y. The differences in the optimal spacing for the staggered, aligned and "best" layout are shown in panel (d-f) and are an effect of the stronger wake effects for the aligned or staggered configuration compared to the "best" layout. Note that for sufficiently large enough streamwise spacing (large enough s_x/s_y) the optimal spacing for the aligned and staggered configuration becomes equal to the "best" layout. Here it is important to note that the figure shows the optimal spacing and not the profitability, which together with effects of maintenance costs has also been considered in our work. In addition we note that determining the profitability per turbine gives us insight in the required (nondimensionalized) revenue that is necessary to operate a wind-farm for a given a and β while the profitability can also be maximized per land area, which results in different optimal spacings.

In short, we have extended the work of Meyers and Meneveau (20) on the determination of the optimal spacing in very large wind-farms using analytical models. We now included the effect of the cable cost, the maintenance costs, the wind-farm layout, and the influence of maximizing the profitability instead of the normalized power per unit cost, in the analysis. However, it is emphasized that for the design of an actual wind-farm local effects and restrictions should always been taken into account. An analytical analysis as shown here is useful to provide insight in the main trends and to develop intuition of the factors that are important for the actual design of wind-farms.

References

[1] P. B. S. Lissaman, *Energy Effectiveness of Arbitrary Arrays of Wind Turbines*, J. of Energy **3**, 323 (1979).

[2] N. O. Jensen, *A note on wind generator interaction*, Risø-M-2411, Risø National Laboratory, Roskilde (1983).

[3] I. Katić, J. Højstrup, and N. O. Jensen, *A simple model for cluster efficiency*, European Wind Energy Association Conference and Exhibition, 7-9 October 1986, Rome, Italy 407 (1986).

[4] J. Choi and M. Shan, *Advancement of Jensen (PARK) wake model*, EWEA Conference, Vienna, February 2013 (2013).

[5] A. Peña and O. Rathmann, *Atmospheric stability-dependent infinite wind-farm models and the wake-decay coefficient*, Wind Energy (2013).

[6] M. Bastankhah and F. Porté-Agel, *A new analytical model for wind-turbine wakes*, Renewable Energy **70**, 116 (2014).

[7] G. Marmidis, S. Lazarou, and E. Pyrgioti, *Optimal placement of wind turbines in a wind park using Monte Carlo simulation*, Renewable Energy **33**, 1455 (2008).

[8] A. Emami and P. Noghreh, *New approach on optimization in placement of wind turbines within wind farm by genetic algorithms*, Renewable Energy **35**, 1559 (2010).

[9] A. Kusiak and Z. Song, *Design of wind farm layout for maximum wind energy capture*, Renewable Energy **35**, 685 (2010).

[10] B. Saavedra-Moreno, S. Salcedo-Sanz, A. Paniagua-Tineo, L. Prieto, and A. Portilla-Figueras, *Seeding evolutionary algorithms with heuristics for optimal wind turbines positioning in wind farms*, Renewable Energy **36**, 2838 (2011).

[11] R. J. A. M. Stevens, D. F. Gayme, and C. Meneveau, *Coupled wake boundary layer model of wind-farms*, Submitted to J. Renewable and Sustainable Energy (2014).

[12] B. G. Newman, *The spacing of wind turbines in large arrays*, Energy conversion **16**, 169 (1977).

[13] N. O. Jensen, *Change of surface roughness and the planetary boundary layer*, Quart. J. R. Met. Soc. **104**, 351 (1978).

[14] S. Frandsen, *On the wind speed reduction in the center of large clusters of wind turbines*, J. Wind Eng. and Ind. Aerodyn. **39**, 251 (1992).
[15] S. Emeis and S. Frandsen, *Reduction of horizontal wind speed in a boundary layer with obstacles*, Bound-Lay. Meteorol. **64**, 297 (1993).
[16] S. Frandsen, R. Barthelmie, S. Pryor, O. Rathmann, S. Larsen, J. Højstrup, and M. Thøgersen, *Analytical modelling of wind speed deficit in large offshore wind farms*, Wind Energy **9**, 39 (2006).
[17] M. Calaf, C. Meneveau, and J. Meyers, *Large eddy simulations of fully developed wind-turbine array boundary layers*, Phys. Fluids **22**, 015110 (2010).
[18] C. Meneveau, *The top-down model of wind farm boundary layers and its applications*, J. of Turbulence **13**, 1 (2012).
[19] R. J. A. M. Stevens, *Dependence of optimal wind-turbine spacing on wind-farm length*, Submitted to Wind Energy (2014).
[20] J. Meyers and C. Meneveau, *Optimal turbine spacing in fully developed wind farm boundary layers*, Wind Energy **15**, 305 (2012).
[21] R. J. A. M. Stevens, D. F. Gayme, and C. Meneveau, *Generalized coupled wake boundary layer model: applications and comparisons with field and LES data for two real wind farms*, Submitted to Wind Energy (2015).

14

An Experimental Investigation on the Surface Water Transport and Ice Accreting Processes Pertinent to Wind Turbine Icing Phenomena

Prof. HU, Hui [1]

[1] Department of Aerospace Engineering, Iowa State University

Corresponding Author: huhui@iastate.edu

Wind turbine icing represents the most significant threat to the integrity of wind turbines in cold weather. Ice accretion on turbine blades would decrease power production of the wind turbines significantly. Ice accretion and irregular shedding during wind turbine operation would lead to load imbalances as well as excessive turbine vibration, often causing the wind turbine to shut off. Icing issues can also directly impact personnel safety due to falling and projected large ice chunks. It should be noted that the icing hazard is often most severe in the locations which are best suited for wind turbine sites, such as northern latitudes, off-shore wind farms and high altitudes (i.e. mountains). Wind turbines in these regions are more prone to water contamination and icing in cold weather. Advancing the technology for safe and efficient wind turbine operation in atmospheric icing conditions requires the development of innovative, effective anti-/de-icing strategies tailored for wind turbine icing mitigation and protection. Doing so requires a keen understanding of the underlying physics of complicated thermal flow phenomena pertinent to wind turbine icing phenomena, both for the icing itself as well as for the water runback along contaminated surfaces of wind turbine blades.
In the present study, a series of experimental investigations were conducted to characterize the transient behavior of wind-driven water film/rivulet flows over a NACA 0012 airfoil model and the dynamic ice accreting process over the airfoil model in order to elucidate the underlying physics of the important microphysical processes pertinent to wind turbine icing phenomena. The experimental study was conducted in an icing research tunnel available at Aerospace Engineering Department of Iowa State University. A suite of advanced flow diagnostic techniques, such as molecular tagging velocimetry and thermometry (MTV), digital image projection (DIP), and infrared (IR) imaging thermometry techniques, were developed and applied to achieve quantitative measurements of the film thickness distributions of the surface water film/rivulet flows and the temperature distributions of the water/ice mixture flows over the airfoil model surface at different test conditions. The new findings derived from the present icing physics study would lead to a better understanding of the important micro-physical processes, which could be used to improve current icing accretion models for more accurate prediction of ice formation and ice accretion on wind turbine blades as well as development of effective anti-/de-icing strategies tailored for safer and more efficient operation of wind turbines in cold weather.

62

CFD Analysis of NACA4415 Airfoil with $\gamma-Re_\theta$ Model considering Natural Transition

Dr. ISLAM, Mazhural [1]

[1] UofC

Corresponding Author: dhwood@ucalgary.ca

Airfoil analysis is essential to wind turbine aerodynamics. In typical operating conditions, airfoils undergo transition from laminar to turbulent flow in the boundary layer in a manner that must be modeled accurately to predict airfoil lift and drag. There are different modes of transition (e.g. natural, by-pass, wake induced, reversed, separated flow) and modeling them is not straight-forward. Over the years, diversified predictions have been developed for the various modes. One of the popular transition models is the local correlation-based $\gamma-Re_\theta$ model of Menter et al. \citep{Menter2004}. The model requires data correlations for the transition length and the critical Reynolds numbers.

54

Aerodynamic Effects of Surface Condition on Wind Turbine Blade Sections

Ms. JOSEPH, Liselle [1]; Prof. DEVENPORT, William [2]; Dr. BORGOLTZ, Aurelien [3]; Mr. FENOUIL, Julien [3]

[1] Center for Renewable Energy and Aerodynamic Testing (CREATe), Virginia Tech

[2] Virginia Tech

[3] CREATe, Virginia Tech

Corresponding Author: liselle@vt.edu

This paper briefly examines the aerodynamic effects of typical wind turbine blade roughness by investigating an appropriate scaling criteria which best relates the roughness configuration to the resulting changes in aerodynamic forces and transition. The wind tunnel test results of two wind turbine blade sections tested with three different roughness samples are presented. The two models, consisting of a 457mm-chord and 800mm-chord airfoils using the DU96-W-180 profile, were tested in the Virginia Tech Stability Wind Tunnel at free-stream Reynolds number based on the chord between 1.5 and 3M. Preliminary analysis of the lift and drag scaling are presented as well as a sample of the transition results.

55

Transition Detection for Low Speed Wind Tunnel Testing using Infrared Thermography

Ms. JOSEPH, Liselle [1]; Dr. BORGOLTZ, Aurelien [2]; Mr. FENOUIL, Julien [2]; Prof. DEVENPORT, William [3]

[1] Center for Renewable Energy and Aerodynamic Testing (CREATe), Virginia Tech

[2] CREATe, Virginia Tech

[3] Virginia Tech

Corresponding Author: liselle@vt.edu

The present study records the process undertaken to develop, implement and validate a transition detection system for continual use in the Virginia Tech Stability Wind Tunnel. The final system developed consisted of two high resolution FLIR A655sc infrared cameras; four 63.5-mm diameter circular windows; aluminum models covered in 0.8-mm silicone rubber insulation and a top layer of ConTact© paper; and a series of 25.4-mm wide rubber silicone fiberglass insulated heaters mounted inside the model and controlled externally by experimenters. Transition results produced by the system were compared to measurements obtained from surface pressure data and stethoscope tests as well as the numerical predictions of XFOIL. The transition results from these four methods were in agreement for two wind turbine models, for at least two Reynolds numbers (between Re=1.5x106 and 3x106) and for several angles of attack on both the suction and the pressure side of the models. The agreement of data suggests that the infrared thermography system is able to detect transition for large aluminum models at low speeds. It is also able to detect transition within 1-s and to identify three dimensional behavior in the flow. In addition, the system was found to be a useful boundary layer flow diagnostic tool for wind tunnel testing.

64

Academic Qualification in Onshore and Offshore Wind Energy within the Framework of the European Academy of Wind Energy and the European Wind Energy Master Program - Examples and Experiences in Germany and Europe

Mr. KAERN, Moses [1]

[1] ForWind - Center for Wind Energy Research

Corresponding Author: moses.kaern@forwind.de

Many different approaches for academic qualification in wind energy have been developing in Europe. The European Academy of Wind Energy (EAWE) provides a framework for the exchange of ideas, scientists, and the development of strategies. The efforts to join forces in university education started more than ten years ago and resulted in the establishment of the European Wind Energy Master.

EAWE started already in 2004 as a network of universities engaged in wind energy research and PhD education. Today, EAWE's 39 members -- universities and research institutions -- formulate and execute joint R projects and coordinate high quality scientific research and education in wind energy. One of the core activities has always been the exchange of scientists, PhD and graduate students, as well as the annual EAWE PhD seminar. EAWE is now responsible for the Scientific Track of European Wind Energy association's Annual Events and organizes the much appreciated biannual conference series "The Science of Making Torque from Wind". Four EAWE members have joined forces to push international education through a joint master program, the European Wind Energy Master (EWEM). The program was established in 2012 by four universities who have long been active in Wind Energy and Offshore Wind Energy research and education: Delft University of Technology, Technical University of Denmark, Carl von Ossietzky University Oldenburg, Norwegian University of Science and Technology. The master program is supported by the European Union through its Erasmus Mundus excellence program. The European Wind Energy Master is an advanced 2 year program dedicated to specialized research within four areas: Wind Physics, Rotor Design, Electric Power Systems, and Offshore Engineering. Students have to choose one of those four tracks and follow that dedicated curriculum. EWEM graduates receive a double degree by the two (of the four) universities who are responsible for the scientific track. Already three cohorts of students have been taken in, and the number of students is stable. EWEM is supported by a network of 43 associated partners from all over the world: research institutions, universities, and companies.

Putting together a joint master program like EWEM would not have been possible without each partner's longstanding experience in research and education. In fact, EWEM strongly depends on the existence of local programs and degrees being able to contribute to such an extensive wind energy program. While the development at the four partner universities has been different because of the different national university policies, wind energy market developments, and research funding schemes, some general issues can be highlighted when looking at the case of the University of Oldenburg. Already in the early 1980'ies University of Oldenburg started research on renewable energies at the Physics Department. The researchers at the Energy Lab were ahead of their time at the forefront of sustainable energy technology research: they studied different renewable energy sources and their integration into one system. First, university education has only been done as specialization within a classical degree, i.e. Physics, but it was extended through the establishment of one of the first master programs for renewables: the Postgraduate Program for Renewable Energy (PPRE) which now, after 27 years of operation, is supported by a network of 400 alumni in over 80 countries. Apart from that, research and education in wind energy has developed further into a highly specialized field at the University of Oldenburg within the Institute of Physics focussing on the physical aspects of wind as a resource for energy conversion -- and branding this field as "Wind Physics". The institutionalization of wind energy research has eventually been brought forward a major step in the year 2004 when ForWind, the Center for Wind Energy Research, has been founded. Today, ForWind and its three partners, the Universities of Oldenburg, Hannover, and Bremen, have gained national and international reputation, making them an interesting partner for a Strategic Research Alliance with the German Aerospace Center (DLR) and the Fraunhofer Institute for Wind Energy and Energy System Technology (IWES) in 2012. So, becoming part of the EWEM consortium in 2012 is an outcome of successful research, networking, and institutional growth over more than two decades -- and that is true also for the three other partners.

In 2006 ForWind has stretched its educational activities to continuing study programs and part-time education

for professionals in wind and offshore wind. The Continuing Studies Program Wind Energy Technology is one year part-time study program covering all aspects related to the planning, development, and operation of onshore wind farms. It addresses professionals from all disciplines -- technical, commercial, legal -- and provides them with a systematic understanding of wind farm projects. Participants should hold a master degree and have at least three years of professional experience. Much emphasis is based on the exchange among the participants of the courses and the exchange of their expertise. Lecturers of the course are known experts in the field, and they come from companies and universities. The graduates gain important competencies to succeed in the highly interdisciplinary wind industry and business. There is a variant to this course devoted explicitly to offshore wind, the Continuing Studies Program Offshore Wind Energy. Due to the nature of offshore wind farm projects the offshore course is taught in English, and the program has just recently established co-operations with a leading UK institution and a company in Denmark. In the last 9 years more than 220 professionals have graduated and form a vital alumni network with regular meetings at trade fairs and other business events.

48

Stepwise Inertial Control Scheme of a Doubly-Fed Induction Generator to Prevent a Second Frequency Dip

Mr. KIM, Keonhui [1]; Mr. KANG, Moses [1]; Dr. MULJADI, Eduard [2]; Prof. KANG, Yong Cheol [3]

[1] Chonbuk National University, Korea

[2] National Renewable Energy Laboratory, US

[3] WeGAT Research Center, and Smart Grid Research Center, Chonbuk National University, Korea

Corresponding Author: keonhuikim@jbnu.ac.kr

If a large disturbance occurs in a power system, to arrest a frequency drop, the conventional stepwise inertial control (SIC) schemes switch the power reference signal of a wind generator (WG) to a stepwise function that is defined in the time domain. In the stepwise reference function, the output of a WG is increased in a stepwise manner and maintained for a predetermined time period; then the output should be reduced fast so that the rotor speed is restored. This fast reduction in the output will inevitably cause a subsequent frequency dip. In addition, since the factors such as overproduction time, underproduction time, extra power and reduced power in the schemes are reciprocally interdependent, special attention is required to choose them to avoid a second frequency dip. However, difficulties will arise in choosing them systematically under all operating wind conditions. Thus, they were chosen heuristically.

This paper proposes a SIC scheme of a doubly-fed induction generator (DFIG) that can increase the frequency nadir while preventing a second frequency dip. Fig. 1 depicts the operational features and test results of the proposed inertial control scheme. The proposed scheme uses a reference function defined in the rotor speed domain, not in the time domain, by connecting the maximum torque limit at the rotor speed prior to a disturbance and the mechanical power at the minimum rotor speed limit (see Fig. 1(b)).

The reference function defined in the above manner shows a gradually decreasing pattern in the time domain as shown in Fig. 1(d). At the initial period of the disturbance, the output power increases to the power determined by the maximum torque limit, and then gradually decreases to the mechanical input power at the minimum rotor speed limit, where the electrical output power matches the mechanical input power. Thus, the rotor speed remains at the minimum limit without decreasing below the minimum operating speed.

The performance of the conventional and proposed SIC schemes was investigated and compared for a 100 MW wind power plant at the wind speed of 9 m/s using an EMTP-RV simulator. The solid, dashed, dash-dotted, and dotted lines are the results for the proposed scheme, conventional 1 SIC [1], conventional 2 SIC [2], and 'w/o inertial control', respectively. As shown in Fig. 1(c), the frequency nadir for the proposed scheme is the largest because the output power of a proposed scheme significantly increases; in addition, this scheme does not cause a second frequency dip. The results show that the proposed scheme significantly increases the frequency nadir without causing a second frequency dip. The full paper will include the test results under various wind conditions.

72

Adjoint Optimization of Wind Turbine Locations for Systems Engineering

Mr. KING, Ryan [1]; Prof. HAMLINGTON, Peter [1]; Ms. DYKES, Katherine [2]; Dr. GRAF, Peter [2]

[1] University of Colorado at Boulder

[2] NREL

Corresponding Author: ryan.nicholas.king@gmail.com

We present work on the development of a high fidelity flow solver for use in sys- tems engineering optimization of wind farm layouts. High fidelity flow models capture atmospheric boundary layer turbulence and turbine wake effects more accurately than existing linear models, and thereby more accurately reflect the power production and turbulence-induced loads within a wind farm. We formulate the optimization of a wind farm layout as a PDE-constrained optimization problem where the fluid flow equations are a PDE constraint and the optimization seeks to minimize the Levelized Cost of Energy (LCOE). To this end, a finite element flow solver has been implemented in the python software framework FEniCS and validated with standard fluid dynamics test cases for lid driven cavity flow and vortex shedding from flow around a cylinder. Additionally, an adjoint optimization framework has been implemented that efficiently solves large gradient based optimization problems. The cost of this adjoint optimization approach is independent of the number of design variables, and is well suited to flow modeling PDE-constrained optimization problems. Use of this adjoint solver is demon- strated with the flow model in several test cases and in optimization of wind turbine actuator disk locations.

1 Introduction

Optimizing wind turbine positions within a wind farm is a difficult problem due to the strong nonlinear coupling between turbine locations, power production, atmospheric boundary layer turbulence, and mechanical loads on turbine components. Traditional approaches to optimizing turbine layouts have focused on maximizing total power output, but this does not take into account the costs of constructing, operating, and maintaining turbines within the farm. If not properly assessed, these costs can become prohibitive even for wind farms where power output is maximized, thereby limiting the economic competitiveness of wind energy compared to other renewable and non-renewable sources of electricity.

In order to develop a more complete accounting of the costs associated with a particular wind farm layout, a systems engineering optimization approach that considers the Levelized Cost of Energy (LCOE) is required. With an LCOE-based optimization routine, tradeoffs between power production, operations and maintenance (O) costs, and construction

costs can be quantified, thus helping developers determine the most economically compet- itive wind farm designs. A key challenge in using LCOE as an optimization metric is in estimating O costs. These costs are due in large part to damage-equivalent loads on mechanical components in turbine drivetrains. As a result, transient turbine loads must be considered alongside power output during the optimization procedure. These loads are strongly coupled to unsteady coherent turbulence caused by wake interactions and atmo- spheric instability, and their accurate prediction places enormous demands on the spatial and temporal resolution of flow field data used in the optimization procedure.

From a computational perspective, only large eddy simulations (LES) have the fidelity and resolution necessary to accurately capture turbulent effects relevant to turbine loading. Many prior layout optimization studies have relied on reduced order models; linear 'frozen turbulence' models assume that there is no interaction between turbines in a farm other than the additive effects of their wakes, and Reynolds Averaged Navier Stokes (RANS) approaches seek only to model the mean flow and cannot capture local, instantaneous turbulent structures associated with fatigue loading. The few studies that have used LES have assumed that turbines are located on regularly spaced grids. A more desirable approach would be to optimize wind turbine layouts using high fidelity flow fields and wake behaviors from LES, but without requiring a regular grid a priori, and while considering the effects of turbine loads, construction costs, and power production.

2 Development of an Adjoint Flow Solver

This general systems engineering approach for optimizing wind farm layouts results in a PDE-constrained optimization problem with a large design space and a single LCOE- based cost function. PDE-constrained optimization of such complex systems is particularly amenable to gradient-based adjoint methods. The design space for wind turbine layouts is sufficiently large to prohibit exploring all of the space using a gradient-free method, and instead requires the fast convergence of gradient-based optimization routines. Adjoint tech- niques are a computationally efficient means of determining the gradient of an objective function at a fixed

cost, regardless of the size of the design space.

The flow solver and adjoint optimization is implemented in a software package called FEniCS, which automates the solution of PDE's using the finite element method. FEn- iCS is written in python, and can be easily integrated with the rest of the NREL Wind Energy System Engineering tools like WISDEM and FUSED-Wind. FEniCS comes with a user-friendly problem solving environment with a mathematical syntax for writing the variational form of PDE problems and meshing the finite element, and automated com- pilers for generating finite element basis functions and assembling the variational forms. The python code is just-in-time (JIT) comiled to C++ for computational speed. FEniCS can interface to common HPC libraries such as PETSc and Trilinos for numerical linear algebra, ParMETIS and SCOTCH for domain decomposition, and MPI and OpenMPI for parallelization. FEniCS is well tested and validated on a number of computational problems in solid and fluid dynamics, eigenvalue problems, and coupled PDE's.

The variational form of finite element problems lends itself well to gradient based op- timization problems. The software package dolfin-adjoint performs a high level automated differentiation and can derive both discrete adjoint and tangent linear models of a forward problem implemented in FEniCS. The discrete adjoint and tangent linear models are import in the gradient based optimization algorithms used in data assimilation, optimial control and error estimation. The automatic differentation routines in dolfin-adjoint treat each forward model as a series of equation solves and therefore derives adjoint and tangent linear models at a higher level of abstraction than traditional algorithmic differentiation which treats forward models as a series of elementary instructions. This higher level of abstraction gives dolfin-adjoint greater flexibility and automation across a wide range of PDE applications. dolfin-adjoint can be implemented on unsteady and nonlinear PDE's, and can also be run in parallel. It can directly interface to the optimization algorithms in SciPy and also contains routines for checking the correctness of the adjoint gradients.

Two flow solvers have been developed, a steady state Reynolds-Averaged Navier Stokes (RANS) solver that implements the Shear Stress Transport (SST) model, as well as an unsteady implicit Large Eddy Simulation (LES). The flow solvers use 2nd degree continuous Galerkin finite elements for the velocity field and 1st degree elements for the pressure field. The unsteady LES simulation implements an incremental pressure correction scheme (IPCS) and Crank-Nicholson timestepping. Wind turbines are represented as actuator disks that project a body force onto the flow. Initial tests on lid-driven cavity flows, flow over cylinders, and flow through actuator disks are used to validate the codes.

Initial Results

Initial results will be presented on the valiation of the RANS and LES codes for canonical test cases like lid-driven cavity flow and flow over a cylinder. Results of the actuator disk simulations will be compared to standard 1D momentum theory. We will show single turbine adjoint optimizations that recover the Betz limit, and higher dimensional optimizations that optimize the layout of many turbines. Insights from the adjoint solution will also be discussed to give insight into gradient based optimization of the turbine locations.

31

Simulating the Variability of Renewable Generation and Demand in RTOs at 353 Penetration

Dr. KIRK-DAVIDOFF, Daniel [1]; Dr. JASCOURT, Stephen [2]

[1] MDA Information Systems LLC University of Maryland, College Park

[2] MDA Information Systems LLC

Corresponding Author: daniel.kirk-davidoff@mdaus.com

Wind and solar generation forecasts are used by electrical grid operators and utilities to predict the amount of electricity that will be required from non-renewable generation facilities. That is, they are typically regarded as contributing to a prediction of effective electrical demand. Electrical demand itself varies strongly and non-linearly with temperature. Thus skillful prediction of effective electrical demand requires good predictions of both demand-weighted temperature and renewable generation. Since electrical prices depend not only on demand, but on expectations of demand, the goal of avoiding spiky electrical prices and reduction of the use of inefficient peaking power units is best served when the joint variability of demand and renewable generation is well understood.

In this presentation we examine the joint variability of modeled electrical demand and wind and solar generation in all the US and Canadian regional transmission organizations (RTOs). We use reanalyzed wind, temperature and insolation from the Climate Forecast System Reanalysis to simulate the demand and renewable generation that would have resulted over the past 33 years if the present renewable infrastructure and temperature-sensitive demand had been present over that period, and then extend the present infrastructure to simulate variability at 353 renewable contribution to electrical demand. Demand sensitivity is based on regression of temperature and electrical demand over the past year (2013) in each RTO. We show that the correlation of demand and renewable generation is a strong function of geography, season, and averaging period (hourly, daily or monthly), identifying those regions where joint variability tends to reduce effective demand variability and those where joint variability tends to increase effective demand variability. While wind generation typically maximizes at night, the intensity of the diurnal cycle varies strongly over the course of the year, while temperature dependent demand variations and solar generation variations are largest in summer, since temperature is more diurnal at that time than in the winter, and the sensitivity of demand to temperature is larger in summer.

We explore the ways in which choices of how and where to expand renewable generation affect the co-variability of renewable generation and demand, and the probability of long periods of low generation in each RTO. We anticipate that this simulation capability will be helpful in planning the needs of the future electrical grid for generating capacity, storage and demand management, as well as for inter-regional power transfers.

21

Aerodynamic Validation of Wind Turbine Airfoil Models in the Virginia Tech Stability Wind Tunnel

Dr. KUESTER, Matthew [1]; Mr. BROWN, Ken [2]; Mr. MEYERS, Timothy [2]; Dr. INTARATEP, Nanyaporn [2]; Dr. BORGOLTZ, Aurelien [2]; Prof. DEVENPORT, William [1]

[1] Virginia Tech

[2] Virginia Polytechnic Institute and State University

Corresponding Author: mkuester@vt.edu

1 Introduction

Accurate predictions of lift and drag are critical for the design and performance evaluation of megawatt- scale wind turbines. Wind tunnel testing is a key component of the design process, as it complements CFD and other prediction tools. Over the last 10 years, the Virginia Tech Stability Wind Tunnel has been used extensively for aerodynamic and aeroacoustic measurements of wind turbine airfoils; however, comparisons of data from Virginia Tech and other wind tunnels showed discrepancies in lift curve slope and maximum lift coe□cient. For a DU96-W-180 airfoil geometry, measurements at Virginia Tech yielded lift curve slopes 3.0% – 5.5% smaller and maximum lift coe□cients 0.04–0.12 smaller than measurements from two large scale European wind tunnels. Although di□erences in lift curve slopes and maximum lift coe□cients are not uncommon in wind tunnel testing (see McCroskey [2] and Troldborg *et al.* [4]), this was viewed as an opportunity to thoroughly investigate airfoil testing in the Virginia Tech Stability Wind Tunnel.

The goal of this work is to investigate and evaluate all aspects of airfoil model testing in the Virginia Tech Stability Tunnel, from model fabrication through data reduction, to explain the di□erences in lift coe□cients between the Virginia Tech Stability Tunnel and other facilities. This work has validated the majority of aspects/procedures of the Virginia Tech Stability Tunnel, including:

- Accuracy of Measured Reference Conditions
  - Static Pressure
  - Dynamic Pressure
  - Temperature
  - Freestream Speed
- Tunnel Flow Quality
- Model Outer Mold Line Accuracy
- Pressure Measurement Fidelity
- Post-Processing Routines
- Corrections for Hard-Walled Boundaries
- Measured Lift/Drag Repeatability

The results presented in the rest of the abstract highlight key findings that warrant further study.

2 Wind Tunnel Facility

These experiments were performed in the Virginia Tech Stability Wind Tunnel.. A thorough description of the tunnel is given by Remillieux *et al.* [3], while a brief description is given here. The wind tunnel is a closed return, low-turbulence tunnel capable of reaching freestream speeds up to 75 m/s. The test section has a 6 ft × 6 ft square cross section. Airfoil models are mounted vertically along the centerline of the test section.

Figure 1: Naphthalene visualization on pressure side of the DU96-W-180 model at $\alpha = 8^{\circ}$ and $Re_c = 3.0$ Million. Left: after naphthalene application. Right: after wind tunnel was held on condition for ∼10 minutes and turned o□.

Lift on airfoil models is measured through both airfoil and wall pressure taps, while drag is measured using a traversing pneumatic wake rake that horizontally spans the entire test section.

A 0.8 m chord DU96-W-180 model was mounted in the aerodynamic test section for this work. This model was constructed at Virginia Tech by the Aerospace and Ocean Engineering Machine Shop. The model is constructed of 50 mm spanwise aluminum laminates that are pinned together and held in compression. The model is rotated to the desired angle of attack through a turntable mounted in the ceiling, and the angle of attack is measured using an encoder on the turntable. A suction system is used to remove the wall boundary layer on both the floor and ceiling to minimize end e□ects. The gap between the model tips and wind tunnel floor/ceiling is nominally five millimeters wide to allow an adequate flow rate through the suction system. Brown *et al.* [1] provide more details regarding the mounting and testing of airfoil models in the Virginia Tech Stability Wind Tunnel.

3 Surface Quality & Boundary Layer Transition

One of the objectives of this work was to determine if model surface quality was tripping the boundary layer and thus a□ecting lift measurements. The Stability Tunnel utilizes infrared thermography to visualize boundary layer transition on airfoil models; however, this measurement is typically made with a thin insula- tive material on the airfoil surface. For this work, naphthalene visualization was used to visualize transition on the clean DU96-W-180 model without any surface treatments.

Figure 1 shows an example of the before and after photographs from a naphthalene visualization. In this technique, naphthalene is dissolved in acetone and pressure sprayed onto the model. The tunnel is then set to the test condition, and the model is rotated to the desired angle of attack. The naphthalene sublimates at a rate proportional to shear stress, so the naphthalene disappears rapidly from the model where the boundary layer is turbulent. The flow is turned o□ once a clear transition front is observed.

Naphthalene visualization was performed at several angles of attack between zero and eight degrees at

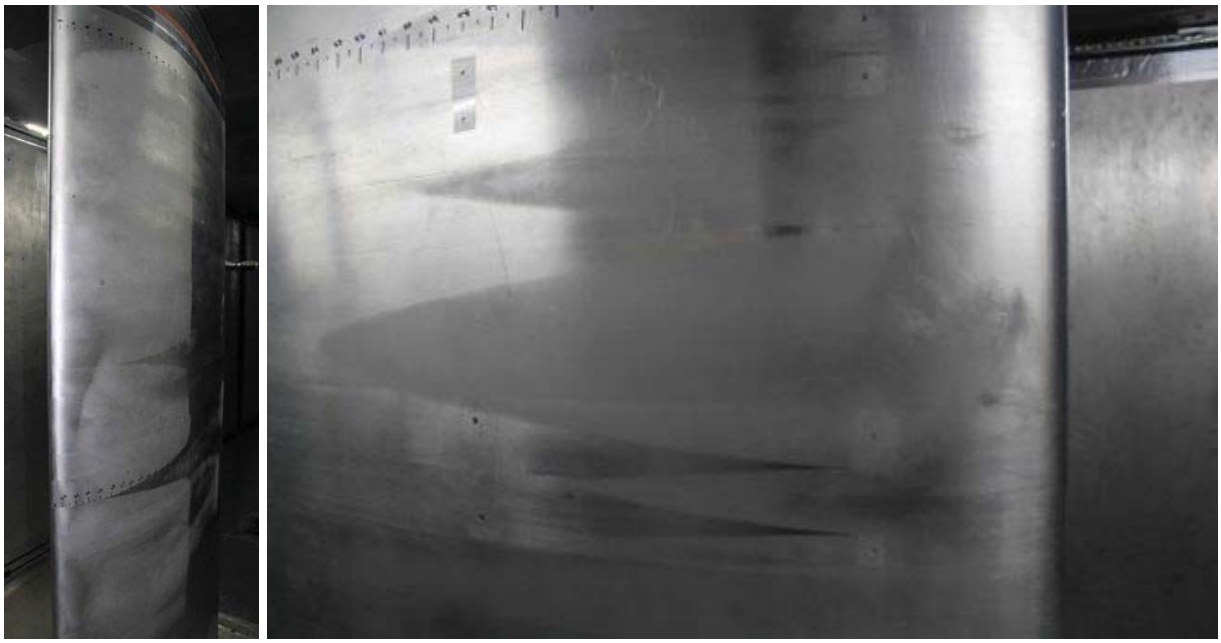

Figure 2: Naphthalene visualization on the DU96-W-180 model at Re_c = 3.0 Million. Left: suction side at α = 0 degrees, flow from left to right. Right: pressure side at α = 8 degrees, flow from right to left. Turbulent wedges caused by forty-micron-thick tape and surface defects at laminate edges.

Re_c = 3.0 Million. The naphthalene showed that small surface defects at the edges of laminates caused turbulent wedges. In addition, forty-micron-thick tape, which were covering threaded holes on the pressure side of the model, was also tripping the boundary layer and creating turbulent wedges. Figure 2 shows examples of tape and laminate edges tripping the boundary layer on both the pressure and suction sides of the airfoil model.

After each naphthalene visualization, surface defects that caused turbulent wedges were were lightly sanded and polished until as many turbulent wedges were removed as possible. Figure 3 shows the effect of sanding/polishing defects on lift. Improving the model surface finish improved the lift curve slope (measured between 0 & 5 degrees) over 3% and slightly raised the maximum lift coefficient. Because of this finding, naphthalene visualization is a standard procedure for tests on airfoil models in the Stability Wind Tunnel to ensure the model surface finish is not prematurely causing boundary layer transition.

4 Corrections for Model Deflection

Another focus of the validation testing was assessing model deflection/flexure under aerodynamic loading. As a first step towards this goal, a laser distance sensor was installed into the starboard wall of the test section. The laser hits the model near 1/3 span, approximately eight inches below the pressure taps. This sensor continuously measures the distance between the wall and the airfoil model, and the model angle of attack can be inferred from the model profile and the laser position/orientation.

A one time calibration was used to determine the laser's position and orientation relative to the model center of rotation. With the wind turned off, the model was rotated between –20° and 20° angle of attack in 1° increments. The angle of attack and measured laser distance at each point was used by an optimization routine which calculated the position and orientation of the laser relative to the model center of rotation. This calibration was then used to determine the angle of attack of the model, given the distance measurement from the laser. The residuals from the calibration data showed that the laser could measure model angle of attack to within ± 0.02 degrees.

Comparisons between the angles of attack measured by the encoder and the laser proved that the model (or model mounting system) was deflecting under aerodynamic loading. Figure 5 compares $\alpha_{encoder}$ and

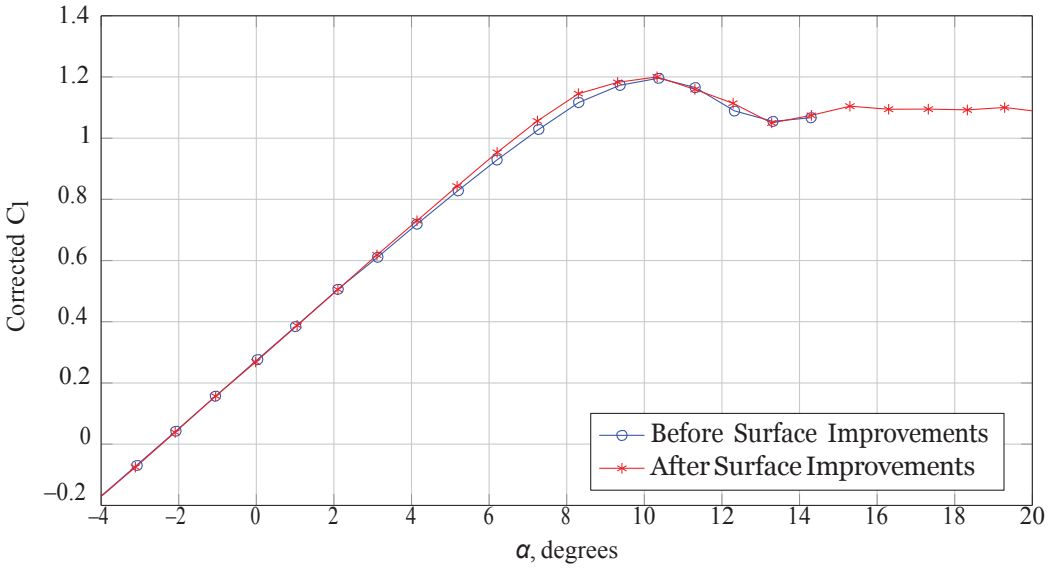

Figure 3: Lift curve improvements at Re_c = 3.0 Million after improving the surface quality.

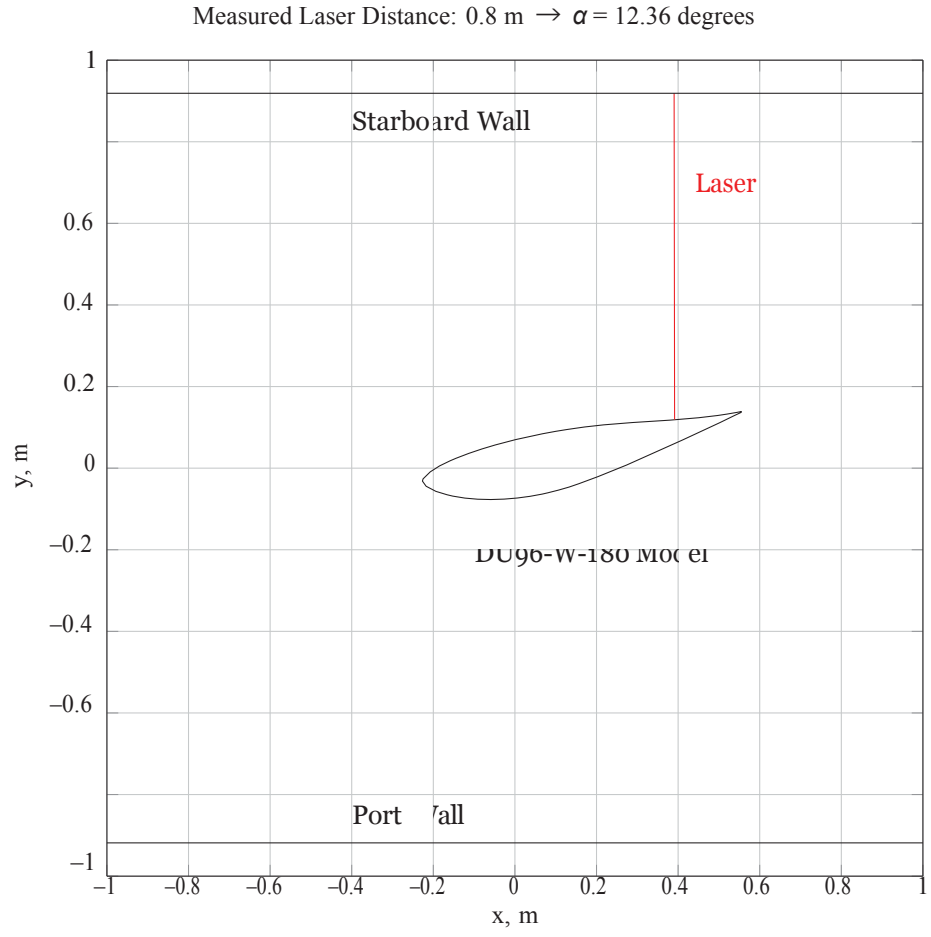

Figure 4: Setup of the laser distance sensor. Flow travels from left to right.

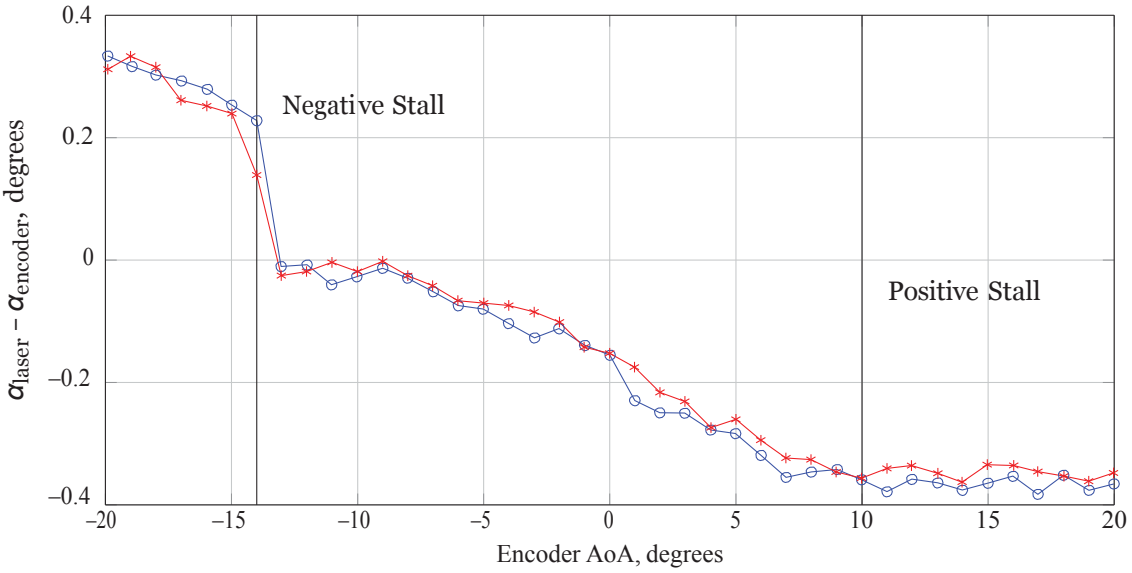

Figure 5: Di□erence between encoder angle of attack and laser angle of attack at Re_c = 3.0 Million

α_{laser} for two low angle lift polars at Re_c = 3.0 Million. The di□erence between the encoder and the laser shows a repeatable rotation of the model under aerodynamic loading. A large change in the moment coe□cient across negative stall creates a sudden change in laser angle of attack. In the linear range of the lift curve, the di□erence between the encoder and the laser angles steadily decreases. At and beyond positive stall, the di□erence remains constant at -0.35 degrees.

The laser measurement confirms that the model is deforming at the spanwise position where the laser hits the model. Camera measurements taken while the model was under aerodynamic load suggest that the deformation is nearly constant along the model span and may be caused by rotational deflection within the model mount. Based on this result, we assume that the laser is measuring the true angle of attack for the entire model. Future validation testing in February-April 2015 will utilize four lasers to measure the model position at multiple spanwise and chordwise locations to confirm this assumption. In addition, the wind tunnel is constructing a loading rig to measure model deflections under simulated aerodynamic loads.

Figure 6 shows the lift curve of the DU96-W-180 plotted using both the encoder angle of attack and the laser angle of attack. The lift curve slope (calculated between zero & five degrees) based on the laser is 1.6% larger than than the lift curve slope based on the encoder. Moving forward, laser measurements will become the standard angle of attack measurement in the Stability Wind Tunnel.

5 Ongoing Work

This work is part of an ongoing e□ort at the Stability Wind Tunnel to validate our measurements of lift and drag on wind turbine airfoil models. Additional e□orts this spring (February-April 2015) will focus on the following areas:

- Pressure Taps:
  - Size
  - Tripping E□ects
- Model Flexure Using Four Laser Sensors
- Tip Conditions
  - Boundary Layer Suction System
  - Size of Gap Between Wall And Model

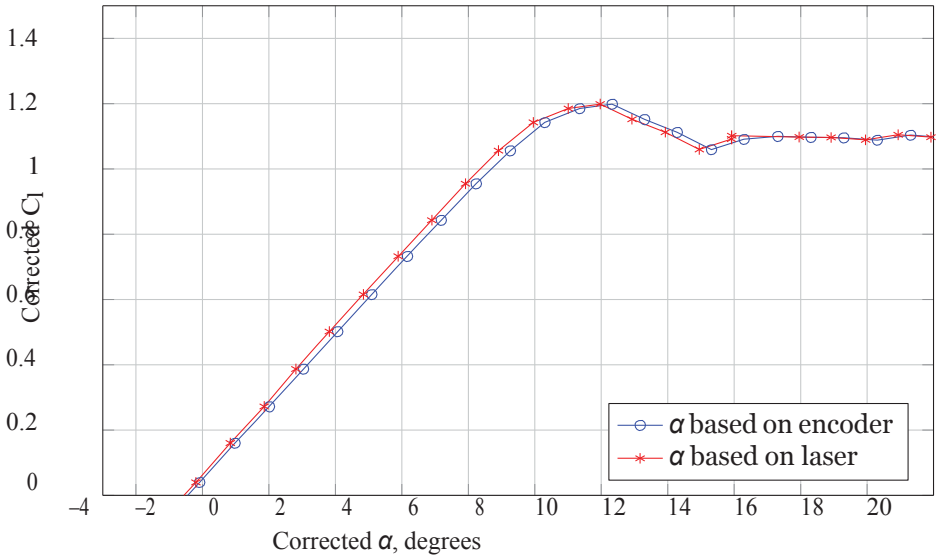

Figure 6: Lift curve of the DU96-W-180 based on encoder angle of attack and laser angle of attack

References

[1] K. Brown, W. Devenport, and A. Borgoltz, *Exploiting the characteristics of kevlar-wall wind tunnels for conventional aerodynamic measurements*, AIAA Paper 2014-2110.

[2] W. McCroskey, *A critical assessment of wind tunnel results for the NACA 0012 airfoil*, tech. rep., DTIC Document, 1987.

[3] M. C. Remillieux, E. D. Crede, H. E. Camargo, R. A. Burdisso, W. J. Devenport, M. Ras- nick, P. V. Seeters, and A. Chou, *Calibration and demonstration of the new Virginia Tech Anechoic Wind Tunnel*, AIAA Paper 2008-2911.

[4] N. Troldborg, C. Bak, H. Aagaard Madsen, and W. R. Skrzypinski, *DAN-AERO MW: Final Report*, tech. rep., DTU Wind Energy, 2013.

20

Using Maintenance Options to Optimize Wind Farm O&M

Mr. LEI, Xin [1]; Prof. SANDBORN, Peter [2]; Dr. GOUDARZI, Navid [2]; Mr. BAKHASHI, Roozbeh [1]; Mr. KASHANI-POUR, Amir [1]

[1] University of Maryland - CALCE

[2] University of Maryland, CALCE

Corresponding Author: sandborn@umd.edu

When remaining useful lives (RULs) are predicted for turbines in a wind farm, decision-makers face the challenge of determining when to perform predictive maintenance. To address this question, this paper applies a predictive maintenance options model to both single turbines and entire offshore wind farms managed via Power Purchase Agreements (PPAs), considering the uncertainties in wind, the accuracy of the forecasted RULs, and discrete maintenance opportunities. The optimum maintenance plan for the turbines in a farm is not the same as the optimum maintenance plan for individual turbines managed in isolation due to the constraints provided by the PPA.

0

MODEL AND PROCEDURES FOR RELIABLE NEAR TERM WIND ENERGY PRODUCTION FORECAST

Mr. LI, Jiale [1]; Prof. YU, Xiong (Bill) [1]

[1] Case Western Reserve University

Corresponding Author: jxl780@case.edu

Accurate and reliable prediction of wind energy production is important for the operational management of wind farm as well as for the stability of electrical grid with renewable energy integration. This paper describes a model and procedure that accurately predict wind energy production using weather forecast. An aerodynamic model is used to predict the wind speed distribution with elevation from the 24 hour forecasted wind speeds at three hours intervals. The model considers the effects of factors such as ground topology, land cover, etc. on the wind speed distribution. Therefore, it is applicable for different types of territories. The simulated wind speed, at time interval of 15 minutes, is then used together with the factory or calibrated turbine production curve to predict the energy production in 24 hours. The model and procedures for wind energy production forecast are validated on a 100kw prototype research wind turbine installed on the campus of CWRU. The actual energy production data in different seasons from the prototype wind turbine was analyzed and compared with that by model forecast. It was found this new model-based forecast method provide more reliable and accurate prediction of wind energy production, compared with alternative methods. The potential application of this wind energy forecast method include to improve the management of wind farm operations, to evaluate the electric power storage demand, to optimize the market values of wind energy , and to assist the electric grid integration of renewable energies.

42

Wind Forecast Improvement Project2, improving model physics in complex terrain – NOAA's Plans for Improving the Rapid Refresh and High Resolution Rapid Refresh Models

MARQUIS, Melinda [1]; OLSON, Joseph [2]; BIANCO, Laura [2]; DLALALOVA, Irina [2]; MCCAFFREY, Katherine [2]; ECKMAN, Richard [3]; CARLEY, Jacob [4]; CLINE, Joel [5]; KENYON, James [2]; PICHUGINA, Yelena [2]; CHOUKULKAR, Aditya [2]; BANTA, Robert [2]; WILCZAK, James [6]

[1] NOAA ESRL

[2] University of Colorado/CIRES and NOAA/ESRL

[3] NOAA/ARL

[4] I.M. Systems Group and NOAA/NCEP

[5] DOE Wind and Water

[6] NOAA/ESRL

Corresponding Author: melinda.marquis@noaa.gov

The Department of Energy is leading a second Wind Forecast Improvement Project (WFIP2), which will aim to improve modeling of complex flow. The National Oceanic and Atmospheric Administration (NOAA) will collaborate with DOE and its national labs, and the team led by Vaisala, which includes academic, utility and renewable energy partners.

WFIP2 aims to improve model physics and bridge models that describe multiple scales in complex flow. Observations collected during a 12-18 month field campaign in an area bounded by the Columbia River Gorge and Vansycle Ridge will be used for model verification and assimilation. Scales of physical phenomena of interest range from meso-beta (20-200 km) through the meso-gamma (2-20 km) to the microscale (< 1 km). Physical phenomena of particular interest include frontal passages, gap flows, convective outflows, mountain waves, topographic wakes, and marine pushes.

The instrumentation for the field campaign, which will begin in the summer of 2015, includes radar wind profilers, sodars, lidar wind profilers, scanning Doppler lidars, microwave radiometers, sonic anemometers, ceilometers, range gauges, high resolution microbarographs, surface energy budget sensors. Sensors on tall towers and wind turbines will also be used.

NOAA's 13-km Rapid Refresh (RAP; spanning North America) and 3-km High-Resolution Rapid Refresh (HRRR; covering the CONUS) will be the primary forecast models for this study. The RAP and HRRR are hourly updating assimilation and model forecast system, capable of assimilating many types of observations, including near-surface and aircraft in-situ observations as well as radar reflectivity and satellite radiances. The RAP produces 18-h forecasts and the HRRR produces 15-h forecasts every hour, both using the Advanced Research version of the Weather Research and Forecast (WRF-ARW) model as the forecast model component. The HRRR uses the RAP for lateral boundary conditions. Within the HRRR, a concurrent 750-m nest will be used to develop scale-aware physical parameterization during WFIP2. Model improvements at all scales will be made available to the public via the WRF-ARW repository.

NOAA will assimilate special WFIP2 observations, using them to verify the operational RAP and HRRR forecasts. Selected cases that are poorly forecast and deemed important to wind power production will be re-simulated with modifications to key physical parameterizations (boundary layer, surface layer, etc.) in an attempt to reduce forecast errors. The most significant model improvements as well as the collective model improvements will further be tested in retrospective experiments involving the full RAP and HRRR domains in order to ensure robust improvements for general weather prediction as well as the complex flows of focus in this project.

Retrospective runs will also be run by NOAA's hourly-updated North American Mesoscale Rapid Refresh (NAMRR) system, which includes the full 12-km North American domain and the 3-km CONUS nest domain.

67

One Team's Participation in the Inaugural Collegiate Wind Competition – Lessons Learned and Experiences Gained

Prof. MILES, Jonathan [1]; Mr. LOOS, Blaine [1]; Ms. PANGLE, Remy [1]

[1] James Madison University

Corresponding Author: milesjj@jmu.edu

Context: Wind energy education has been offered to undergraduate students through traditional courses, capstone projects, international programs, and internships offered at James Madison University (JMU) for more than fifteen years. The Department of Integrated Science and Technology (ISAT) at JMU has produced hundreds of majors who have enrolled in courses that teach wind modules, more than one hundred of whom have conducted a senior capstone project and/or an in-depth study in an international setting that focuses on wind energy and associated applications. JMU's participation in the inaugural Collegiate Wind Competition (CWC) sponsored by the U.S. Department of Energy (DOE) provided an opportunity to create new and intensive opportunities for students who share a passion for wind energy and seek opportunities to gain real-world experience that involves design, development, and research in this important field.

Justification: James Madison University participated in the inaugural Collegiate Wind Competition, which culminated in a two-day contest among ten institutions of higher education in Spring 2014. The JMU proposal was led by the Department of Integrated Science and Technology and supported by the Center for Wind Energy (CWE) at JMU, an interdisciplinary center that emphasizes Research, Education and Outreach while addressing the interests of JMU, Virginia and surrounding states, industry, and other stakeholders. Nearly thirty students from nine different majors comprised a team, supported by faculty and staff, that addressed the goals developed for the competition. The three primary elements of the competition were to (i) design, prototype, and test a small, light-weight wind turbine tailored for battery charging and powering small electronic devices; (ii) assess and address the market barriers associated with the turbine designed and develop a practical, flexible business plan; and (iii) research a market topic of particular relevance to the region where each competing institution is situated and present on that topic.

Results: The JMU team that participated in the inaugural Collegiate Wind Competition was supported by an interdisciplinary team of faculty and staff, and was represented by twelve of its own at the contest which was hosted at Windpower 2014. The team placed fifth out of ten overall, with students reporting a high degree of satisfaction with the experience overall. The approach taken at JMU during the Academic Year 2013-14 to guide the large student team through its preparations included the application of novel teaching methodologies and exposure to unique resources. The resulting model is being refined and will be applied toward future wind competition activities.

Conclusions: The Collegiate Wind Competition provides a platform for innovative and impactful teaching of wind turbine design, development, and testing, as well as relevant business-related topics and accompanying market issues. The lessons learned and experiences gained are being applied toward the development of new curriculum models and will inform future undergraduate teaching of wind energy and related topics.

5

Modifications to RANS Turbulence Model for Use in Urban Wind Resource Assessment

Mr. MOHAMED, Rif [1]

[1] University of Calgary

Corresponding Author: conjecture23@gmail.com

A new turbulence model, MW, is developed for use in the computational flow over an urban landscape. It addresses the stagnation-point anomaly found in simulations over buildings with the standard k- E and negates the introduction of negative normal stresses which come about in the presence of large mean strain rates. MW was tested for a flow over a building and it performed better than the models of Yap and Durbin. It was also able to predict a larger recirculation region at the lee of a steep hill which is an improvement to the standard k- E.

51

SMALL SCALE ROTOR TESTING TO CHARACTERIZE THE INGESTED TURBULENCE INTO WIND TURBINES

Mr. MURRAY, Henry [1]; Dr. ALEXANDER, William [1]; Prof. DEVENPORT, William [1]

[1] Virginia Tech

Corresponding Author: henryiv4@vt.edu

This abstract relates the results of turbulence ingestion measurements on a small scale breaking rotor in the Virginia Tech Stability Tunnel to wind turbines. It presents the results of PIV and phased array measurements from the experiment that characterize the ingested turbulence into the rotor and extrapolates the conclusions to a full scale wind turbine.

74

Design of closed loop control for a wind turbine system coupled to a CV transmission system

Santiago M. Novoa[1], Nilabh Srivastava[2], Luciano Castillo[3], Beibei Ren[3].

1. *Dept. of Electrical Engineering, Texas Tech University, Lubbock, TX 79409, USA.*
2. *Dept. of Mechanical Engineering, University of North Carolina at Charlotte, Charlotte, NC 28223, USA.*
3. *Dept. of Mechanical Engineering, Texas Tech University, Lubbock, TX 79409, USA.*

Grid integration of renewable energy sources has proven to be a popular and challenging problem that has been extensively studied and continues to be a focus of interest. Most modern wind energy conversion systems utilize power electronics converters/inverters to maintain voltage phase, frequency and magnitude at the grid-dictated values.

While power electronics is an expanding area of interest, currently available solutions report high failure rates and elevated monetary costs. In this paper we investigate the dynamic analysis of a gearless wind turbine coupled to an induction generator based on the dynamical understanding proposed *by Ericson and Srivastava* that describes both the steady state and the shifting behaviours of the V belt CVT. The Model uses the dynamics published by Carbone-Mangialardi to explain this relationship during creep mode shifting, and the dynamics by Shafai in Slip Mode shift, which provides thorough detail on the inertial interactions between the belt and the pulleys of CVT.

Using Matlab/Simulink, we incorporate the CVT model into a wind turbine model coupled to an induction generator. The entire turbine/rotor – CVT/generator is coupled to the grid through the conventional grid- and rotor-side converters. By controlling the driver axial forces of the CVT we intend to be able to control low- and high-speed shaft speeds (i.e. perform speed control) to obtain maximum wind energy capture before the wind cut-out speed and provide an alternative to pitch control afterward.

The intent is to understand how control inputs of the CVT affect power through the entire drivetrain to meet the objectives of:

a) Maximal power extraction from the wind
b) Better quality power for grid integration
c) Tracking the grid demands without degrading the CVT performance

The results for the overall integrated powertrain are presented and discussed in detail with the CVT and the induction generator operated in ***closed loop*** configuration. The simulations were all performed utilizing real wind data taken from a met tower in the South plains area, the data was sampled at 50 Hz.

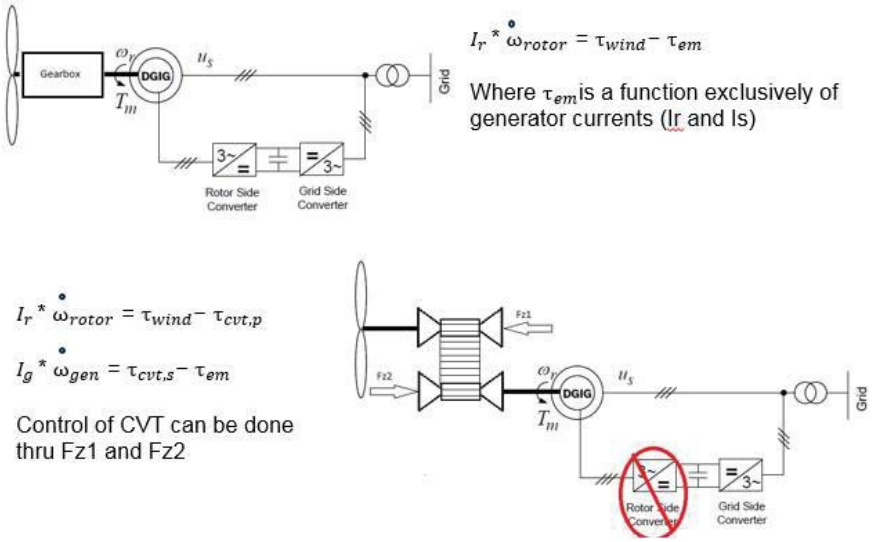

Fig.1 – Gearbox vs. CVT based wind turbine systems

- A CVT can improve energy capture (wider speed range)
- A CVT can downsize pitch control
- A CVT can downsize, if not completely eliminate, speed control needed on HSS and/or LSS. Traditionally, speed control on LSS and HSS is done by RSC (Significant reduction of power electronics, 25% of failures in wind energy industry is due to power electronics)
- A CVT can downsize switching electronics needed to ensure a constant grid frequency of 60 Hz.

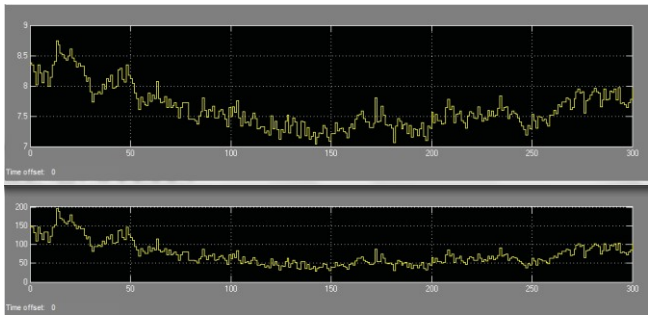

Fig.2 – Wind speed and Aerodynamic Torque vs time for met data obtained in the South plains region.

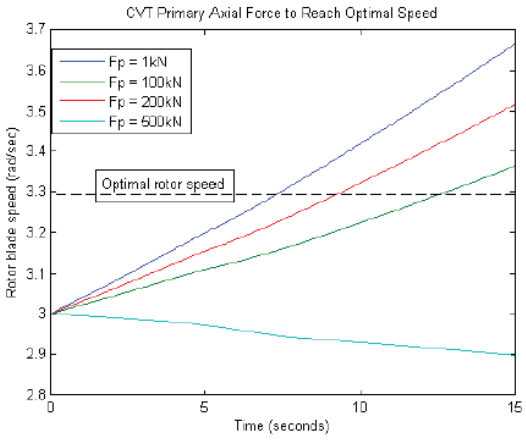

Fig.3 – LSS optimal rotor speed vs CVT primary axial forces.

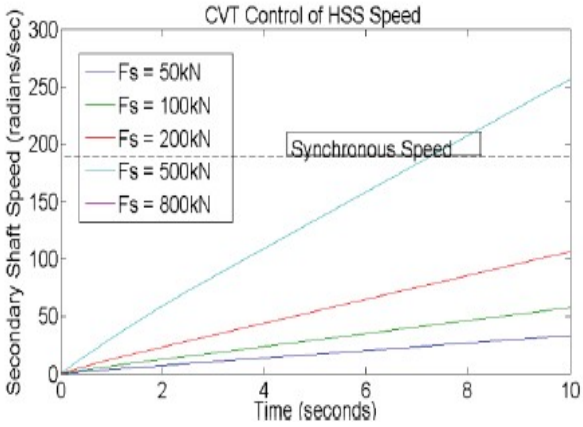

Fig.4 – HSS optimal rotor speed vs CVT primary axial forces.

57

Analysis of Tower Shadow Effects on the UAE Rotor Blades

Mr. NOYES, Carlos [1]; Dr. LOTH, Eric [2]; QIN, Chao [2]

[1] The University of Virginia

[2] the University of Virginia

Corresponding Author: ccn5cw@virginia.edu

A leading obstacle hindering the development of wind turbines to extreme scale is the structural integrity of the blades. Downwind rotors have been shown to give structural advantages for larger systems. However, there is an added aerodynamic complication from the tower shadow. This paper presents and analyzes a previously unpublished subset of data collected by NREL during an extensive wind tunnel campaign for Unsteady Aerodynamic Experiment Phase VI (UAE Phase VI). The experimental data includes relative flow fields, aerodynamic blade forces, and root blade flapwise bending moments, from upwind turbines, downwind turbines and downwind turbines with the use of an aerodynamic tower fairing. It is shown that the tower shadow can have a severe and negative effect on these variables, leading to higher bending stresses. The use of a tower fairing can greatly reduce these detrimental effects. To better interpret this data, predictions using an aeroelastic wind turbine code, FAST, was used to model the experimental conditions. The differences between the experimental data and the computational predictions are attributed to unsteady effects of the wake. This suggest that wake modeling for downwind turbines may require modifications to capture physically realistic tower shadow effects.

56

Wind Turbine Tower Fairing Geometries to Decrease Shadow Effects

Mr. NOYES, Carlos [1]; Dr. LOTH, Eric [1]; Mr. FUHRMAN, Jay [1]

[1] the University of Virginia

Corresponding Author: ccn5cw@virginia.edu

Tower fairings are a promising method to reduce wake for down wind turbines, with the drawback that the performance may be lost at high angles of attack. For example, the E863 airfoil has a much smaller wake than a cylinder at 0o but a similar wake at 20°. This study investigates various fairing geometries focusing on impact of a rounded trailing edge on the wake for an angle of attack of 20°. Models were designed and manufactured of the E863 fairing and two fairings with circularly rounded trailing edges, E863r40 and E863r45. The modified fairings having a thickness ratio of 403 and 453 respectively. The fairings were tested in a water tunnel at Reynolds number based on diameter of 6.82x104 using dye for flow visualization and particle image velocimetry for wake quantification. Instantaneous, averaged and root mean squared values of velocity deviation and flow angle were analyzed for all the models. It was shown that both of the modified trailing edge fairings (with rounding) performed better than the unmodified aerodynamic fairing at 20°. In particular, the E863r45 performed better than the E863r40 and performed comparably to the cylinder at 20°. However at 0°, the E863 and the E863r40 showed little wake instability, and were better than the E863r45 (and far better than the cylinder).

4

Non-intrusive sensing of air velocity, humidity, and temperature using tunable diode laser absorption spectroscopy

Prof. MA, Lin [1]; Mr. PARK, Suhyeon [2]

[1] Department of Aerospace and Ocean Engineering, Virginia Tech

[2] Department of Mechanical Engineering, Virginia Tech

Corresponding Author: linma@vt.edu

This work will report the non-intrusive sensing of air velocity, humidity, and temperature using tunable diode laser absorption spectroscopy (TDLAS), and discuss the potential applications of such sensors for in situ monitoring and active control for wind energy. The sensing technique utilizes the absorption features of water vapor in ambient air to monitor multiple flow parameters including velocity, humidity, and temperature simultaneously and non-intrusively [1-3]. The TDLAS technique does not require pre-calibration or seeding and extensively employs fiber-optics technologies to facilitate its implementation. As a result, the sensor enjoys advantages such as low maintenance cost and scalability, which are especially attractive characteristics for practical deployment in power generation systems such as wind turbines.

In this work, we will discuss the fundamentals of TDLAS technologies and the results obtained in a series of laboratory demonstrations. Figure 1 shows a schematic to illustrate the concept of TDLAS. The output of a laser diode (both in terms of it power and wavelength) was changed by modulating its driving current (for example, a 2 kHz ramp signal in this work). As a result such modulation, the wavelength of the output scans across a certain spectral range (near the 1392 nm for example in this work) to detect an absorption line of water vapor. Typically, the output of the laser were split into three parts using fiber couplers. The first part, a small portion (103 in this work) of the output, was fed into a Mach-Zehnder interferometer (MZI) to monitor the wavelength scan during the modulation as shown. The rest of 903 of the output was then split into two equal parts to be used as the probe beams. The probe beams are pitched at an angle and directed into the target flow as shown. The transmitted laser beams are detected by two photodiodes at the opposite side of the flow, whose signals are then collected by a data acquisition systems for further analysis. In the signal analysis, the magnitude of the absorption peak was used to determine the concentration of the water vapor in the measurement region, the relative strengths of two absorption peaks to determine the temperature, and the Doppler shift between the two beams to determine flow velocity [2].

A set of example measurements is shown in Figure 2 below to illustrate the data analysis mentioned above. The results show an absorption peak near 1392 nm, measured by two probe laser beams, one crossed the flow at -45 degrees (slide blue line) and the other at 45 degrees (dashed red line). As mentioned above, the absolute magnitude of such absorption signals (defined as absorbance as shown in Figure 2) is used to determine the concentration of water vapor. As shown in Figure 2, the absorption signals peak at different wavelengths because the Doppler shift caused by the flow. This Doppler shift (L'w) was calculated to be 4x10/\(-4) cm-1 for this measurement as shown in the inset of Figure 2, based on which the flow velocity was determined to be 12.4 m/s.

In this measurement, the target flow (which was generated by a small open jet tunnel) was also characterized by hotwire for comparison purposes. Figure 3 shows the flow velocity measured at multiple locations by the hotwire. We can see the velocity followed a distribution in the measurement region. The velocity distribution peaked at 20 m/s at the center of the flow, and the arithmetic mean of distribution was 11.7 m/s. In comparison, the TDLAS technique determines a line-of-sight integrated measurement of 12.4 m/s.

In summary, the above example demonstrated the advantages of the TDLAS technique for monitoring multiple flow properties simultaneously and non-intrusively. Due to the advancement and maturity in diode lasers and fiber technologies, such technique is especially attractive for in situ application in practical systems.

43

Integrating Real World Case Studies into Wind Energy Graduate Education

Dr. PATTISON, Chris [1]; Dr. SWIFT, Andrew [1]; Dr. MORTSTOCK, Kim [2]; Dr. ELKINTON, Chris [2]

[1] Texas Tech University

[2] DNV GL

Corresponding Author: andy.swift@ttu.edu

Wind power continues to grow rapidly as a fuel source for the electric power industry in the US. Recent data for 2014 show that wind power in Texas alone delivered in excess of 10 percent of the annual electrical energy consumed in the state. With this growth has emerged the need for a professionally educated national workforce to support the industry and sustain future growth. With the original support of the Texas Workforce Commission in 2008, both undergraduate and graduate wind energy education programs have been established at Texas Tech University. A series of multidisciplinary courses have been developed by the six full-time faculty to support the degree and certificate programs. Total wind energy student course enrollments over approximately 20 wind energy courses offered each semester are averaging 400 to 500. The offerings are both face to face (in-class) and by distance delivery.

Starting in Fall 2014 TTU partnered with DNV GL to offer real-world case studies as part of the graduate course offerings. Four case studies were offered in each of two graduate classes – Advanced Technical Wind Energy I and Advanced Managerial Wind Energy I. The case studies covered technical, environmental, and site management topics for a single turbine project, a multi-turbine power plant, an offshore installation, and wind turbine technology innovations. The case studies were delivered remotely allowing students to benefit from real-life examples and the interaction with members of the wind industry. This presentation will discuss an outline of the cases, best practices for integrating industry participation to maximize student benefit, and effective delivery methods - what worked well and what can be improved.

46

Offshore Low-Level]et properties from offshore lidar measurements in the Gulf of Maine

Dr. PICHUGINA, Yelena [1]; Dr. BANTA, Robert [2]; Dr. BREWER, Alan [2]; Dr. CHOUKULKAR, Aditya [1]; Dr. MARQUIS, Melinda [2]; Dr. HARDESTY, Michael [1]; Dr. WEICKMANN, Ann [1]; Dr. SANDBERG, Scott [2]

[1] CU Boulder/NOAA

[2] NOAA

Corresponding Author: yelena.pichugina@noaa.gov

The Low Level Jet (LLJ), an atmospheric flow phenomenon well known as an important source for wind power production in the U.S. Great Plains, is not well characterized or understood in offshore regions considered for wind-farm development, due to a lack of wind measurements having needed precision and vertical resolution at turbine rotor heights. These measurements are also needed to verify whether numerical weather prediction (NWP) forecast models are able to predict offshore LLJ speed, height, direction, and other properties, such as shear. To begin to fill this knowledge gap, in this paper, we have analyzed ship-borne Doppler lidar measurements taken in the Gulf of Maine from 09 July to 12 August 2004. The lidar observing system, NOAA /ESRL's High Resolution Doppler Lidar (HRDL), features high-precision and high-resolution wind measurements and a motion compensation system to provide accurate wind data with a static pointing-angle precision of 0.15°, and dynamic precision < 0.5° despite ship and wave motions (Pichugina et al. 2012, J. Appl. Meteor., 51, 327-349). Fine-resolution wind profiles (15-min time resolution and 15-m vertical resolution) obtained from the water surface up to 1 km, were used to statistically characterize LLJ events, including frequency of occurrence, jet speed maxima, and the height of these maxima.

LLJ structure was evident in the lidar-measured wind profiles, often during nighttime and transitional periods, but also during the day on occasion. The LLJ strength for the entire experiment ranged from 5 to 20 m s-1 with a mean value of 9.4 m s-1 and a median value of 8.7 m s-1. A high frequency (about 483) of jet maxima was observed below 200 m above sea level (ASL) as shown in Figure 1, although for some episodes of strong winds (> 15 m s-1), jet maxima were found at 500-600 m ASL.

The existence of LLJs can significantly modify wind profiles, producing vertical wind-shears of 0.03 s-1 or more across the rotor layer. The strong speed and directional shear through the rotor layer during LLJ events, as well as the enhanced winds and turbulence, may all act to increase turbine loads, since the top and bottom tips of the blades would operate in different wind regimes. Additionally, the deviation of LLJ-shape profiles from standardized profiles often leads to significant errors in rotor-layer wind speeds and the calculated wind resource power assessments, such as by using the power-law relation, as will be shown by examples. The shear exponent computed from lidar-measured wind speeds at 10 m and 100 m ASL showed diurnal and other nonsystematic variations ranging from 0.09 to 0.24, with mean value of 0.16.

The paper will also present statistics and distributions of wind flow parameters aloft in the turbine rotor layer of the marine boundary layer over a range of heights and under various atmospheric conditions, and show diurnal variations of many flow-related quantities critical to wind energy. It will discuss discrepancies in power estimates using measured hub-height and rotor equivalent winds. Such results cannot be captured by surface measurements or by remote sensing instruments with a coarse vertical resolution of data.

12

Analysis of Turbine Wake Characteristics by using Proper Orthognal Decomposition(POD) and Triple Decomposition Methods

Mr. PREMARATNE, Pavithra [1]

[1] Iowa State University

Corresponding Author: huhui@iastate.edu

In the present study, we report the progress made in our efforts to examine the wake flow characteristics behind a commonly-used three-bladed horizontal-axis wind turbine. A series of experiments were performed in a large-scale wind tunnel with a scaled wind turbine model placed in a typical Atmospheric Boundary Layer (ABL) wind under neutral stability conditions. In addition to measuring dynamic wind loads acting on the model turbine by using a force- moment sensor, a high-resolution digital particle image velocimetry (PIV) system was used to achieve detailed flow field measurements to quantify the characteristics of the turbulent vortex flow behind the turbine model. Besides conducting "free-run" PIV measurements to determine the ensemble-averaged statistics of the flow quantities such as mean velocity, Reynolds stress, and turbulence kinetic energy (TKE) distributions in the wake flow, "phase-locked" PIV measurements were also performed to elucidate further details about evolution of the unsteady wake vortex structures in relation to the position of the rotating turbine blades. The detailed flow field measurements were used to validate the analytical models for the velocity deficit prediction in turbine wakes. Proper Orthogonal Decomposition (POD) method was employed in the present study for the data reduction of the PIV measurement results to identify the high energy modes that dominate the turbulent kinetic energy distributions in the turbine wakes. Triple Decomposition (TD) approach was also used to analyze the phase-locked PIV measurement results to elucidate the underling physics related to the intensive turbulent mixing process in the wake flow, which would promote the vertical transport of kinetic energy to entrain more high-speed airflow from above to re-charge the wake flow behind the wind turbine model.

33

Investigation of Dynamic Loading for 13.2 MW Downwind Pre-Aligned Rotor

Dr. QIN, Chao [1]; Prof. LOTH, Eric [1]; Dr. LEE, Sang [2]; Dr. MORIARTY, Patrick [2]

[1] University of Virginia

[2] National Renewable Energy Laboratory

Corresponding Author: chaoqin@virginia.edu

To alleviate the mass-scaling issues associated with conventional upwind rotors of extreme-scale turbines, a downwind rotor concept is considered that uses fixed coning to align the non-circumferential loads for a given steady-state condition. This alignment can be pre-set to eliminate downwind blade moments for a given steady-state condition at rated wind speed and to minimize them for other conditions. The alleviation in downwind dynamic loads may enable a reduced structural blade mass as compared with a conventional upwind rotor. To examine the potential impact of this design, FAST simulations were conducted for a 13.2 MW rated turbine at steady-state conditions for two rotor configurations with similar power outputs: 1) a conventional upwind rotor with three blades and 2) a downwind pre-aligned rotor with two blades. The rotor mass was reduced by approximately 253 for the downwind pre-aligned configuration. In addition, the damage equivalent loads on the blades were reduced more than 603 for the downwind pre-aligned configuration. However, additional work is needed to investigate this concept at turbulent inflow conditions and for extreme events.

63

An Analytical Procedure for Evaluating Aerodynamics of Wind Turbines in Yawed Flow

Prof. RAJAGOPALAN, R Ganesh [1]; Ms. GUNTUPALLI, Kanchan [2]; Mr. FISCHELS, Mathew [3]; Mr. NOVAK, Luke [4]

[1] Professor, Department of Aerospace Engineering, Iowa State University

[2] Aerospace Engineer, Sukra Helitek Pvt. Ltd., India

[3] Graduate Student, Department of Aerospace Engineering, Iowa State University

[4] Aerospace Engineer, Sukra Helitek Inc., USA

Corresponding Author: kanchan@sukra-helitek.com

A new analytical method for evaluating the performance of wind turbines in yawed flow is presented. The method, based on momentum theory, relates the yaw angle to the tip-path-plane orientation of the turbine rotor and
the non-dimensional deficit velocity. The analytical calculations are compared with results from Rot3DC, a kernel within the RotCFD software package, an integrated environment for rotors. Rot3DC, a 3-D Navier-Stokes based module, can simulate one or more Horizontal Axis Wind Turbines (HAWT) and uses the concept of momentum sources to compute the turbine performance and flowfield in a self contained manner. Rot3DC simulations are validated against NREL Phase-II experiments. Analytical results for yawed turbines correlate well with Rot3DC and are found to be within 103 error margin for the extreme yaws considered. The developed analytical formulation provides a simple model for quantification of turbine performance in yawed flow and can be used as an input to onboard feedback systems for yaw control.

15

Engaging a Multidisciplinary Group of Students in Wind Energy Education through the Planning and Execution of a KidWind Challenge at]ames Madison University

REMY, Remy [1]; Dr. JON, Jonathan [2]; Dr. KYLE, Kyle Gipson [3]

[1] Pangle

[2] Center for Wind Energy at JMU

[3] James Madison University

Corresponding Author: panglerm@jmu.edu

The Center for Wind Energy (CWE) at James Madison University (JMU) has hosted Virginia KidWind Challenge for the last three years. During the spring semester, 2015, Remy Pangle, Education and Outreach Coordinator for the CWE, and Dr. Jonathan Miles, professor in the Department of Integrated Science and Technology (ISAT) and Director of the CWE, partnered with Dr. Kyle Gipson, professor in the Department of Engineering, to launch a new course for students majoring in Education, Engineering, Hospitality, ISAT, and Psychology. This course combines disciplines associated with these majors with the primary goal to plan and execute the Eastern Finals of the KidWind Challenge at JMU. Students from each major bring a unique set of skills to the table: Education, the ability to identify age-appropriate activities for teams when they are not competing during the event; Engineering, the technical skills for providing guidance to teams and coaches; Hospitality, the logistical knowledge for planning the event; ISAT, the ability to bring all disciplines together and facilitate communication as well as manage the project; and Psychology, the knowledge of assessment so the group can understand the impact their event has on K-12 student.

19

Temporal Coherence in Turbulent Wind Simulation and Atmospheric Data

Ms. RINKER, Jennifer [1]; Dr. GAVIN, Henri [1]; Dr. CLIFTON, Andrew [2]

[1] Duke University

[2] National Renewable Energy Laboratory

Corresponding Author: jmr64@duke.edu

Abstract: Wind turbine design loads are calculated by simulating many turbulent wind fields and using them as input to a turbine model (e.g., the FAST 5 MW model [1]). The model outputs are then used to extrapolate the load that corresponds to a particular return period, which is called the design load. Unfortunately, the stochastic turbulence simulation methods recommended in the IEC 61400-1 design standard [2] produce wide-sense stationary turbulent turbulent fields, whereas real wind is known to be nonstationary (i.e., it has time-varying mean and variance) [3]. This is important, as the authors have found that nonstationarity in the turbine inflow increases both the magnitude and the variability of extrapolated design loads. A novel methodology, called temporal coherence, can be used to generate nonstationary turbulent wind fields for design load calculations with only simple modifications of existing stochastic simulators such as TurbSim [4]. Additionally, temporal coherence can be used to quantify the degree of nonstationarity in data. The main objective of this paper is the empirical calibration of a temporal coherence model that can be used to generate samples of wind parameters (the "classical" parameters U, σ_u, and L and the novel parameters ρ and μ, defined below) that match the conditions at the National Wind Technology Center (NWTC) near Boulder, CO.

Temporal coherence differs from the standard stochastic methods by creating a correlation between phases at different frequencies. It is similar to spatial coherence, but instead of correlating phases at the same frequency but different locations, there is a correlation between phases at different frequencies but the same location. This correlation is easily implemented using phase difference distributions (PDDs), which were first investigated in earthquake engineering for the stochastic simulation of accelerograms [5]. PDDs create the phase correlation by prescribing a non-uniform probability distribution on the difference between the phases at frequencies i and $i+1$. This phase correlation causes consistent constructive interference in the time domain, which concentrates the signal energy (see Fig. 1). The more concentrated the PDD, the more the signal energy is concentrated in the time domain and the more nonstationary it is. A uniform PDD, which has no concentration, corresponds to a stationary signal [6]. The location of the PDD mode controls the location of the energy "packet" in the time domain (see Fig. 1). To generate a turbulent wind record, the only procedural difference from the standard methods is that a sample of the phase differences is first generated using a PDD model with the user-specified concentration and location parameters (denoted by ρ and μ, respectively). Then, these phase differences are cumulatively summed to produce the phases, after which the Fourier magnitudes are prescribed using a specified spectrum, and finally an inverse Fourier transform produces the time history with temporal coherence.

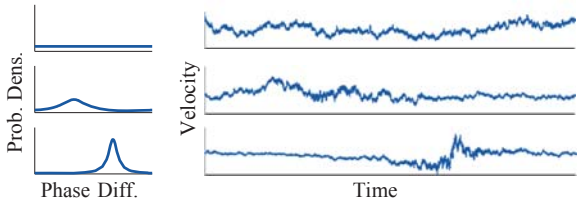

Figure 1: Effect of phase difference distribution (left) on time history (right)

In many cases, it is valuable to generate turbulent fields whose parameters reflect the conditions at a site of interest. In this paper, a joint probability distribution of five wind pa-

rameters (the 10-minute mean wind speed U, standard deviation σ_u, Kaimal length scale L, concentration parameter ρ, and location parameter μ) is calibrated using wind data recorded by sonic anemometers at six different heights at the NWTC. This distribution can be used to draw samples of wind parameters for wind simulations, and the samples are guaranteed to have similar probability characteristics as the real data at the site.

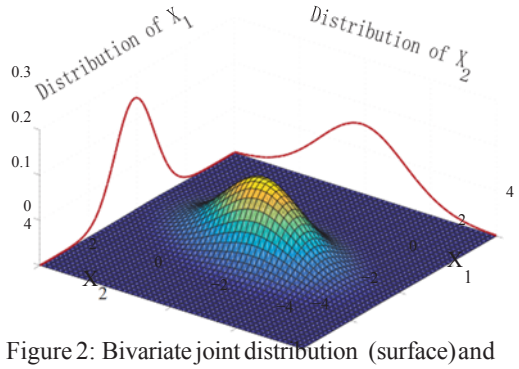

Figure 2: Bivariate joint distribution (surface) and marginals (red lines)

To fit the joint distribution, the five parameters of interest were extracted from each 10-minute wind record that passed a basic screening procedure for minimum wind speed and direction (to exclude the wake from a nearby turbine). The samples were then separated by height. This yielded a 5-dimensional hypercube for each height, where the five parameters extracted from each wind record correspond to a point in a hypercube. Because joint distributions are completely characterized by the marginal distributions and the correlations between the standardized variates (see Fig. 2), the marginal distributions and correlations of the parameter samples at each height were calculated. For the marginal distributions, using a single distribution for all of the data led to errors in the higher quantiles, so generalized Pareto (GP) distributions were used to model the data in the upper quantiles. The marginal distributions for the concentration parameter revealed that over 93% of all records in the screened dataset were nonstationary with 99% confidence. The correlations of the standardized variates were determined by trans- forming the wind parameters to a standard normal space through the empirical cumulative distribution function (CDF) and the inverse normal CDF and then calculating the Pearson correlation coefficient of the standardized variates.

The data analysis reveals three important facts. First, the best marginal distributions were not those that are traditionally assumed (e.g., Weibull for U, lognormal for σ_u, etc.), and the distribution type that was found to best fit the data often varied by height. Second, the use of a single distribution to model each parameter produced large errors in the upper quantiles, which prompted the use of a "composite" distribution with a separate distribution for the tail. Finally, over 93% of the analyzed wind records were classified as nonstationary with 99% confidence, demonstrating the importance of using nonstationary stochastic wind simulation methods and models, such as the one developed here, for the calculation of design loads.

References

[1] J. M. Jonkman, S. Butterfield, W. Musial, and G. Scott, "Definition of a 5-MW reference wind turbine for o□shore system development," National Renewable Energy Laboratory, Golden, CO, Tech. Rep. NREL/TP-500-38060, February 2009.

[2] International Electrotechnical Committee, *IEC 61400*, International Electrotechnical Commission Std., 2005.

[3] M. Nielsen, G. C. Larsen, J. Mann, S. Ott, K. S. Hansen, and B. J. Pedersen, "Wind simulation for extreme and fatigue loads," Risø National Laboratory, Roskilde, Denmark, Risø-R-1437(EN), January 2004.

[4] B. J. Jonkman and L. Kilcher, "TurbSim user's guide: Version 1.06.00," National Re- newable Energy Laboratory, Tech. Rep., September 2012.

[5] H. Thráinsson and A. S. Kiremidjian, "Simulation of digital earthquake accelerograms using the inverse discrete Fourier transform," *Earthquake Engineering & Structural Dy- namics*, vol. 31, no. 12, pp. 2023–2048, 2002.

[6] M. Shinozuka and C.-M. Jan, "Digital simulation of random processes and its applica- tions," *Journal of Sound and Vibration*, vol. 25, no. 1, pp. 111–128, 1972.

6

Coupled Time-Domain Aero-Hydro-Elastic Simulations of Offshore Floating Wind Turbines

SALEHYAR, Sara [1]; ZHU, Qiang [2]

[1] PhD Candidate, UC San Diego

[2] Associate Professor, UC San Diego

Corresponding Author: sssalehy@ucsd.edu

Compared with their land-based counterparts, offshore wind turbines possess clear advantage in their easy access to steady wind and mitigated impact upon human society. In terms of the abundance of offshore wind resource, the U.S. is ranked second in the world. Therefore, the development of offshore wind turbines is essential for our energy independence. Most of the offshore wind resources in U.S. (and elsewhere in the world) are located in places with water depth larger than 30 meters, so that it is critical to develop deep water wind turbine technology.

Offshore wind turbines installed in waters deeper than 60 meters usually have flexible mooring systems and are thus called floating systems. Existing designs of the floating wind turbines (except for the mooring systems) are borrowed from land based systems, especially the Horizontal Axis Wind Turbines (HAWT). However, it is clear that in deep water these turbines work under completely different conditions from land based or shallow water ones. On the other hand, these floating wind turbines are structurally different from any existing ocean platforms. Therefore, existing design codes for land based wind turbines or offshore structures cannot be directly applied. Dedicated experiments, numerical models, and prototype developments are requested to prove the feasibility and robustness of these devices and to explore special design requirements.

A linear frequency-domain model is suitable in studying long term responses of floating wind turbines excited by small to medium ocean waves, but it is not able to simulate large structure motions. It is also not convenient to study transient problems (due to the broadness of the frequency bandwidth involved as well as nonlinear effects). To study these effects, a nonlinear time-domain analysis is needed.

In our research, we have developed a nonlinear, coupled, hydrodynamic, aerodynamic and mooring cables model to study the responses of offshore floating wind turbines in time domain. For illustration, a spar-buoy-type floating wind turbine is used as a sample problem (Fig. 1)

Our hydrodynamic model is based upon 3D Mixed-Eulerian-Lagrangian (MEL) method. The basic procedure of free-surface simulation in this method is: (1) Assuming that the flow is potential, solve the boundary-value problem based on the location of the free surface and obtain its velocity; (2) update the position of the free surface based upon its velocity. The first step is done by a boundary-element model, in which singularities are distributed on the wetted surface of the body as well as the free surface. The second step is done using a 4th order Runge-Kutta time marching technique. A sample wave field around the tower of the turbine is illustrated in Fig. 2.

An unsteady wind-blade interaction model based on boundary elements has been developed to calculate the aerodynamic forces. This method avoids the inaccuracy associated with the slender-body approach and the quasi-static assumption in the currently popular Blade-Element-Momentum technique. This method achieves fully-3D and fully-unsteady simulations of the wind-blade interactions (Fig. 3). Specifically, this approach allows the accurate calculation of the wind-induced damping and added mass in relatively high frequencies.

A fully nonlinear cable dynamics model is used to simulate dynamics of the mooring system. In this model the bending, stretching, and torsional stiffnesses of a cable are all accounted for. With a dual Euler-Lagrangian approach this model is capable of simulating cables with arbitrary configurations and deformations.

These models enable fully nonlinear simulations of the dynamic responses of floating wind turbines, which are critical in studying the dynamics of these offshore structures in extreme conditions.

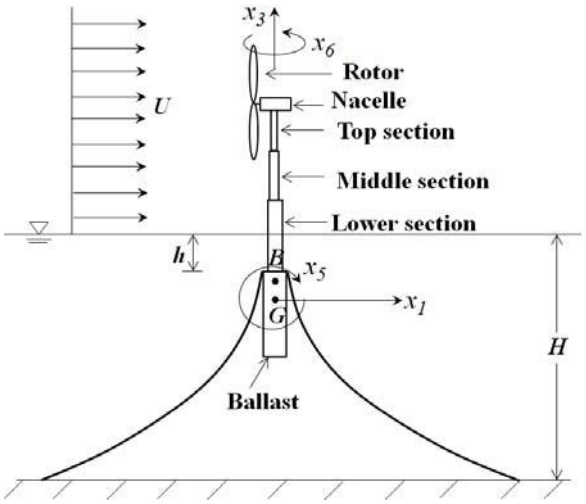

Figure 1: A 5 MW floating wind turbine based on the spar-buoy design.

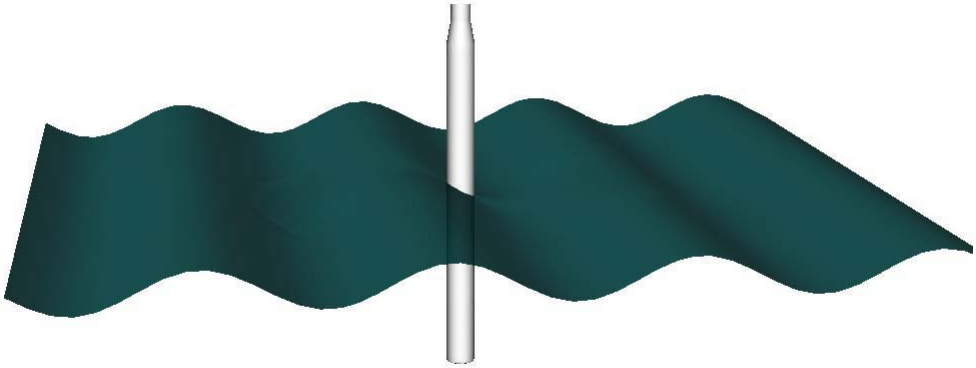

Figure 2: A sample wave field around the tower of the turbine.

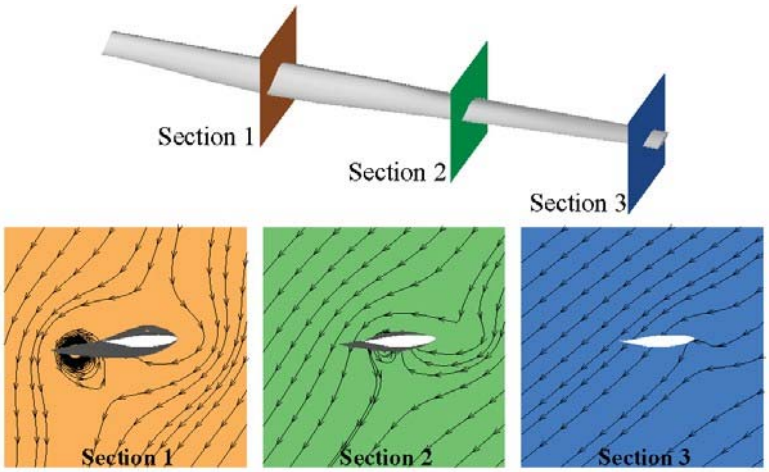

Figure 3: Cross-sectional views of the flow field near a blade.

49

Noise and Vibration Issues of Wind Turbines and Their Impact – A Review

Dr. SAMANTA, Biswanath [1]; Mr. SAAVEDRA, Rudolf [1]

[1] Georgia Southern University

Corresponding Author: bsamanta@georgiasouthern.edu

This paper presents a systematic review of current literature on the issues of noise and vibration of wind turbines and their impact on human health and wild life. The paper reviews the literature on the issues of noise and vibration in wind turbines, the generation mechanisms, the propagation, the impact on human health and wild life. The current status of technology and future developments to mitigate the health and environmental impacts of wind turbine noise and vibration are also reviewed. The paper includes a review of current standards on measurement of acoustic noise of wind turbines and data analysis.

60

Studying wind farm frequency regulation using high fidelity wind farm simulations

Mr. SHAPIRO, Carl [1]; Mr. MARTINEZ-TOSSAS, Luis [1]; Prof. MENEVEAU, Charles [1]; Prof. GAYME, Dennice [1]

[1] Johns Hopkins University

Corresponding Author: cshapir5@jhu.edu

Introduction: In the past, relatively insignificant installed wind power capacity meant that grid operators did not need wind power plants to participate in frequency regulation services. Over the past decade, however, wind power production has grown dramatically, with wind penetration levels exceeding 15% in several countries, such as Denmark, Portugal, and Spain [1]. As a result, grid operators are reevaluating frequency regulation requirements for wind farms. A number of system operators now require active curtailment of wind power for over-frequency regulation, and some system operators are also considering under-frequency regulation requirements for wind power plants [2].

Frequency regulation is provided by matching active power generation and demand over many time scales, ranging from seconds to hours, to maintain a stable grid frequency [3]. Recent studies have shown the feasibility of using stand-alone wind turbines for short- to medium-term frequency regulation by modulating the real power delivered through active power control [4, 5]. Active power control in wind farms, however, is complicated by aerodynamic interactions between turbines. When a wind farm changes operating conditions to provide frequency regulation, the wakes from upstream turbines will a□ect downstream wind conditions, thereby changing the power output of downstream turbines and potentially leading to unintended conse- quences. Therefore, a better understanding of these interactions is needed to develop e□ective controllers for wind farm frequency regulation.

In the current work, we study the use of wind farms for secondary frequency regulation, where participat- ing generators track a power production signal from the grid operator over a period ranging from minutes to an hour [3]. We propose using large eddy simulations (LES) [6, 7], a high fidelity simulation technique that numerically solves the filtered Navier-Stokes equations, coupled with the actuator line model (ALM) [8, 9]. This study is a first step towards demonstrating the usefulness of this approach, which allows for simulation of the aerodynamic impact of changes in the turbine operating state. First, we demonstrate that the qual-

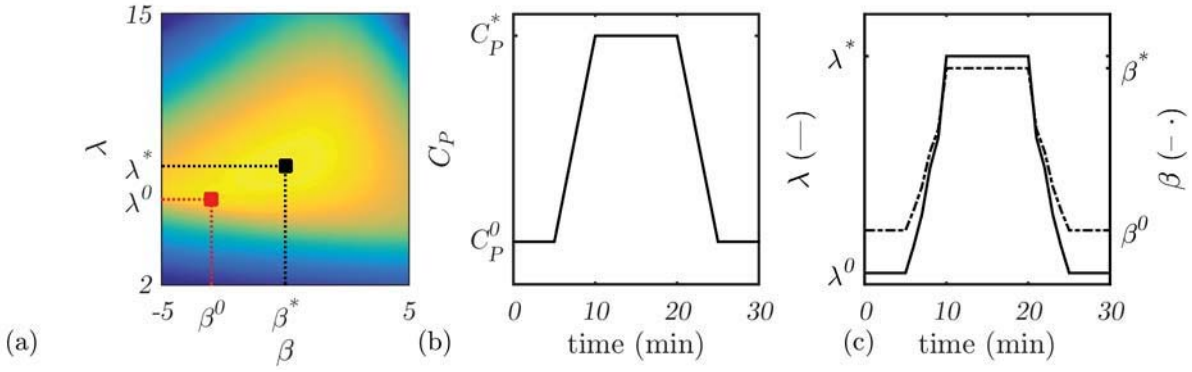

Figure 1: (a) Power coe□cient curve as a function of tip speed ratio, λ, and blade pitch angle, β, showing both the optimal (black) and range of possible derated (red) operating conditions. (b) An example grid operator power generation signal, shown in terms of the power coe□cient, and (c) a possible operating trajectory to follow this signal.

itative nature of the power coe□cient curves used in prior active power control approaches for stand-alone turbines can be replicated with LES-ALM on relatively coarse grids. We then illustrate the large e□ect of changes in operating conditions on downstream power production and the potentially complicated nature of these e□ects. Finally we discuss the implications of these results in terms of the development of frequency regulation controllers.

Prior work: Secondary frequency regulation is achieved by taking advantage of power coe□cient curves generated using simplified aerodynamic models [4, 5], for example based on blade element momentum (BEM) theory [10]. Traditional control strategies track an optimal power coe□cient, C_P^*, that occurs at a unique optimal blade pitch angle, β^*, and optimal tip speed ratio, λ^* [11]. Secondary frequency regulation controllers operate at a derated state, C_P^0, β^0, and λ^0, which leaves room for increased power generation by moving to the optimal state [4, 5]. As an example, a hypothetical power coe□cient curve is shown in Figure 1(a) with the optimal and derated operating states indicated on the axes. The wind turbine can follow a given power production signal provided from the grid operator, shown in Figure 1(b), by following a trajectory from the derated to optimal conditions, as shown in Figure 1(c).

LES-ALM power and thrust coefficients: In order to e□ectively study the impact of wake interactions and other turbulent flow characteristics on frequency controller e□cacy, it is important to reproduce certain trends in the power and thrust coe□cients of a real wind turbine. The power coe□cient should have a unique optimal value, and the thrust coe□cient should increase with increasing blade pitch angle and tip speed ratio. Given the relatively coarse grid resolution used in LES and the filtering of blade forces onto the LES grid, we need to employ a series of simulations to produce power and thrust coe□cient curves for the LES-ALM system.

These curves are generated by simulating a NREL 5MW reference turbine [12] with a steady uniform inflow velocity $U_\infty = 8$ m/s in a domain with streamwise and spanwise lengths of 2.048 × 1.024 km and a grid resolution of $\Delta x = \Delta y = \Delta z = 8$ m. Blade pitch angles and tip speed ratios are varied from -4 ° to 6 ° and 6 to 10, respectively, to generate the power and thrust coe□cient curves shown in Figure 2. These curves indeed replicate the qualitative behavior of curves generated from BEM theory. In particular, the power coe□cients have a peak at an optimal tip speed ratio and blade pitch angle, and the thrust coe□cients increase with increasing blade pitch angle and tip speed ratio.

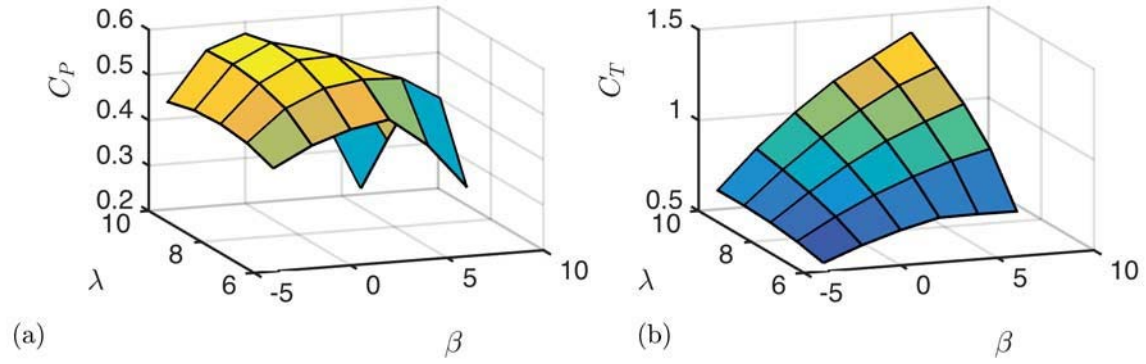

Figure 2: (a) Power and (b) thrust coe□cients as function of tip speed ratio, λ, and blade pitch angle, β, generated with LES-ALM using an inflow velocity of $U_\infty = 8$ on grid with $\Delta x = \Delta y = \Delta z = 8$ m.

Turbine interactions: The e□ects of active power control on downstream turbines are studied in a small wind farm with 24 turbines arranged in 4 streamwise rows and 6 spanwise columns in a $\pi \times \pi \times 1$ km domain, as shown in Figure 3. Inflow conditions are simulated using a concurrent precursor simulation [6] of the atmospheric boundary layer with the same domain size and grid resolution. Starting at time $t = 0$ we change the blade pitch angle of the the turbines in the first row and look at the response of the downstream turbines. Three cases are investigated, $\beta = 1\,^\circ$, $\beta = -1\,^\circ$, and $\beta = -2\,^\circ$, and power production P for each case is compared to the power production of the control case P_C with no changes in blade pitch angle, as shown in Figure 4.

Pitching to feather (negative pitch angles) reduces the thrust coe□cient, resulting in higher upwind

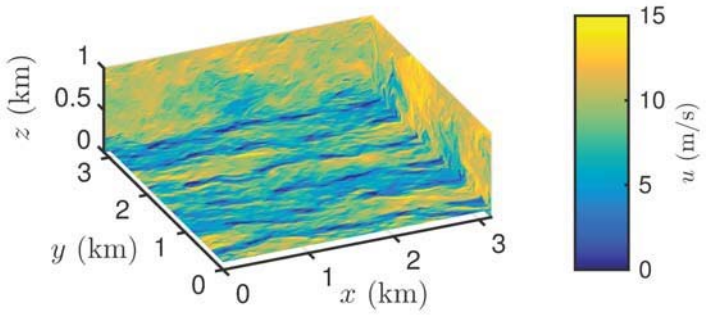

Figure 3: Streamwise velocity of wind farm with 24 turbines. Flow is in the positive x-direction, and wakes are clearly visible behind each turbine.

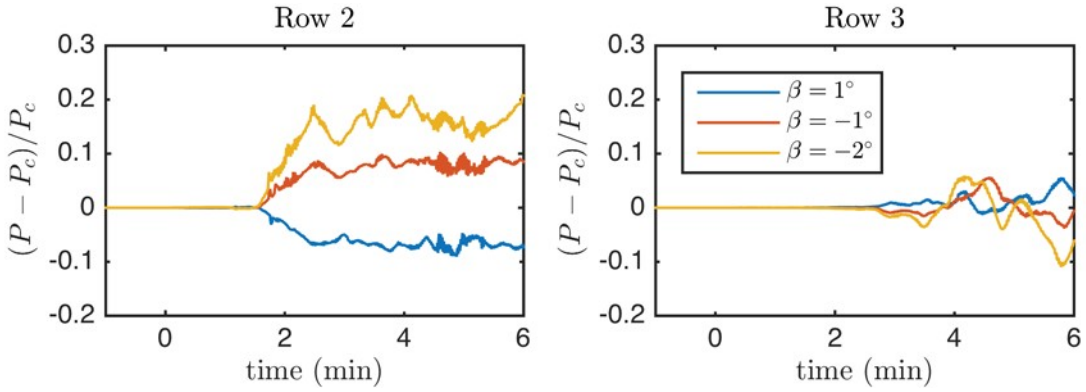

Figure 4: Average change in power production across each row P to the control case P_c for three treatment cases, where the first row of turbines are pitched to a set angle at $t = 0$.

velocities and power production for the downstream turbines. Conversely, pitching to stall (positive pitch angles) results in lower upwind velocities and power production for the downstream turbines. The change in power production for the downstream turbines has a time delay roughly equal to the convective time scale between turbines (i.e. the time that it takes for the wind to travel from one row to another). This time is 1.64 minutes for a hub-height velocity of roughly 8 m/s. Furthermore, the change in power output is large, corresponding to 10–20% of the power output in the control case.

These inter-turbine interactions will have interesting economic implications for wind farm frequency con- trollers. While the time delay between turbines could complicate frequency regulation control by reducing operational flexibility, the large relative e□ect of operational changes on downstream turbines could be lever- aged to reduce the size of the steady-state derate (i.e. the di□erence between the operating power coe□cient, C_P^0, and the optimal power coe□cient, C_P^*) that is used to increase power production while providing frequency regulation service. Reducing the derate would have large economic benefits by increasing steady state power production when the grid operator does not call for frequency regulation services. Additional economic benefits could be realized through reduced structural loading caused by the control strategy.

This work is supported by the National Science Foundation (SEP 1230788 and IIA 1243482, the WINDIN- SPIRE project).

References

[1] Wiser, R. *et al.* 2012 Wind technologies market report. Tech. Rep. DOE/GO-102013-3948 (2013).

[2] Mohseni, M. & Islam, S. M. Review of international grid codes for wind power integration: Diversity, technology and a case for global standard. *Renewable and Sustainable Energy Reviews* **16**, 3876–3890 (2012).

[3] Rebours, Y. G., Kirschen, D. S., Trotignon, M. & Rossignol, S. A survey of frequency and voltage control ancillary services—Part I: Technical features. *IEEE Transactions on Power Systems* **22**, 350– 357 (2007).

[4] Ma, H. & Chowdhury, B. Working towards frequency regulation with wind plants: combined control approaches. *IET Renewable Power Generation* **4**, 308–316 (2010).

[5] Aho, J. *et al.* A tutorial of wind turbine control for supporting grid frequency through active power control. *American Control Conference* 3120–3131 (2012).

[6] Stevens, R. J., Gayme, D. F. & Meneveau, C. Large eddy simulation studies of the effects of alignment and wind farm length. *Journal of Renewable and Sustainable Energy* **6**, 023105 (2014).

[7] Stevens, R. J., Graham, J. & Meneveau, C. A concurrent precursor inflow method for large eddy simulations and applications to finite length wind farms. *Renewable Energy* **68**, 46–50 (2014).

[8] Martínez-Tossas, L. A., Churchfield, M. J. & Leonardi, S. Large eddy simulations of the flow past wind turbines: actuator line and disk modeling. *Wind Energy* (2014).

[9] Martínez, L. & Meneveau, C. A study of two subgrid-scale models and their effects on wake breakdown behind a wind turbine in uniform inflow. *Bulletin of the American Physical Society* **59** (2014).

[10] Burton, T., Jenkins, N., Sharpe, D. & Bossanyi, E. *Wind Energy Handbook* (John Wiley & Sons, 2011).

[11] Johnson, K. E., Pao, L. Y., Balas, M. J. & Fingersh, L. J. Control of variable-speed wind turbines: Standard and adaptive techniques for maximizing energy capture. *IEEE Control Systems Magazine* **26**, 70–81 (2006).

[12] Jonkman, J. M., Butterfield, S., Musial, W. & Scott, G. Definition of a 5-MW reference wind turbine for o□shore system development. Tech. Rep. NREL/TP-500-38060 (2009).

38

A Fixed-Wake Vortex Line Method for Aerodynamic Analysis and Optimization of Multi-Rotor Wind Turbines

Mr. ROSENBERG, Aaron [1]; Prof. SHARMA, Anupam [1]

[1] Iowa State University

Corresponding Author: sharma@iastate.edu

The objective of this paper is to extend the xed wake vortex lattice method (VLM), used to evaluate the performance of single-rotor wind turbines (SRWT), for use in analyzing dual-rotor wind turbines (DRWT). VLM models wind turbine blades as bound vortex laments with helical trailing vortices. Using the Biot-Savart law, it is possible to calculate the induction in the plane of rotation allowing for a computationally inexpensive, yet accurate, prediction of blade loading and power performance. This paper presents a method for modeling the additional vortex system introduced by a second rotor while taking into account the singularities that occur when the trailing vortices from the upstream turbine interact with the bound vortices of the down-stream turbine. Time averaging is done to account for the rotors operating at di erent rotational velocities. This method will be used to predict the performance of the DRWT introduced in Rosenberg et al. (2014). This turbine consists of a large, primary rotor behind and a smaller, auxiliary rotor. Blade loading and power performance obtained with VLM will be compared to the LES results of the same con guration presented in Moghadassian et al. (2015).

53

Flare Reduction Technique for Near-Surface Airfoil Boundary Layer Measurements with Laser Diagnostics

Dongyun Shin, Daniel R. Cadel, and K. Todd Lowe
Department of Aerospace and Ocean Engineering
Virginia Tech, Blacksburg, Virginia

A laser flare reduction technique involving a new application of transparent-material additive manufacturing and semitransparent fluorescent surface treatment is demonstrated for near-wall boundary layer velocity measurements on an airfoil. This work is of interest to the wind energy community, as near-wall measurements can lead to more accurate models and design tools for new blade designs with minimum drag. Further, detailed, near wall validation data may be obtained for comparison to simulations. High reflection from solid surfaces has been a common issue when conducting measurements with laser diagnostic techniques such as Doppler Global Velocimetry (DGV) (Cadel et al. 2014) or Particle Image Velocimetry (PIV) (Prasad et al. 2000). Laser flare is caused by reflected light from the airfoil surface that saturates pixels of a camera sensor, resulting in a loss of information in the measurement region. In order to acquire data in this near-surface region, the laser flare needs to be sufficiently reduced.

Light interacts with surfaces in four ways. It can be scattered from the surface, causing the laser flare; reflected in a highly directional specular reflection; absorbed by a surface material; or transmitted through the material. Several efforts have sought to mitigate the first effect by utilizing the reflection/absorption/transmission properties of certain materials and finishes. Konrath et al. successfully used a combination of reflection and absorption to make optical flow measurements down to the nominal surface (Konrath et al. 2007). Paterna et al. reduced a direct laser light reflection from 7 up to 30 times by using Rhodamine 6G solution (Paterna et al. 2013). Lee et al. also used a Rhodamine 6G solution on a black anodized wing model to reduce the laser flare (Lee et al. 2010).

In the current work, a combination of absorption and transmission was used to reduce laser flare at the surface. Transmission of light through the surface was achieved by using a 3D-printed, transparent section of a DU96-W-180 wind turbine blade airfoil (Figure 1). The 2 inch-span section was assembled at center-span of a multi-laminate, 32 inch span model. By letting a portion of the light pass through the surface, the degree of scattering and reflection was reduced. Absorption was achieved by employing a fluorescent dye similar to that used by Lee et al. (2010) Frequency-doubled lasers such as Nd:YAG-, Nd:YLF-, and Nd:YVO_4-based systems are commonly used in velocimetry techniques, including PIV and DGV. A fluorescent dye known as Rhodamine 6G (Rh6G) was selected because of its high absorption at the 527 nm and 532 nm wavelengths emitted by these lasers. The subsequent peak re-emission of light at 570 nm (Zehentbauer et al. 2013) was rejected from images via a narrow band-pass filter passing 513 nm – 538 nm, in front of the camera lens. Since Rh6G emits in the yellow-orange color range, the camera sensor detects a minimal amount of surface-scattered green light.

In the course of development, several combinations of surface preparations, treatments, and model materials were tested. The best flare reduction was obtained by using the transparent airfoil segment with the Rh6G surface treatment applied, such that the Rh6G surface treatment absorbed the scattered light due to the index of refraction changes and re-emitted at high wavelength, while the transparent laminate transmitted some of the light not absorbed by the Rh6G. Using this mechanism, it was identified that the highest flare reduction occurred with a solution of Rhodamine 6G, ethanol, and

transparent paint in preliminary tests. Ethanol was chosen as a solvent because Rh6G has a high solubility in ethanol. The recipe for this optimal solution was found experimentally after a review of

the available literature, mainly Paterna et al. (2013), and Lee et al. (2011). As shown in Figure 1, the fluorescent paint mixtures were applied using a standard airbrush.

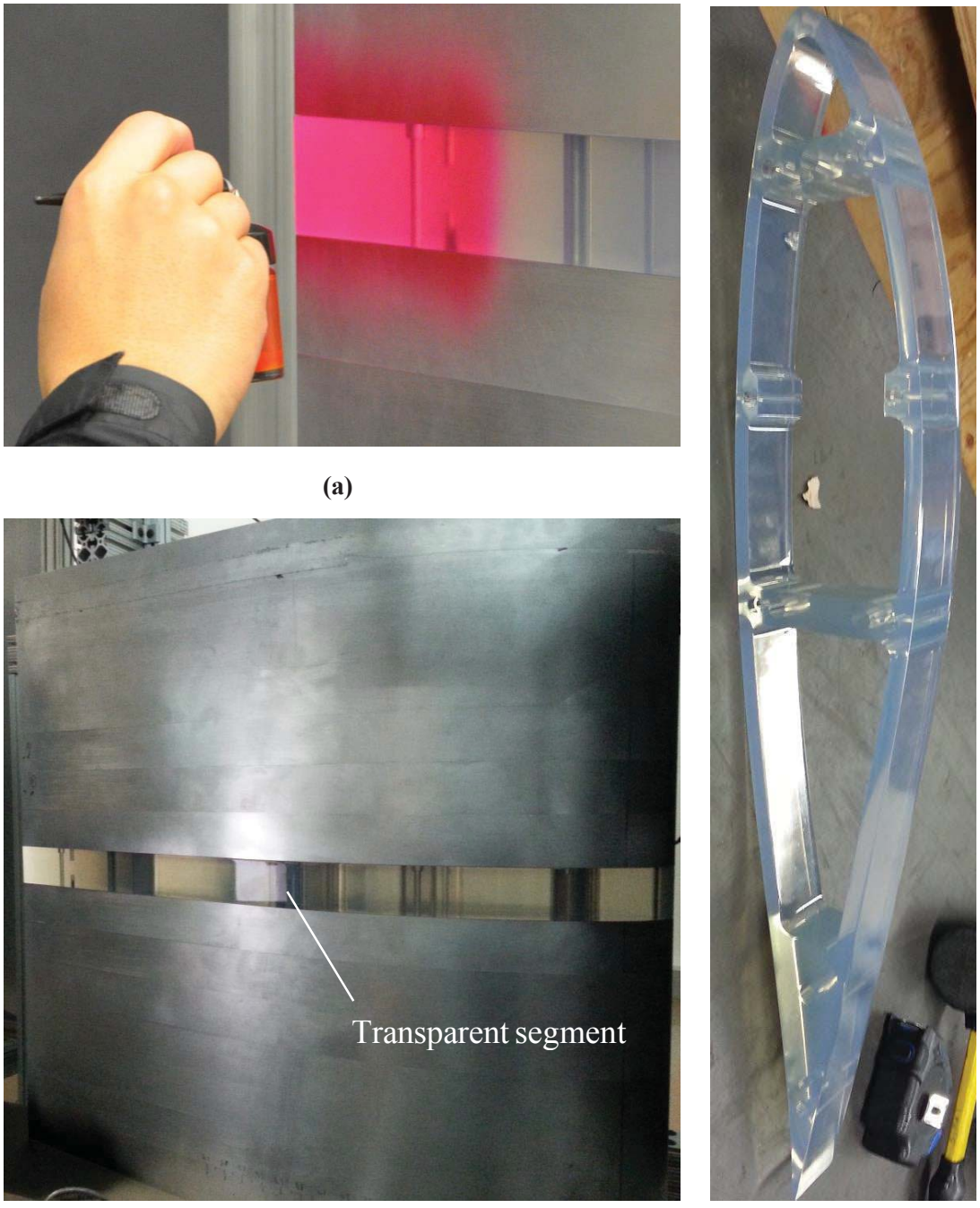

(a) **(b)** **(c)**

Figure 1. Spraying Rh6G solution with airbrush on the transparent airfoil segment (a), DU96-W-180 airfoil model with transparent segment at center span (b), 3D transparent airfoil segment (c)

Pierce et al. found the choice of camera viewing angle to be the most straightforward way to achieve a reduction in observed surface flare (Pierce et al. 2011). By giving 90 degrees of angle between the camera lens and the plane of the airfoil surface, the solid angle from the camera sensor to the solid surface is minimized. This 90 degree angle is referred to as a 'grazing angle'.

The current flow measurements were made in the Virginia Tech Open Jet Wind Tunnel facility with planar PIV. This facility has a 0.7m x 0.7m of exit and powered by a 30 hp BC-SW Size 365 Twin City centrifugal fan capable of up to 15m3/s. At a maximum fan speed of 1180 RPM, the flow exits the 5.5:1 contraction at 30m/s. In this experiment, the airfoil was fixed at 0 degree of angle of attack with constant free-stream flow resulting in a chord Reynolds number of 887,000. A laser light sheet was directed perpendicular to the transparent airfoil segment in the streamwise/wall normal plane. By imaging the Sebecate (DEHS) seeding, the displacement of the seeding particles can be calculated, from which velocity may be inferred.

A quantitative measure of the laser flare is presented in Figures 2 for four different cases: untreated metal (baseline), treated metal, untreated transparent, and treated transparent. All four cases exhibit nearly the same level of maximum flare, directly on the surface, where the camera is saturated. Just away from the surface, however, all signals drop at different rates, approaching an apparently asymptotic state beyond x = 70 pixel units (on the order of serveral millimeters). The close-up region of interest is shown in Figure 3. In this region, the smallest intensity decrease occurred with the baseline case due to a high level of scattering from the surface to the flow. Figure 3 exhibits clearly why the reated transparent case performed best. It decreased the most and provided a higher signal-to-noise ratio, nearer to the surface, than any other methods.

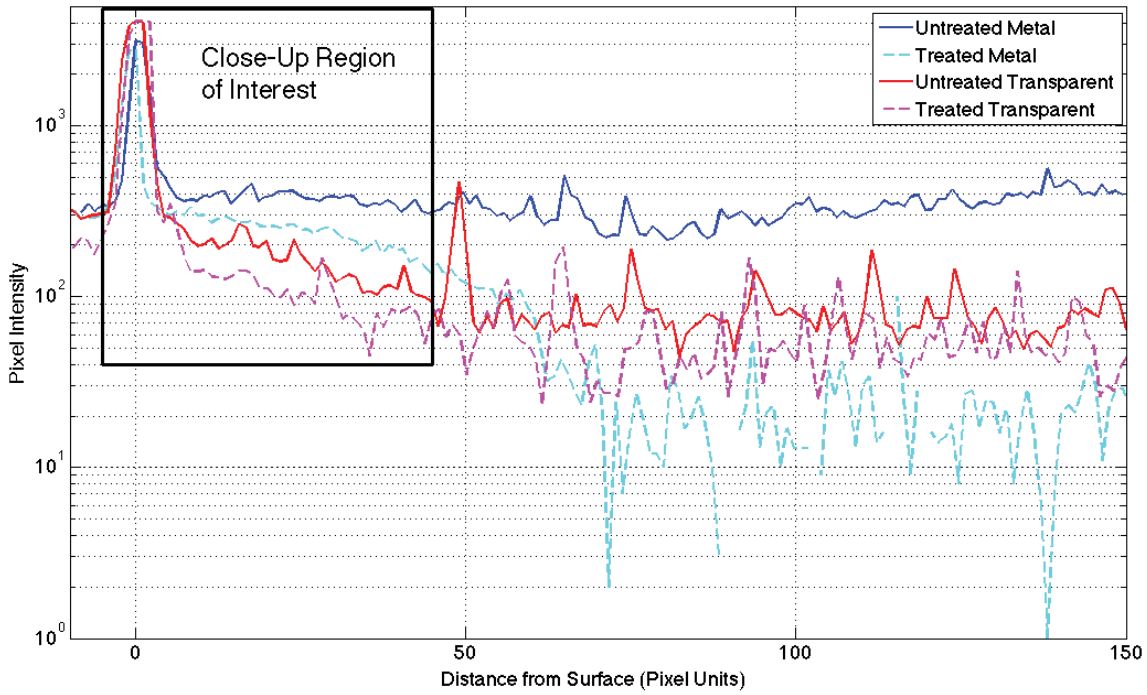

Figure 2. Profiles of camera pixel intensity along a trajectory normal to the surface just upstream of the model trailing edge. All signals have the same approximate peak intensity, and all but the baseline reach approximately the same steady state value at a sufficient distance from the surface

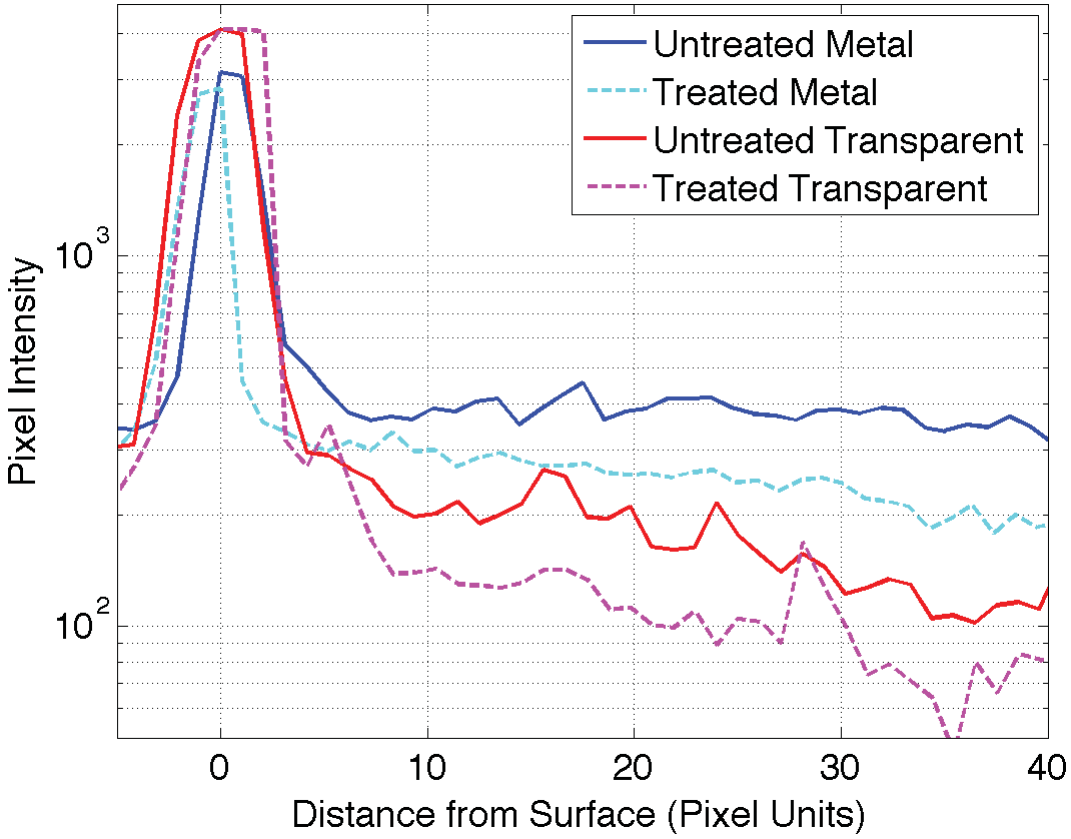

Figure 3. Close-up view of the pixel intensity profiles near the surface of the model. The Rh6G treated transparent laminate exhibits the fastest drop-off in intensity in this region, making it best suited amongst these cases for resolving near-wall particles.

A map of mean velocity magnitude is shown in Figure 4. Data were acquired at 5000 Hz using sequential image correlation with a minimum of 1000 images. Velocity profiles at x/c = 0.95 and the trailing edge are presented in Figures 5 and 6, respectively, for the transparent laminate with Rh6G treatment. With the surface treatment, PIV could obtain the velocity profile within 4.94 mm from the airfoil surface. The results show that the combination of the surface treatment and transparent segment is a very promising technique that can reduce the intensity of laser flare effectively. By developing this technique further, better measurement of the velocity profile near the surface is expected.

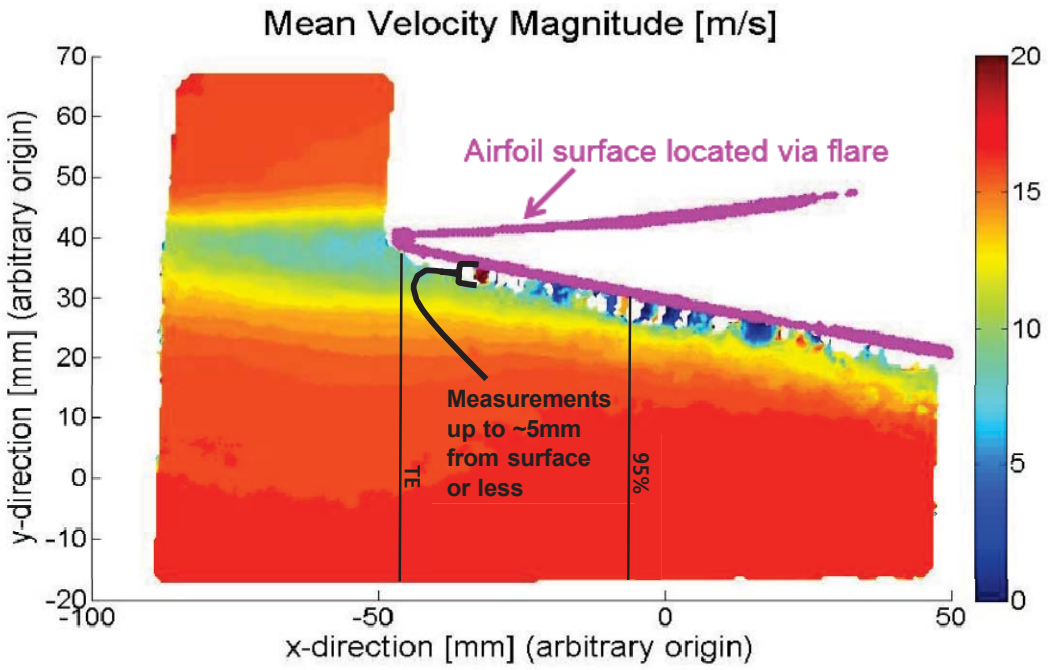

Figure 4. The mean velocity profile in boundary layer of the airfoil.

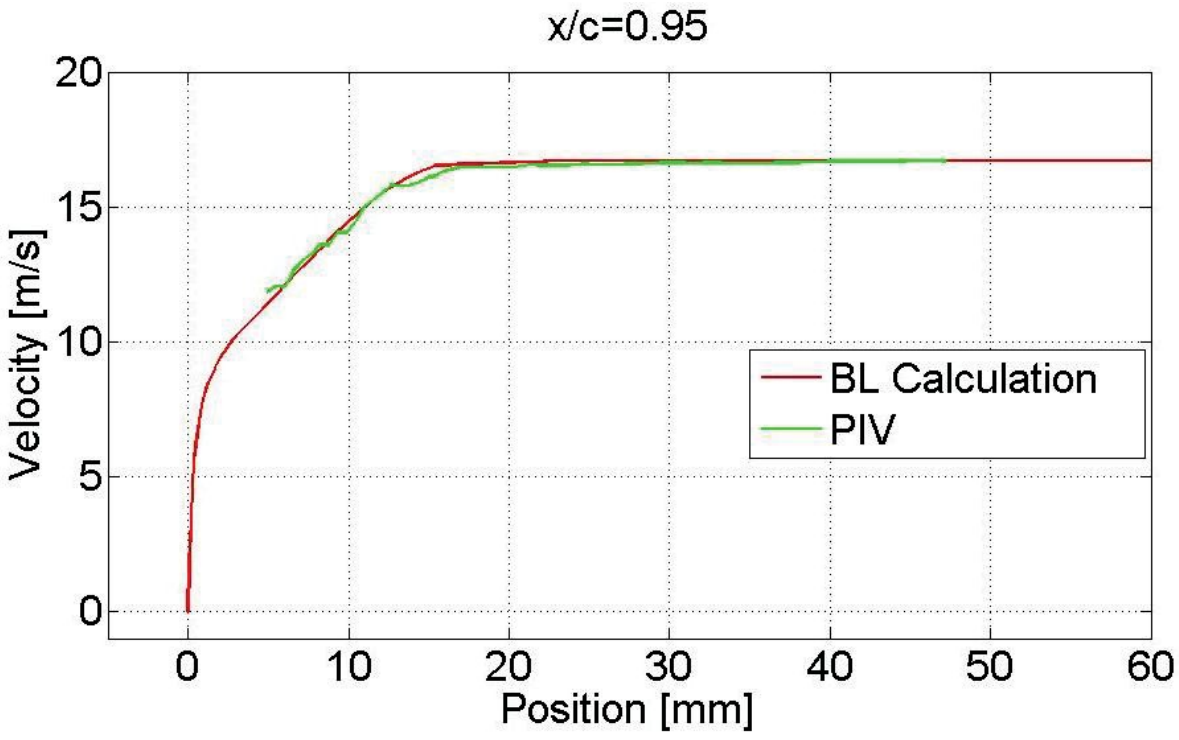

Figure 5. Comparison between Boundary layer calculation and PIV result at x/c =0.95 of the airfoil.

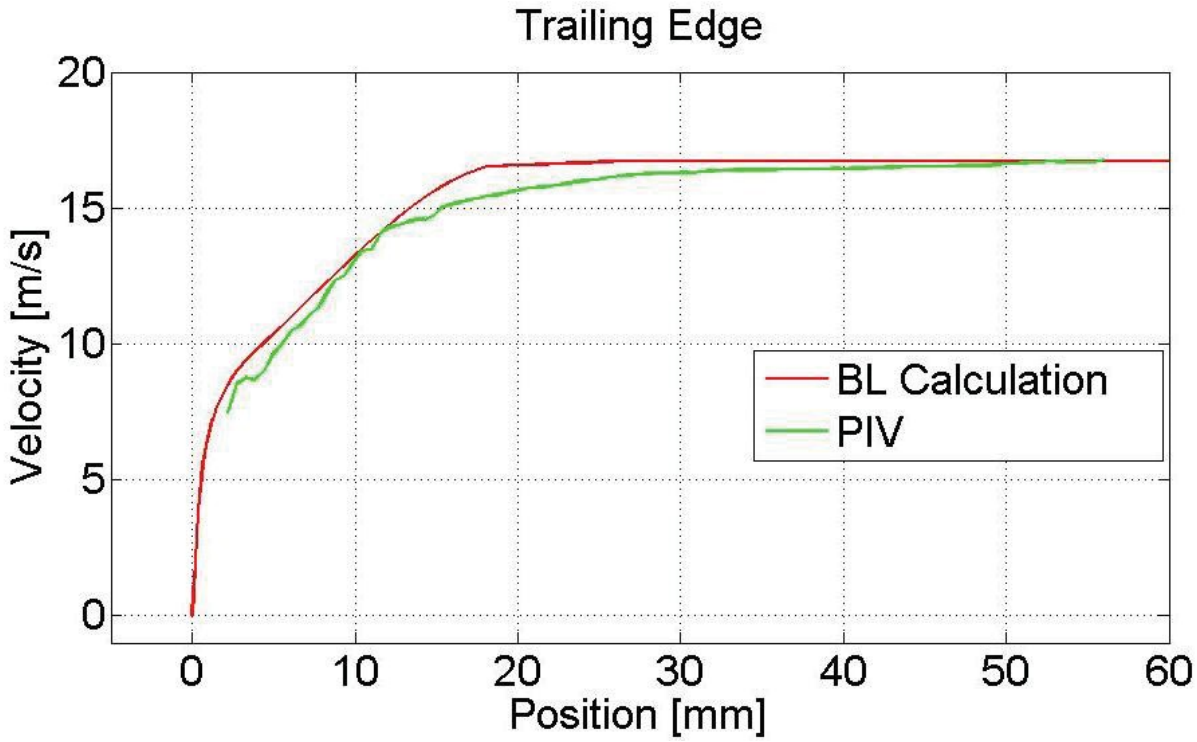

Figure 6. Comparison between Boundary layer calculation and PIV result at trailing edge of the airfoil.

Reference

Cadel DR, Ecker T, Lowe KT. 2014 Time-Domain Cross-Correlation Scan DGV (CCS-DGV) for Mean-Velocity Boundary Layer Measurements 52nd Aerospace Sciences Meeting; 2014; AIAA 2014-1104.

Prasad AK. 2000 Particle image velocimetry Current Science, Vol. 79, No. 1, 2000.

Konrath R, Klein C, Schro¨der A, Kompenhans J. 2007 Combined application of pressure sensitive paint and particle image velocimetry to the flow above a delta wing Exp. Fluids;2008; 44:357–366.

Paterna E, Moonen P, Dorer V, Carmeliet J. 2013 Mitigation of surface reflection in PIVmeasurements Meas. Sci. Technol. 24;2013; 057003

Pierce AJ, Lu FK. 2011 New Seeding and Surface Treatment Methods for Particle Image Velocimetry 49th AIAA Aerospace Sciences Meeting including the New Horizons Forum and Aerospace Exposition;2011;AIAA 2011-1164.

Schröder A, Agocs J, Frahnert H, Otter D, Mattner H, Kompenhans J, Konrath R. 2006 Application of Stereo PIV to the VFE-2 65° Delta Wing Configuration at Sub- and Transonic Speeds 24th Applied Aerodynamics Conference;2006;AIAA 2006-3486.

Meyers JF, Lee JW, Cavone AA. 2010 Boundary layer measurements in a supersonic wind tunnel using Doppler global velocimetry 15th Int. Symp. on Applications of Laser Techniques to Fluid Mechanics; Lisbon, Portugal, 05-08 July, 2010.

Lee T. 2010 PIV study of near-field tip vortex behind perforated Gurney flaps Exp. Fluids; 2011; 50:351–361; doi:10.1007/s00348-010-0933-x

Chennaoui M, Angarita-Jaimes D, Ormsby MP, Angarita-Jaimes M, McGhee M, Towers CE, Jones AC, Towers DP. 2008 Optimization and evaluation of fluorescent tracers for flare removal in gas-phase particle image velocimetry *Meas. Sci. Technol.* 19; 2008; 115403 (8pp) doi:10.1088/0957-0233/19/11/115403.

Zehentbauer FM, Moretto C, Stephen R, Thevar T, Gilchrist JR, Pokrajac D, Richard KL, Kiefer J. 2013 Fluorescence spectroscopy of Rhodamine 6G: Concentration and solvent effects Spectrochimica Acta Part A: Molecular and Biomolecular Spectroscopy 121 (2014) 147–151.

71

Convergence of Extreme Loads for Offshore Wind Turbine Support Structures

Mr. STEWART, Gordon [1]; Prof. LACKNER, Matthew [1]; Prof. ARWADE, Sanjay [2]; Prof. MYERS, Andrew [3]; Mr. HALLOWELL, Spencer [3]

[1] University of Massachusetts Amherst

[2] University of Massachusetts

[3] Northeastern University

Corresponding Author: gmstewar@gmail.com

Extreme loads of wind turbines are historically difficult to predict through simulation due to uncertainty in input conditions as well as in the simulation models. In addition, many long time series must be simulated for the statistics of the peak loads to become stationary. Offshore wind turbines require even more simulation due to the addition of stochastic wave loading. Floating offshore wind turbines, the subject of this paper, experience free-body motion as a result of wind and wave loading, and the phasing of wind turbulence, turbine motion, and large waves can be very influential in determining extreme loading. The International Electrotechnical Commission's 61400-3 standard covers loads analysis of offshore wind turbines, including only cursory references toward floating offshore wind turbines. This IEC design standard requires six 1-hour simulations to estimate extreme loads, which is not long enough for convergence of the statistics of peak loads for offshore turbines, especially floating turbines, which have higher and more variable loads due to platform motion.

In this paper, 50-year wind and wave conditions are synthesized from data from the National Oceanographic and Atmospheric Administration's (NOAA's) floating data buoys for a suite of ocean sites suitable for floating or fixed bottom offshore wind turbines. The simulation software used in this paper is FAST, developed by the National Renewable Energy Laboratory, which is a coupled aero-hydro-servo-elastic wind turbine design tool. The current version of FAST which is used in this research includes second-order hydrodynamic effects, which may be important sources of loading in extreme conditions for certain floating platforms. TurbSim is used to create full-field turbulent wind files using the mean wind speed determined from the buoy data, while the hydrodynamics module within FAST handles the wave height time series using a JONSWAP spectrum. The OC3 spar buoy and the OC4 semi-submersible floating platforms are used as examples of realistic platform designs and a monopile is used as the fixed bottom example. A large number of 1-hour simulations are run to determine the convergence characteristics of each platform at each ocean site. These results are discussed and recommendations for future revisions of the design standard are made. Future work concerning various methods that will reduce the simulation cost of determining the converged extreme load will also be discussed.

18

Experimental Study of Turbulence Influence on Wind Turbine Performance

TALAVERA, Miguel [1]; Dr. SHU, Fangjun [1]

[1] New Mexico State University

Corresponding Author: matl06@nmsu.edu

Regarding the issue about unmatched Reynolds number for downscaled wind turbine tests in wind tunnels, a study of the performance characteristics of a model wind turbine operating in the wake of another turbine of the same model under laminar and turbulent inflow was performed. The distance between the two turbines was set at 5, 10, and 15 turbine diameters. In the laminar inflow case, due to the low recovery rate in the wake of the front turbine, the efficiency of the rare turbine has been greatly reduced even when the distance was 15 diameters. To address this issue, turbulent inflow was created using an active grid system installed between the contraction and test-section of the wind tunnel; the maximum turbulence intensity can reach 203. Velocity fields upstream and in the wake of the turbine were measured using a 2D-PIV system; 1000 pairs of images were acquired for each location to achieve statistical convergence. It was found that by using turbulent inflow the efficiency of both the upstream and the downstream turbine was highly improved. Also, it was found that the efficiency of both turbines is highly related to the turbulence intensity in the inflow. At a constant tip speed ratio for the upstream turbine of 10.3, and a distance of 5 diameters between them, the efficiency for the downstream turbine was 4.1 times higher than in laminar case; for 10 and 15 diameters with the same conditions it was 2.71, and 2.48 times higher respectively. The maximum efficiencies reached for the downstream turbine were 38.53, 34.53, and 24.63 for 15, 10, and 5 diameters of distance between respectively. Therefore, despite the low Reynolds number, a high efficiency close to the field was reached using turbulent flow created by an active grid system.

METHODS AND RESULTS

Experimental Setup

In this study, two-blade wind turbines with a 20.3cm diameter (D=20.3cm) were used. Two wind turbines were installed in a low-speed wind tunnel with test-section dimension of 1.4mx1.4mx14.6m. Distance between the wind turbines was adjustable. An active grid system was used to generate controllable inflow turbulence. An ATI Nano force and torque sensor was used to measure the efficiency of the turbines and a 2D planer PIV system was used to measure the flow fields up- and downstream of the turbines. A schematic of the experimental setup was presented in Figure 1, in which the distance between the two turbines was set at 10D.

(Please see figure in the attached file.)
Figure 1. Wind turbines array and PIV testing sections

Efficiency Measurements

Using a torque sensor (NANO 7 IP68) mounted on the wind turbines the harvested energy and efficiency of the turbines were studied. These experiments were conducted in two turbines, operated with one turbine in the wake of another under laminar and turbulent flow inflow conditions. Two variables were manipulated in the experiment: the distance between turbine and turbine, e.g. 5D, 10D and 15D (, where D is the diameter of the turbine); and the tip-speed-ratio (TSR) of the upstream wind turbine. For the laminar case, the tip speed ratio of the upstream wind turbine was set at 8 different ratios within the rage of 5.6-8.9. And for the turbulent case, within the range of 4.7-10.9. For both cases, the harvested energy was calculated using the product of torque and the angular speed of the turbine. Some results of the downstream turbine are presented in figure 2, in which the upstream wind turbine tip speed ratio was set at 10.3 for turbulent flow, and 5.6 for laminar flow.
(Please see figure in the attached file.)
Figure 2. Downstream wind turbine power coefficient versus tip speed ration for a) 5 diameters, laminar flow, b) 5 diameters, turbulent flow, c) 10 diameters, laminar flow, d) 10 diameters, turbulent flow, e) 15 diameters, laminar flow, f) 15 diameters, turbulent flow.
From Figure 2, great improvement in turbine efficiency was found when the inflow is turbulent. For the case using a 5D distance, the maximum efficiency was 4.1 times higher using turbulent flow. For the 10D and 15D distances, the maximum efficiency was 2.71 and 2.48 times higher respectively. Which provided efficiencies

much closer to the ones in the field than the laminar performance.

PIV Measurements

To understand why the wind turbine performance increased in turbulent flow condition, 2D PIV measurements were taken in various regions. In each region, 1000 pairs of particle images were acquired to achieve statistical convergence. The locations for PIV measurement were shown in Figure 1. These locations were chosen to study the flow recovery downstream of the turbines and the influence of turbulence intensity. For each conditions, flow upstream of the front turbine was also measured. The PIV measurements were performed using a high (103) and low (33) turbulence intensity in the inflow so a comparison on the flow using these two can be made.

In figure 3, the velocity profiles for the four regions under high and low turbulence intensity are presented, notice that the velocity magnitude has been normalized using the free stream velocity. The corresponding turbulence intensity contours were presented in figure 4. In region 1, the inflow is approximately uniform before approaching the wind turbine. In regions 2 and 3, the turbulence intensity was still higher for the high turbulent inflow case, which caused fast velocity recovery in the wake. This explained the significantly greater efficiency in the rare wind turbine under turbulent inflow conditions.

(Please see figure in the attached file.)

Figure 3. Normalized velocity profile in the 4 measurement regions indicated in Figure 1. First row: high turbulence intensity (TI=103); second row: low turbulence intensity (TI=33)

In region 4 the turbulence intensity was comparable to that in regions 2 and 3, approximately 303, for both low and high TI cases (see figure 4). The velocity profiles for this section were similar as well (figures 3). This is because the turbulence intensity downstream of the second turbine is almost independent of the inflow turbulence, due to the disturbance generated by the two turbines.

(Please see figure in the attached file.)

Figure 4. Turbulence intensity in the 4 measurement regions indicated in
Figure 1. First row: high turbulence intensity (TI=103); second row: low turbulence intensity (TI=33)

CONCLUSIONS

An experimental investigation has been performed to find a solution regarding the issue of unmatched Reynolds number for downscaled wind turbines test in wind tunnels. A wind turbine was tested operating in the wake of another turbine under turbulent inflow conditions with different turbulence intensity. It was found that the efficiency of both turbines, upstream and downstream, had highly improved when the inflow was turbulent. Also PIV measurements were taken in the wake of both wind turbines. It was concluded that the flow recovery in the wake downstream of the first wind turbine highly depends on the turbulence intensity in the inflow. For a higher turbulence intensity, a faster recovery has been observed. However, it was also found that the flow recovery downstream the second turbine was almost not influenced by the initial turbulence intensity. At this point the flow was greatly affected by the two wind turbines and the initial conditions of the inflow, in terms of turbulence, were no longer important.

52

A Cost Benefit Analysis of Electricity Generation

THOMSON, Heather [1]; Dr. KEMPTON, Willettt [1]

[1] University of Delaware

Corresponding Author: hthomson@udel.edu

This talk presents a cost-benefit analysis of three main fuels for electricity generation, namely coal, natural gas, and wind. This analysis incorporates social costs and benefits along with traditionally utilized private costs and benefits. The author has recently completed a study monetizing the visual and auditory amenity and disamenity of wind turbines and coal fired power plants, and also natural gas plants, by extension. This analysis utilizes that study and other recent studies on the impacts of electricity generation on water use, wildlife, and property values, among others, as well as other impacts well documented in the literature. Therefore it is the most current cost-benefit analysis of electricity generating facilities. It then examines the policy implications of the analysis.

7

Freewake simulation and POD analysis of two non-aligned turbines in a row

Dr. TUGLUK, Ozan [1]; Dr. SEZER-UZOL, Nilay [2]; Dr. UZOL, Oguz [3]

[1] METUWIND METU/Ankara

[2] TOBB University of Economics and Technology, Ankara, Turkey

[3] Department of Aerospace Engineering, Middle East Technical University (METU), Ankara, Turkey

Corresponding Author: tugluk@metu.edu.tr

The present paper is composed of two main parts. In the first part, the test case for NTNU's blind-test workshop 3 geometry is simulated using an in-house GPU accelerated free-wake code. In the second part, the unsteady database created by the free-wake simulation is used to perform a Proper Orthogonal Decomposition (POD or Karhunen-Loeve decomposition). POD of wind turbine wakes was formerly performed on various studies based on high-fidelity CFD data. While free-wake simulations present lower fidelity solutions in comparison to well-resolved, high-order CFD simulations, they are computationally less expensive, enabling longer time integration of turbine wakes. Furthermore the use of the emerging streaming architectures (in the present case Graphics Processing Units) dramatically accelerates the free-wake simulations, exploiting the inherent parallelism in the underlying algorithms.

24

Effects of Tip Injection and Mie Vanes on the Performance of a Model Wind Turbine Rotor

Mr. ABDULRAHIM, Anas [1]; Ms. ANIK, Ezgi [1]; Prof. UZOL, Oguz [1]

[1] METU Center for Wind Energy

Corresponding Author: uzol@metu.edu.tr

This paper presents the results of an ongoing experimental investigation of the effects of tip injection, as well as V-shaped Mie Vanes on the performance of a model wind turbine rotor. Experiments are conducted by placing a three-bladed horizontal axis wind turbine rotor at the exit of an open-jet wind tunnel facility. It is observed that tip injection has significant effects on the power and thrust coefficient variations especially at higher TSR values beyond max CP TSR. Results of the effects of tip injection as well as Mie vanes on the power and thrust coefficient variations with Tip Speed Ratio (TSR) for several wind speeds and comparisons with baseline data will be presented in the final paper.

Characterizing long-time variations in fully developed wind-turbine array boundary layers using Proper Orthogonal Decomposition

Claire VerHulst, Charles Meneveau

Johns Hopkins University, Department of Mechanical Engineering and Center for Environmental and Applied Fluid Mechanics, Baltimore, MD,
cverhul1@jhu.edu and meneveau@jhu.edu

ABSTRACT

Temporal variation of wind-farm power production is caused, in part, by the presence of large-scale flow structures in the turbulent atmospheric boundary layer. Such structures can span several thousand meters, and they interact with the wind turbines in a non-trivial fashion. The purpose of this study is to identify the flow features and characterize their evolution in time. To unambiguously identify structures in the complex atmospheric flow around a wind farm, snapshot proper orthogonal decomposition (POD) has previously been applied to thousands of three-dimensional turbulent velocity fields around an infinitely large array of wind turbines [1]. The POD analysis determined the flow structures, spanning the entire domain, that contributed the greatest time-averaged fraction of turbulent kinetic energy in the domain. The most prominent spatial features identified in the atmospheric flow using POD are classified into one of three types: roller modes, oblique modes, and shear modes. The previous study focused on entrainment of mean kinetic energy, which replenishes the flow in the fully developed region. The current study examines the time evolution of the atmospheric large-scale structures (i.e. POD modes) and their impact on power production in a fully developed wind farm.

For this analysis, large eddy simulations (LES) with periodic boundary conditions in the horizontal directions are used to simulate an infinite array of wind turbines. In cases where the streamwise extent of the wind farm exceeds the height of the atmospheric boundary layer by an order of magnitude, the wakes merge such that the flow becomes fully developed and is well represented by an infinite wind farm. In this state, there is a balance between the roughness of the wind farm and the forcing of the atmospheric boundary layer. This fully developed region, the focus of the present study, is especially relevant to future wind farms that would be necessary to reach the goal of 35% of North American electricity from wind by 2035.

The 24 wind turbines that are explicitly included in the domain, arranged in an aligned configuration, are modeled using an actuator disk method [2] with low resolution requirements that permit the simulation of large domains over very long time periods. In this analysis, the neutral atmospheric flow is simulated using the Lagrangian scale-dependent dynamic model [3] in a 3 km x 3 km domain. The simulation is driven by a constant, imposed pressure gradient and run for an equivalent of 72 hours under stationary conditions. At each time, the complex three-dimensional velocity field is projected onto a Proper Orthogonal Decomposition (POD) basis, determined from the previous analysis, to identify time-scales associated with high-energy large-scale features in the outlying boundary layer flow. The variation in time of each POD mode is represented by a single scalar coefficient, $a^k(t)$, where k is the mode number. Sample time-series for the three types of POD modes are shown in Figure 1 with each coefficient normalized by its standard deviation.

Each of the three types of POD modes is found to have a unique imprint on the time-scales of the flow. The roller modes, which contribute the most to the kinetic energy entrainment [1], have very long time vari- ations which correspond to meandering of high- and low-speed streaks in the domain. The oblique modes, which are characterized primarily by streamwise variation, capture advection of velocity perturbations, and they therefore have a dominant frequency of variation which corresponds to the mean transport time between wind turbine rows. The shear modes vary in time over long time-scales and this variation strongly correlates with power production in the wind farm. The implications of these results are addressed by considering the relationship of the POD modes to unsteadiness in wind farm power generation and fatigue loading, as well as entrainment of kinetic energy which replenishes the flow in the very large wind farms considered in this analysis.

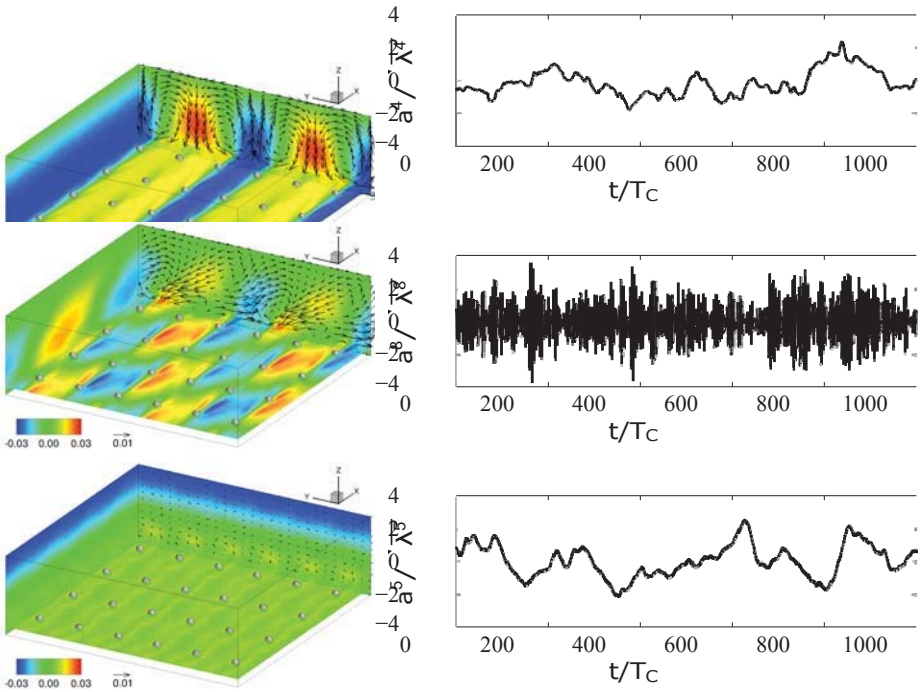

Figure 1: Temporal variation of sample roller, oblique, and shear modes is shown relative to T_C, the mean advection time between turbine rows. The standard deviation of the k^{th} POD time coefficient, $a^k(t)$, is given by the square-root of the POD mode energy, λ^k.

ACKNOWLEDGEMENTS

CV was supported by an NSF graduate fellowship grant and IIA-1243483, the WINDINSPIRE project.

REFERENCES

[1] C. VerHulst and C. Meneveau, "Large eddy simulation study of the kinetic energy entrainment by ener- getic turbulent flow structures in large wind farms," Phys. Fluids, vol. 26, 025113, 2014.
[2] R. Mikkelsen, "Actuator Disk Methods Applied to Wind Turbines, Tech. Univ. of Denmark, 2003.
[3] E. Bou-Zeid, C. Meneveau, and M. Parlange, "A scale-dependent Lagrangian dynamic model for large eddy simulation of complex turbulent flows," Phys. Fluids, vol. 17, no. 2, 025105, 2005.

3

Thermal management of energy storage systems based on battery modules

Prof. MA, Lin [1]; Mr. WANG, Haoting [2]; Mr. HE, Fan [2]

[1] Department of Aerospace and Ocean Engineering, Virginia Tech

[2] Dept of aerospace and ocean engineering, Virginia Tech

Corresponding Author: linma@vt.edu

Electricity generated from wind power is growing rapidly in recent years. As an intermittent energy source, the wind energy needs to be stored appropriately at times. Lithium ion batteries, which have large capacity and energy density, are becoming a good option for the wind energy storage [1]. However, thermal management of the batteries represent a technical challenge due to the heat generation during charging and discharging, especially at high rates. The challenge is further complicated by the dynamics nature of the processes, the wide range of environmental conditions under which the batteries are used, and the relatively narrow temperature for optimal battery operation (typically limited between 0 to 40 °C [2]). High temperature causes problems like reduced battery life, thermal runaway, even fire hazards.

This work will discuss the thermal management issues of Li-ion battery modules. In this work, combined experimental and modeling studies of battery thermal management will be reported. The experimental platform used is shown in Figure 1, consisting of a wind tunnel, battery modules with multiple cells, and control and sensing instrumentation. Using the platform, experimental data were obtained and will be reported under various cooling configurations.

The experimental results were then used to validate modeling efforts, and furthermore to guide the optimization and active control of the thermal management. As an example, Figure 2 shows a set of comparative results to illustrate the benefit of such optimization and active control. The results obtained in three different cases were shown. Case 1 shows the application of a simple unidirectional cooling flow to a pack of batteries, case 2 shows the application of a reciprocating flow (i.e., the cooling flow changes its direction periodically [3]), case 3 shows the application of active control to the cooling flow, and lastly a case where no cooling was applied is also shown for benchmarking purposes. Figures 2 shows the agreement between the experimental and modeling results, and the benefits of using reciprocating flow and active control in terms of managing the temperature with minimal cooling power consumption. These results illustrate the value of the combined experimental and modeling approach for the study of battery systems for dynamic energy storage.

9

A Wind Tunnel Study on the Aeromechanics of Dual-Rotor Wind Turbines

Prof. HU, Hui [1]; Mr. WANG, Zhenyu [2]

[1] Department of Aerospace Engineering, Iowa State University

[2] Iowa State University

Corresponding Author: huhui@iastate.edu

In the present study, we report our recent efforts to develop a novel dual-rotor wind turbine (DRWT) concept to improve aerodynamic efficiency of isolated turbines as well as wind farms. The DRWT concept employs a secondary, smaller, co-axial rotor with two objectives: (1) mitigate losses incurred in the root region of the main rotor by using an aerodynamically optimized secondary rotor, and (2) mitigate wake losses in DRWT wind farms through rapid mixing of turbine wake. Mixing rate of DRWT wake will be enhanced by (a) increasing radial shear in wind velocity in wakes, and (b) using dynamic interaction between primary and secondary rotor tip vortices. Velocity shear in turbine wake are tailored (by varying secondary rotor loading) to amplify mixing during conditions when wake/array losses are dominant. The increased power capacity due to the secondary rotor can also be availed to extract energy at wind speeds below the current cut-in speeds, in comparison to conventional single-rotor wind turbine (SRWT) design.

For a DRWT system, the two rotors sited on the same turbine tower can be set to rotate either in the same direction (i.e., co-rotation DRWT design) or at opposite directions (i.e., counter-rotating DRWT design). It should be noted that a counter-rotating rotor concept (i.e., the rotors rotate at opposite directions) has been widely used in marine (e.g., counter-rotating propellers used by Mark 46 torpedo) and aerospace (e.g., Soviet Ka-32 helicopter with coaxial counter-rotating rotors) applications to increase aerodynamic efficiency of the systems. The recent work Ozbay et al. (2015) reveal that, with the two rotors in counter-rotating configuration (i.e., counter-rotating DRWT design), the downwind rotor could benefit from the disturbed wake flow of the upwind rotor (i.e., with significant tangential velocity component or swirling velocity component in the upwind rotor wake). As a result, the downwind rotor could harvest the additional kinetic energy associated with the swirling velocity of the wake flow. With this in mind, the effects of relative rotation direction of the two rotors on the aeromechanics performances of DRWTs (i.e., co-rotation DRWT design vs. counter-rotating DRWT design) and the turbulent mixing process in the DRWT wakes are also evaluated in the present study.

The experimental study was performed in a large-scale Aerodynamics/Atmospheric Boundary Layer (AABL) Wind Tunnel located at the Aerospace Engineering Department of Iowa State University. Scaled DRWT and SRWT models were placed in a typical Atmospheric Boundary Layer (ABL) wind under neutral stability conditions. In addition to measuring the power outputs of the DRWT and SRWT systems, static and dynamic wind loads acting on the test models were also investigated to assess the effects of the secondary, smaller, co-axial rotor in either counter-rotating (rotors rotate at opposite directions) or co-rotating (rotors rotate at same direction) configuration on the power production performance and the resultant dynamic wind loads (both aerodynamic forces and bending moments) acting on the DRWT models. Furthermore, a high-resolution stereoscopic Particle Image Velocimetry (Stereo-PIV) system was also used to make both "free-run" and "phase-locked" measurements to quantify the transient behavior (i.e., formation, shedding and breakdown) of unsteady wake vortices and the flow characteristics behind the DRWT and SRWT models. The detailed flow field measurements were correlated with the power output data and dynamic wind loading measurements to elucidate underlying physics for higher total power yield and better durability of wind turbines operating in turbulent non-homogenous atmospheric boundary layer (ABL) winds.

69

An evaluation of power performance for a small wind turbine in turbulent wind regimes

Nicholas J. Ward[1], and Susan W. Stewart[2]

Abstract

An evaluation of power performance field tests for a 2.4 kW Skystream wind turbine was carried out with respect to turbulent wind regime characteristics. The wind turbine is located at the Sustainability Experience Center on the Penn State University Park campus. A power curve was determined with respect to manufacturer specifications and in situ wind regime data generated from anemometers. This approach was accomplished in comparison to International Electrotechnical Commission (IEC) standards and power performance studies for small-scale distributed wind turbines [1]. The site specific data was generated at the Skystream turbine to verify manufacturer specifications and evaluate turbine performance with respect to turbulence. TurbSim was used to investigate power performance studies by integrating site specific turbulence parameters into the wind regime. The output data was then processed in WT_Perf in order to evaluate load and power performance for the wind turbine.

The first aspect of this study analyzed the turbine's performance at its location with respect to manufacturer specifications for the Skystream 3.7. The wind speeds were measured via anemometers on the tower at two different heights. These wind speed measurements were extrapolated to hub height via the Power Law in Equation 1, adapted from Sunderland et al (2013), where v and v_{ref} are the wind speeds at hub height h and anemometer height h_{ref} respectively with a power law exponent α of 0.238 [2].

$$v = v_{ref}\left(\frac{h}{h_{ref}}\right)^{a} \quad (1)$$

The data at each 3 s time step were collected via meterological packages for temperature, air density, pressure, wind speed and direction as well as power output from the turbine. The respective standard deviations for the three different anemometers were calculated in post processing. Figure 1 shows the results for 15 months of collected data from June 2013 to September 2014 at 1 min time steps in comparison with the manufacturer's power curve. Figure 2 compares that data with 10 minute intervals for IEC standards and Sunderland et al (2013) [1,2].

[1] Graduate Student, John and Willie Leone Department of Energy & Mineral Engineering, The Pennsylvania State University
[2] Assistant Professor & Research Associate, Aerospace Engineering and Research Associate, Architectural Engineering, The Pennsylvania State University

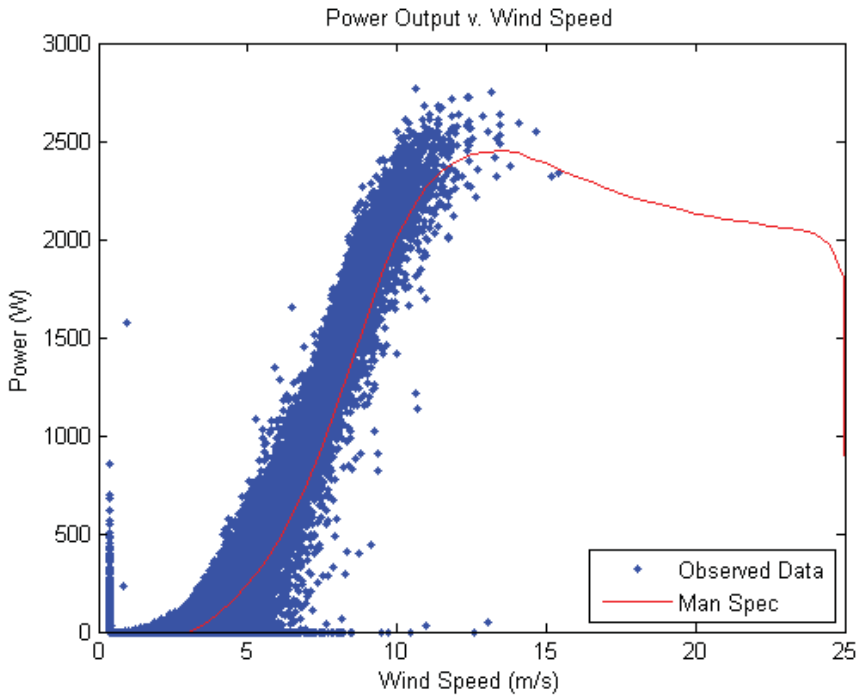

Figure 1: Skystream 3.7 Turbine Performance at Penn State's Sustainability Experience Center

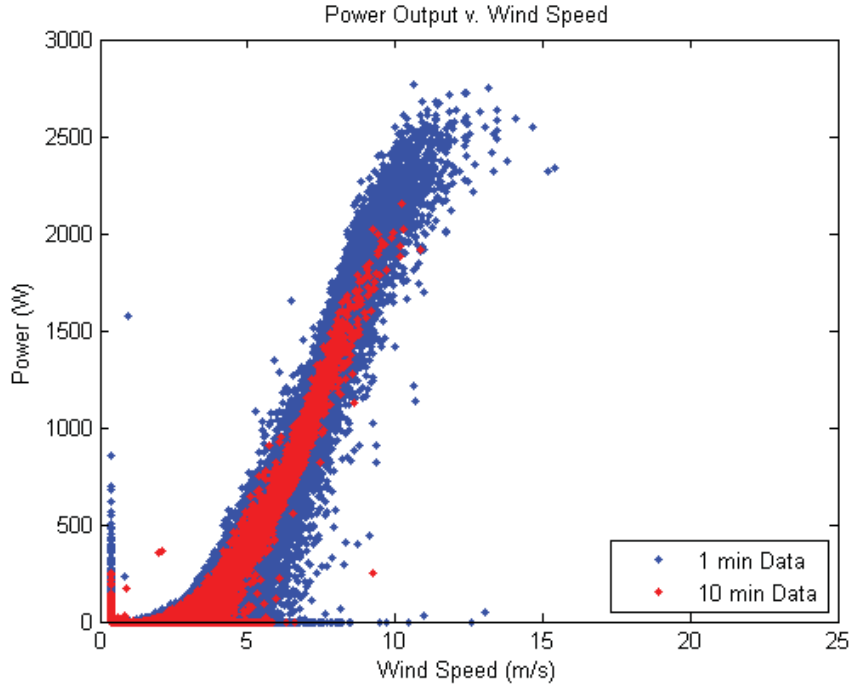

Figure 2: Power Curve for Measured and IEC Standard Time Intervals

From Figures 1 and 2, the wind turbine exhibits characteristics of overperformance compared to manufacturer specifications. Turbulence is preponderant for this wind turbine because of neighboring trees. The repercussion of this interaction is impeded turbine performance for the

given location. The turbulence was quantified at each time step as turbulence intensity (TI) in Equation 2,

$$Tl = \frac{\sigma_U}{} \tag{2}$$

where the standard deviation σ_u and annual average wind speed v- are determined from Equations 3 and 4 at each time step [3].

$$a_u = \frac{1}{N_s - 1} \sum_{i=1}^{N_s} (u_i - v\text{-})^2 \tag{3}$$

$$v\text{-} = \frac{1}{N_s} \sum_{i=1}^{N_s} u_i \tag{4}$$

These turbulence intensities were calculated at each time step from Equation 3 for each anemometer. In order to provide an empirical formulation for turbulence interactions with the wind turbine, a statistical comparison with wind industry practices for wind speeds is proposed. The frequency of turbulence intensity magnitudes for a range of wind speeds can be determined from the Weibull distribution in Figure 3.

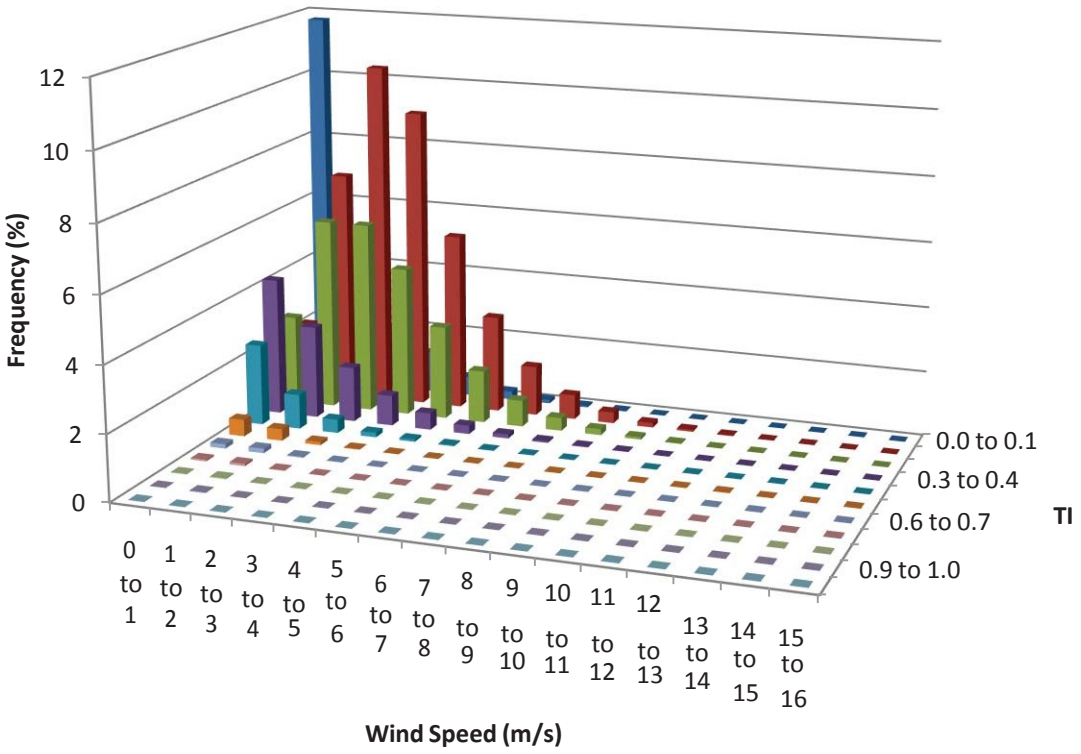

Figure 3: Three-Dimensional Weibull Distribution of Wind Speeds and Turbulence Intensities

Figure 3 indicates that for a wind speed range of 0 to 16 m/s, the turbulence intensity occurs most often between 0.1 and 0.2. These turbulence intensities provide important information on power output for the wind turbine. The turbulence intensities determine a similar statistical

approach for wind speeds (i.e. Weibull distribution) at the turbine hub. The power output can therefore be quantified with respect to the turbulence intensities experienced by the wind turbine. This power output was quantified with respect to measured and IEC standard time intervals for small scale wind turbines in Figure 4 [1]. These results also correlate well with Skystream power curve results from Albers (2009) [4].

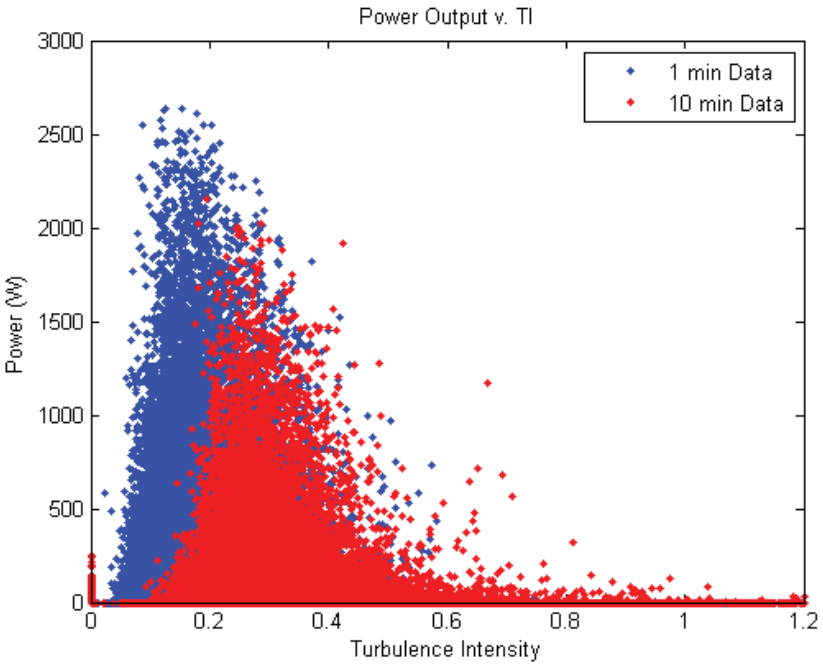

Figure 4: Power Output with respect to Turbulence Intensity for the Skystream 3.7

The results in Figures 3 and 4 indicated a statistical correlation between power performance and turbulence intensity compared to the local Weibull distribution, which enables faster computational prediction of turbine loads given real data. This also enables a more standardized approach for predicting stochastic loads due to turbulence, which can be accomplished in future works. This study demonstrated significant promise in wind turbine performance by providing a new method for assessing and analyzing turbulence interactions.

References

[1] IEC 61400-12-1. Power performance measuring of electricity generating wind turbines. IEC, 2005. 2-90. Print.

[2] Sunderland, Keith et al. "Small Wind Turbines in Turbulent (urban) Environments: A Consideration of Norma and Weibull Distributions for Power Prediction." *J. Wind Eng. Ind. Aerodyn.*, 121 (2013): 70-81. Web.

[3] Manwell, J.F., J.G. McGowan, and A.L. Rogers. *Wind Energy Explained: Theory, Design and Application*. 2nd ed. John Wiley & Sons, 2002. Web.

[4] Albers, A. "Turbulence and Shear Normalization of Wind Turbine Power Curve." (1994): 4. Print.

61

Impact of Hurricane Wind/Wave Misalignment on the Analyses of Fixed-Bottom]acket Type Offshore Wind Turbine

Dr. WEI, Kai [1]; Prof. ARWADE, Sanjay R. [1]; Prof. MYERS, Andrew T. [2]; Dr. VALAMANESH, Vahid [2]; Prof. PANG, Weichiang [3]

[1] University of Massachusetts Amherst

[2] Northeastern University

[3] Clemson University

Corresponding Author: kaiwei@umass.edu

A high risk of hurricane is threatening the development of offshore wind energy in the east coast of the United States. Hurricane loads on an offshore wind turbine, namely wind and waves, not only exert large demands but also have rapidly changing characteristics, especially wind and wave directions. Waves are, in general, inert to rapid changes, whereas wind can change its properties within very short time scales. Misalignment of local winds and propagating ocean waves occurs regularly in a hurricane environment. It is a common practice to design monopile support structures for offshore wind turbines (OWTs) under extreme conditions by the highest wind/wave loads when they are assumed to come from the same direction. However, this co-directional wind/wave assumption can be hazardous for non-axisymmetric fixed bottom support structures for deeper water such as jackets due to their sensitive capacity to loading directions. The goal of this work is to examine the impact of wind/wave misalignment on the extreme loads and structural response under hurricanes. We select a fixed-bottom jacket type offshore wind turbine located in a water depth of 50m as the example structure. The hurricane induced wind and wave loads on the structure system are calculated from a reduced set of 1000 simulated full-track hurricane events, selected from a database of 200,000 years of simulated hurricanes, to represent the hazard of Nantucket, Massachusetts. The meteorological ocean (met-ocean) conditions and wind/wave directions for each hurricane are identified from the track data by physical models. The wind direction, wave direction at different time and location and the orientation of structure are included to capture the misalignment impact on the structural analyses over a wide range of possible engineering designs and conditions. It will let us clearly understand the impact of wind/wave misalignment on the analyses of a jacket-type support structure.

41

Meteorological analysis of large power-error events in the Wind Forecast Improvement Project (WFIP) data set

WILCZAK, James [1]; BIANCO, Laura [2]; DJALALOVA, Irina [2]; GOTTAS, Daniel [1]; NEIMAN, Paul [1]; OLSON, joseph [2]

[1] NOAA/ESRL

[2] CIRES/University of Colorado

Corresponding Author: james.m.wilczak@noaa.gov

Electric grid and utility operators rely on numerical weather prediction model forecasts of power production from wind plants. Of greatest concern are instances when the models either greatly over-forecast or greatly under-forecast the amount of power that a wind plant or group of wind plants will produce. We use one year of observation and model data from the Wind Forecast Improvement Project (WFIP) to analyze the characteristics of large power error events. WFIP was a joint DOE, NOAA, and private sector field campaign whose goal was to improve wind forecasts for the wind energy industry. Observations were collected during WFIP for a 12 month period in 2011-2012 in two study areas within the United States, one in the Northern Great Plains, and one in west Texas.

Large error events are defined on the basis of the 3 hour running mean of the difference between forecast and observed power, aggregated within each of the two WFIP study areas. Using 6 hour forecasts from the 3 km resolution NOAA/High Resolution Rapid Refresh (HRRR) model, and observed pseudo-power derived from anemometers on 127 tall tower sites in the two WFIP study areas, we find 27 events in the North Study Area with aggregate error greater than 203 of capacity, and 31 events in the South Study Area with aggregate error greater than 303 of capacity over the WFIP year-long field program. These events are categorized according to season, meteorological condition, being an over- or under-forecast, and length of the event. We also compare statistics to large errors calculated using the 13km resolution NOAA/Rapid Refresh model (RAP), and to errors calculated for individual tower locations (instead of the aggregated power).

59

Modifications of the k-kL-w Transition Model based on Pohlhausen and Falkner-Skan Profiles

Dr. FURST, Jiri [1]; Dr. WOOD, David [2]

[1] University of Prague

[2] UofC

Corresponding Author: dhwood@ucalgary.ca

We will present novel modifications of the three-equation k-kL-u: eddy viscosity model proposed by Walters and Cokljat [1] for the adverse pressure gradient flows that occur on wind turbine blades and airfoils. The original model was based on the k-u: framework with an additional transport equation for laminar kinetic energy which allows the prediction of natural or bypass laminar-turbulent transitions. The model uses only local information and is, therefore, easily implemented in modern CFD codes including Fluent and OpenFOAM. The original model shows very good agreement with experimental data for zero pressure gradient flows (see e.g. [1]) but it delays the transition for adverse pressure gradient flows at low free-stream turbulence levels [2]. Both stability analysis and experiments show that the pressure gradient has a big influence on transition [3].

13

High speed and multidimensional flow characterization based on nonintrusive optical techniques

Mr. WU, Yue [1]; Mr. LEI, Qingchun [2]; Prof. MA, Lin [1]

[1] Department of Aerospace and Ocean Engineering, Virginia Tech

[2] Department of Mechanical Engineering, Virginia Tech

Corresponding Author: linma@vt.edu

This work will report our work on high speed and multidimensional flow characterization using nonintrusive optical techniques, and discuss their application and relevance to wind energy systems. We will describe two example techniques to obtain velocity and flow field measurements. The first technique involves Particle Image Velocimetry (PIV) to obtained 2D (two-dimensional) velocity measurement with temporal resolution up to 10 kHz. The second technique attempts to extend the PIV technique to 3D velocity and flow measurements by combining Mie scattering imaging with computed tomography.

36

Computational Modelling of Solidity Effects on Blade Elements with an Airfoil Profile for Wind Turbines

Mr. YAN, Haoxuan [1]

[1] University of Calgary

Corresponding Author: hayan@ucalgary.ca

The aim of this project is to investigate the aerodynamic performances of airfoil, especially NACA 4415, using the method of Computational Fluid Dynamics. The NACA 4415 was modeled and meshed in ICEM and then was simulated by using transition SST (shear stress transport) 4-equation model in ANSYS Fluent 15.0 with different Reynolds number and various angles of attack. Lift, drag, pressure distribution and wall shear stress were highly focused during post-processing. The computational results were compared with Xfoil and experimental data collected by The Ohio State University (OSU) in 1996. User Defined Functions (UDF) were also tested during the calculations in order to find the most optimal results. In addition to the isolated airfoil, this project also investigated the cascade effect of blade elements with a NACA 4415 airfoil profile with different solidities (ranges from 0.05 to 0.4). While the typical range for a 3-blade horizontal wind turbine is from 0.021 to 0.11 [1]. Aerodynamics of the airfoil will be influenced by different solidities.

68

Aerodynamics and Aeroacoustics of Spanwise Wavy Trailing Edge Flatback Airfoils: Considering Structural Benefits

YANG, Seung Joon [1]; Prof. BAEDER, James D. [2]

[1] Graduate Student

[2] Professor

Corresponding Author: sjyang@umd.edu

The spanwise wacy trailing edge design considering its structural benefits was proposed and studied. The three dimensional RANS-LES simulation has been performed to reveal the aerodynamic and aeroacoustic behaviors of the newly proposed wavy trailing edge design.

39

LARGE-EDDY SIMULATION OF SWiFT TURBINES UNDER DIFFERENT WIND DIRECTIONS *

XIAOLEI YANG[(1)], DANIEL FOTI[(1)], CHRISTOPHER L. KELLEY [(2)] & FOTIS SOTIROPOULOS[(1)]

[(1)] St. Anthony Falls Laboratory, Department of Civil, Environmental, and Geo- Engineering, University of Minnesota, 2 Third Avenue SE, Minneapolis, MN 55414, USA

[(2)] Sandia National Laboratories, Albuquerque, NM 87185 and Livermore, CA 94550, USA

Turbine wake interaction is a key factor affecting wind farm performance and dynamic loadings on turbine structure. The Scaled Wind Farm Technology (SWiFT) facility (Barone and White 2011; Berg et al. 2014), which is located at the Reese Technology Center near Lubbock, TX, USA, is specifically designed to enable investigating turbine wake effects at field scale. Three turbines (rotor diameter D = 27 m, hub height 31.5 m) forming a 3D-, 5D-, and 6D-length triangle (see Figure 1) have been installed. In this work, systematic study on wake interaction of the three SWiFT turbines, and how wake interaction affecting the power output and dynamic loadings under three different wind directions will be carried out.

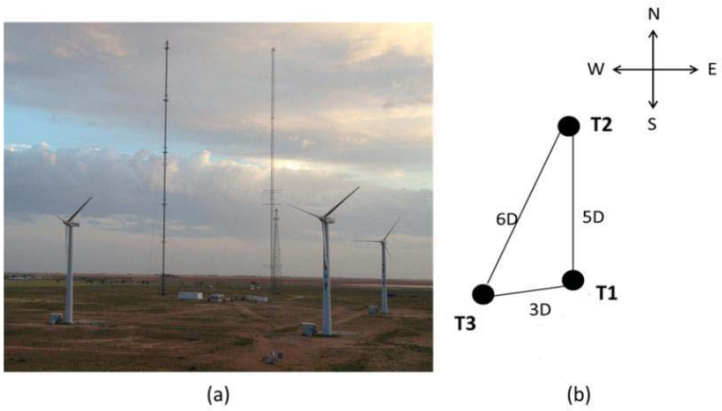

Figure 1: Field view of the three SWiFT turbines (a) and schematic of the turbine locations (b).

The VWiS (Virtual Wind Simulator) code (Yang et al. 2014b; Yang, Kang and Sotiropoulos 2012; Kang, Yang and Sotiropoulos 2014) developed at Saint Anthony Falls Laboratory, University of Minnesota is employed in the present simulations. In VWiS, the wind field is computed by solving the three-dimensional, unsteady, spatially-filtered continuity and Navier-Stokes equations. A dynamic Smagorinsky subgrid scale model is employed for the unresolved subgrid scales. The governing equations are discretized using second-order accurate, three-point central finite differencing for all spatial derivatives. The discrete equations are integrated in time using the second-order accurate fractional step method. The turbine blades are parameterized using a simplified actuator surface model, which accounts for the blades as separate rotating surfaces formed by the airfoil chords. The forces distributed on each blade are calculated based on a blade element approach. The forces from the actuator surfaces are distributed to the background grid nodes using the discrete delta function proposed in Yang et al. 2009. The nacelle is represented by an improved nacelle model. Implementation of the employed actuator models for the blades and nacelle will be briefly presented.

In this study, the cases considered are from the three most prevalent wind directions: South, West, and Southwest. All three wind turbines rotate with a tip-speed-ratio of 9, the ratio of blade tip velocity to rotor disc-averaged wind speed 1D upwind. The turbulent flow at the inlet is calculated from separate large-eddy simulations. The roughness height of the ground is 0.01 m. The grid spacing near the turbine is D/100. Away from the turbine wake regions, the meshes are stretched in the crosswind and vertical directions. The meshes are uniformly distributed in the downwind direction based on the grid refinement study carried out in Yang et al. 2014a. A sample of the computed results is shown in Figure 2, which shows the instantaneous flowfield for the case with wind blowing from the south. In this case, two turbines (T1 and T3) face the undisturbed incoming wind while the third turbine (T2) lies in the wake of turbine T1. Figure 2 shows the contours of the instantaneous downwind velocity at a horizontal plane located at turbine hub height. Wake meandering, which may significantly increase the dynamic loads on the downwind turbines,

* Sandia National Laboratories is a multi-program laboratory managed and operated by Sandia Corporation, a wholly owned subsidiary of Lockheed Martin Corporation, for the U.S. Department of Energy's National Nuclear Security Administration under contract DE-AC04-94AL85000.

is observed for all the three turbines. In the conference, both instantaneous and time-averaged flowfileds and the statistics of the power output and loads for the three cases will be presented.

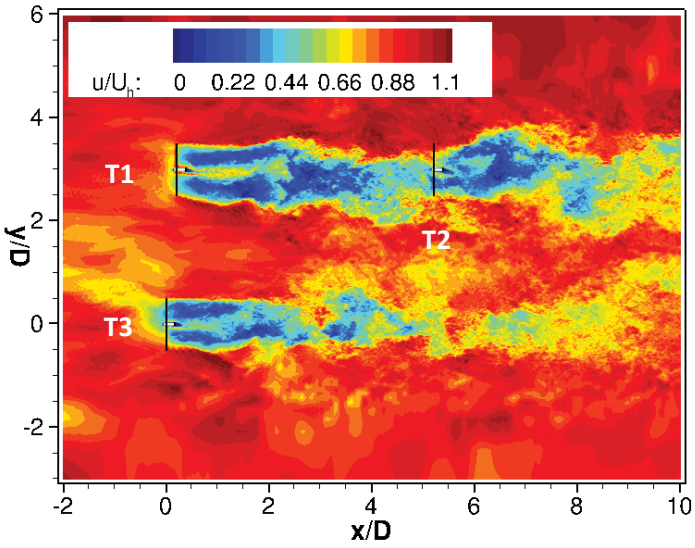

Figure 2: Contours of instantaneous downwind velocity at a horizontal plane located at turbine hub height for wind blowing from the South.

ACKNOWLEDGMENTS

This work was supported by Department of Energy DOE (DE-EE0002980, DE-EE0005482 and DE-AC04-94AL85000). Computational resources were provided by Sandia National Laboratories and the University of Minnesota Supercomputing Institute.

REFERENCES

Barone M. and White J. (2011). DOE/SNL-TTU scaled wind farm technology facility: Research opportunities for study of turbine-turbine interaction. SANDIA REPORT, SAND2011-6522.

Berg J., Bryant J., LeBlanc B., Maniaci D., Naughton B., Paquette J., Resor B., White J. and Kroeker D. (2014). Scaled wind farm technology facility overview. AIAA SciTech, 13-17 January 2014, National Harbor, Maryland, 32nd ASME Wind Energy Symposium, AIAA 2014-1088.

Kang S., Yang X., and Sotiropoulos F. (2014). On the onset of wake meandering for an axial flow turbine in a turbulent open channel flow. Journal of Fluid Mechanics, 744, pp. 376-403.

Yang, X., Boomsma, A., Barone, M., & Sotiropoulos, F. (2014a). Wind turbine wake interactions at field scale: An LES study of the SWiFT facility. In Journal of Physics: Conference Series (Vol. 524, No. 1, p. 012139). IOP Publishing.

Yang X., Sotiropoulos F., Conzemius R. J., Wachtler J. N., and Strong M. B. (2014b). Large-eddy simulation of turbulent flow past wind turbines/farms: the Virtual Wind Simulator (VWiS). Wind Energy, 2014.

Yang X., Zhang X., Li Z. and He G.-W. (2009). A smoothing technique for discrete delta functions with application to immersed boundary method in moving boundary simulations. Journal of Computational Physics, Vol. 228, 2009, pp. 7821-7836.

Yang X., Kang S. and Sotiropoulos F. (2012). Computational study and modeling of turbine spacing effects in infinite aligned wind farms. Physics of Fluids, 24, 115107.

82

System-level simulation of oating platform and wind turbine using high-delity and engineering models

Mr. ZHANG, Di [1]; PATERSON, Eric [1]

[1] Virginia Tech

Corresponding Author: ccdupont@vt.edu

Compared with inland wind farm, the o shore sites has higher energy density, and less environmental and visual impact. It's an attractive energy source for populous coastal cities. However, the marine environment adds more uncertainties in the system, especially for
oating wind turbines. Due to physical conditions,
full-scale testing is usually unpractical, thus system-level simulation is essential in design stage. Cyber Wind Facility(CWF) project aims to provide highly resolved 4D cyber data to answer the key performance questions: structure and turbine loading, shaft torque, platform motion.
In this study, a full-scale NREL 5MW wind turbine and OC3 spar buoy with mooring lines(gure 1) are simulated in open-source code OpenFOAM. The whole system is calculated by three di erent models: actuator-line model(ALM), which calculates aerodynamic force from turbine blades; quasi-static model, which estimates the restoring mooring force in each time-step, and high- delity model for the
oating plat-
form in waves.
The ALM model is less computationally expensive than resolving full turbine geometry, it represents the blades as a set of actuator elements and the loading is distributed along the lines(gure 2). Sectional force at each blade element is computed according to local
ow conditions and airfoil lookup table, the lift and drag
forces are projected onto the
ow as body forces in the momentum equation. The original ALM was developed for xed-bottom turbines (Jha et al., 2014), modi cations are needed to incorporate 6DOF motions from the turbine tower. The
oating platform, i.e. OC3 spar buoy, measures 130m in length with 120m of
total draft(Jonkman, 2010). Single harmony linear waves are generated by wave2Foam library(Jacobsen et al., 2012), numerical beach is included for absorbing waves.
The quasi-static mooring-line model is developed from catenary-line equations(Faltinsen,1990) and it is also implemented in engineering tool HydroDyn(Jonkman, 2007). By calculating the anchor and fairlead position, together with known physical properties of the cable, we can solve both the mooring-line con guration and restoring force. In general, it 1) models individual taut or slack mooring lines; 2) accounts for weight and buoyancy, axial sti ness, and friction from seabed; 3) ignores bending and torsional sti nesses, cable inertia and hydrodynamic forces, and 4) Solves for cable positions and tensions under static equilibrium given the instantaneous fairlead location.
Due to the numerical instability in standard dynamic meshing multiphase solve in OpenFOAM, especially in the presence of large displacement, a modi ed tightly-couple RANS solver(Dunbar, 2013) is used for the high- delity simulation. It features sub-iteration in each time-step to ensure simulation is converged with respect to mesh motion and dynamic relaxation is introduced for faster convergence. Furthermore, it is validated by experimental data of simple 2D cylinder and OC4 semisubmersible platform(Robertson et al., 2014).
In summary, this study integrates ALM and the quasi-static mooring-line model. By using wave generating tool and tighty-coupled solver we can study the 6DOF motion of
oating platform in waves with less
computational resource than fully-resolved high- delity model.

83

A novel rough wall boundary condition for LES of high Reynolds number flows

XIAO, Heng [1]; Prof. DEVENPORT, William [2]; SUN, Rui [2]; LIU, Yu [3]

[1] Department of Aerospace and Ocean Engineering, Virginia Tech

[2] Virginia Tech

[3] Nanjing University of Aeronautics and Astronautics

Corresponding Author: ccdupont@vt.edu

The interactions between of rough surfaces and fluid flows play an important role in turbulence simulation. The understanding of roughness elements at the wall (i.e., buildings and terrain features) to aerodynamics flow is crucial in wind energy from farm identification and assessment to turbine blade design. In this work, we propose a novel rough-wall boundary condition for LES to simulate flows over rough surfaces at high Reynolds numbers. The proposed rough-wall boundary condition consists of two parts: (1) smooth-wall modeling for high Reynolds number flow; (2) wall-modeling for roughness surface.

To reduce the computational costs for high Reynolds number flow, a wall-modeling mesh is applied at the bottom of the boundary layer following (Kawai and Larsson 2012). In this procedure, the wall-modeling mesh will obtain velocity from LES mesh, solve for the shear stress according an equilibrium equation of boundary layer, and provides the calculated wall shear stress back to LES mesh.

To verify the smooth wall-modeling LES part, the simulation of high Reynolds number flow in a channel is performed. The Reynolds number of the verification case is Re_8=u_c 8/u,,3.01x 10 /\5 and the thickness of the wall model is h_wm=0.18. The comparison of normalized streamwise velocity between the experiment, wall-modeling LES and pure LES are shown in the figure below. It is noted that the LES mesh of the modeling LES and pure LES are the same, but the wall-modeling LES will update the shear stress at the wall via wall modeling. Therefore, the wall-model LES results are the combination of the results of the wall-modeling part below h_wm and the LES part above h_wm. From the figure, it is can be seen that the wall modeling improves the results of LES when using relatively coarse grid at the boundary.
Another part of the present model is the simulation of the influence of roughness elements. In the presented rough wall boundary condition, the flow around the roughness element, at the inner region of turbulent boundary layer, is not fully resolved. Instead, a one-layer roughness mesh is used to resolve the geometry of roughness elements. On the roughness mesh, the roughness geometry is adequately represented via the surface elevation. By projecting the instantaneous pressure onto the roughness surface, the instantaneous roughness shear stress is obtained.

Since the smooth-wall and roughness shear stress are obtained, the total wall shear stress is obtained by adding the two parts. Then, the so obtained total wall shear stress is used to correct the flow at the near wall region. The LES mesh size, lix/\+, liy/\+ and liz/\+ (in streamwise, wall-normal, and spanwise directions, respectively) in the present simulations can be as large as 50 to 4000, which is favorable for high-Reynolds number flow simulations in applications of wind turbines. Moreover, the presented wall model can solve roughness elements having size of K/\+ ranging from 100 to several hundred wall units, which can be used to estimate the influence of roughness elements at different sizes.

According to the results from the simulations, the presented rough wall-modeling boundary condition can perform high fidelity simulation for turbulent flow at higher Reynolds number by using a relatively low computational cost. The velocity profiles and Reynolds stress agree favorably with experimental data and numerical results in the literature. Therefore, the merits of the proposed rough-wall model are demonstrated.

80

Understanding Model Uncertainty-An Application of Uncertainty Quantification to Wind Energy

MA, Po-Lun [1]; WHARTON, Sonia [2]; BULAEVSKAYA, Vera [2]; SHAW, William [1]; Dr. BERG, Larry [3]; YANG, Ben [1]; QIAN, Yun [1]

[1] Pacific Northwest National Laboratory

[2] Lawrence Livermore National Laboratory

[3] ATMOSPHERIC SCIENCE AND GLOBAL CHANGE DIVISION

Corresponding Author: ccdupont@vt.edu

Wind resource characterization and short-term wind power forecasts often utilize mesoscale meteorological models such as the Weather Research and Forecasting (WRF) model. Because of the finite nature of the model grid, parameterizations must be used to represent processes that are sub-grid scale, such as those associated with planetary boundary layer (PBL) turbulence. Few published studies have attempted to rigorously define the uncertainty in the simulated wind speed, wind shear, and wind power associated with the assumed constants applied in the PBL and surface layer parameterizations. Likewise, the design of most field studies with the goal of improving PBL parameterizations are based on the intuition of the investigator, rather than an explicit analysis of the causes of uncertainty within the parameterization. In this study we use uncertainty quantification (UQ) to address these shortcomings and provide guidance for the instrument deployments that will be part of the second Department of Energy Wind Forecast Improvement Project (WFIP 2).

The most widely used sensitivity analysis (SA) approach is to conduct "one-at-a-time" (OAT) sensitivity tests that systematically investigate departures of model behavior from the baseline simulation by varying one parameter at a time. However, OAT tests can only evaluate a limited number of parameters at the same time, consider only a small fraction of the total parameter uncertainty space, and are computationally expensive. Another critical limitation of the OAT approach is that it does not allow for the quantification of the effects of interaction among parameters. A more comprehensive method is to populate the statistical distribution of model outputs by simultaneously sampling hundreds or thousands of possible configurations of multiple parameters. The SA, such as analysis of variance and variance decomposition, then use the output distributions to understand the contribution of each parameter (along with any interaction effects it has with other parameters) to the overall variance.

The UQ analysis will be used to document the uncertainty in hub-height wind, wind shear across the rotor diameter, and wind power for WRF simulations completed using the Mellor-Yamada-Nakanishi-Niino (MYNN) PBL parameterization and the recently revised Mesoscale Model 5 (MM5) surface layer scheme for a location in the Pacific Northwest. The UQ results will be used to develop recommendations for the WFIP 2 instrument deployment. An example WRF time series of simulated 80 m wind speed and wind power is shown in the figure below, with each time series resulting from one of 256 individual WRF simulations completed using combinations of different values for 12 PBL parameters. The figure highlights how the uncertainty in the wind speed gives rise to large variations in the wind power that can range from approximately the rated power of 1.6 MW to less than 0.4 MW for a given point in time. Our analysis shows that the WRF simulations of hub-height wind speed are ultimately sensitive to a relatively small number of parameters, including surface roughness length (z0), the von Karman constant, the turbulence kinetic energy (TKE) dissipation rate, the Prandlt Number, parameters associated with the length scales applied in the MYNN PBL parameterization, and to a lesser extent Monin-Obukhov similarity functions during nighttime. These results argue for the measurement of TKE and TKE dissipation rates over the depth of the PBL (or deeper in stable conditions during which the PBL might be quite thin) at a number of locations over the WFIP 2 domain. The day-night changes in the sensitivity point to the need for measurements of the surface sensible heat flux to help determine the static stability at any given time. The relative importance of the various parameters also changes as a function of terrain slope. For example, the relative contribution of the variance associated with changes of a parameter related to the TKE dissipation rate, ranges from 303 in daytime conditions for gentle slopes to nearly 503 during daytime conditions and steep slopes. Overall, the results presented in this work quantify the uncertainty in WRF simulations of hub-height wind speed and wind power in a region of complex terrain, and point to key measurements that should be included as part of WFIP 2.

81

Large Eddy Simulation of Trailing Edge Acoustic Emissions of an Airfoil

WU, Jinlong [1]; Prof. DEVENPORT, William [1]; PATERSON, Eric [1]; SUN, Rui [1]; XIAO, Heng [1]

[1] Virginia Tech

Corresponding Author: ccdupont@vt.edu

The present investigation of trailing edge acoustic emission of an airfoil concerns the e ects of the broadband noise generated by the interaction of turbulent boundary layer and airfoil trailing edge, and the tonal noise generated by the vortex shedding of trailing edge bluntness. Large eddy simulation (LES) is performed on an NACA0012 airfoil with blunt trailing edge at a Reynolds number Rec = 400; 000 based on the airfoil chord length for three di erent con gurations with di erent angles of attack. In order to reproduce and compare with the result from experiment in the literature, numerical tripping is tested and chosen to control the boundary layer development to guarantee a similar boundary layer thickness near the airfoil trailing edge. The near wall region inside the boundary layer is directly resolved by LES simulation with Van Driest damping, in order to obtain the instantaneous data in that region. With these instantaneous data from aerodynamic simulation, the acoustic predication is conducted by the Curle's analogy, which is suitable for stationary surface in free
ow. To validate the numerical solutions, both
ow simulation and acoustic integration results are compared
to experimental data and simulation results available in the literature, and good agreement is achieved. The aerodynamic results show that the similar boundary layer development of experimental result can be reproduced by simulation with a suitable choice of numerical tripping, and the similar instantaneous behavior of
ow inside the boundary layer is therefore guaranteed, which is vital for the acoustic prediction. The aeroacoustic results show that the acoustic prediction changes with the lift and drag force provided by the airfoil. Basically speaking, it's a result that the unsteady force around the surface is closely related to the mean force provided by an airfoil, which means that the noise control of a given airfoil is coupled with the optimization of its aerodynamic performance. As for the approximation made in the implemetation of Curle's analogy, it is shown in the aeroacoustic results that the airfoil can be treated as a compact point only if low frequency acoustic emission is of interest, and such kind of approximation can cause obvious problem if very high frequency acoustic emission is concerned.

84

Combined Offshore Wind, Wave, Storage System Power and Cost Predictions

Combined Offshore Wind, Wave, Storage System Power and Cost Predictions

Jocelyn Kluger, Themis Sapsis, Alexander Slocum

Massachusetts Institute of Technology jociek@mit.edu

The motivation of this work is to significantly increase the power generated by an offshore wind turbine installation and to optimize its renewable power integration into the electrical grid. Our general strategy for achieving this is to combine an oscillating water column (OWC) wave energy converter and an offshore renewable energy storage (ORES) device to the offshore wind installation.

In OWCs, a chamber has an inlet submerged below the water surface and an outlet open to the ambient air above the water surface. Wave motion at the inlet pushes air through the outlet. The outlet is typically fitted with a Wells turbine, which rotates due to the air flow past it. The Wells turbine blades are designed so that both outwards and inwards air flows rotate the turbine in the same direction. This mechanical rectification greatly increases the robustness of the WEC to different sea states with different wave characteristics than compared to a point absorber system (a "buoy" wave energy converter).

Ten years of on-shore OWC installations have proven the machines to be well-suited for the sea environment with few moving parts and dynamical robustness to different sea states. The system may be installed at the same time as a new FWT or retrofit to an existing FWT. The FWT and OWC can share the same mooring and electricity transmission lines, greatly reducing the

cost of the wave energy converter (mooring and transmission lines typically comprise 28% the cost of a 3.6 MW FWT and 60% the cost of a 1 MW floating OWC).

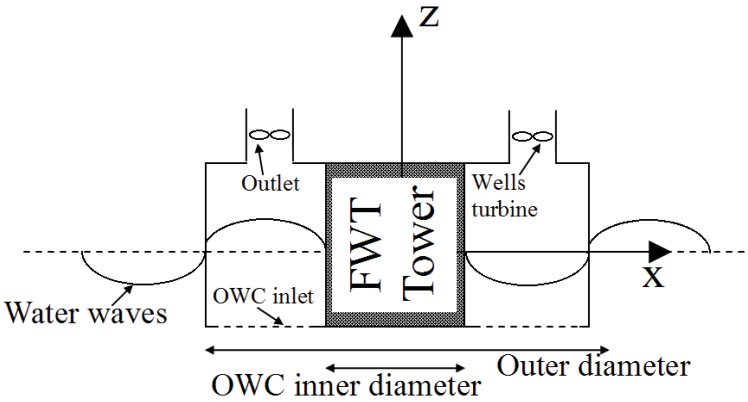

Figure 1: Sketch of a design where an array of oscillating water columns encircles a floating wind turbine

In this work, we use a first-order model of the OWC hydrodynamics and thermodynamics to predict the power generated by the OWC turbine. We consider both a linearized model for frequency-domain analysis and a full nonlinear model that is numerically simulated in MATLAB. We further use linear hydrodynamic theory to predict the lateral and vertical forces

transmitted by the OWC to the FWT based on the OWC geometry and the interface between the OWC and FWT.

Additionally, we model at a system level the combined FWT-WEC-ORES-transmission line device. We note that ocean wave power is less variable than wind power, and may lessen variations in the FWT-WEC device generated power. We assign to the ORES device an energy storage capacity, and power absorption and release efficiency. We model transmission line losses for a given line length. We consider typical power demands of electric grid customers.

The overall goal of this study is to minimize the levelized cost of energy (LCOE) for the offshore device. We maximize the power generated by the OWC and make its performance robust to different sea states via controls or intentional nonlinear geometry. We consider different OWC configurations for reducing the hydrodynamic heave and lateral forces induced on the FWT tower. An optimal OWC design requires no or minimal additional mooring lines to the FWT system. Additionally, it is desirable that the offshore FWT-OWC-ORES system performs well in terms of its source-to-grid power efficiency, power supply-to-power demand matching, and minimized transmission line cost. Finally, we predict the capital expenditures, lifetime, and maintenance costs of the device for computing its LCOE.

77

Turbine-mounted LIDAR Validation

EHRMANN, Robert [1]; GUADAYOL, Marc [1]; ARORA, Dhiraj [1]

[1] ALSTOM Power Inc.

Corresponding Author: devenport@vt.edu

Introduction

As wind turbines become larger and more flexible, methods of reducing structural mass to reduce the cost of energy are being investigated. One method of fatigue reduction is a turbine-mounted LIDAR preview controller. LIght Detection and Ranging (LIDAR) have become well established in the wind industry as an atmospheric measurement tool. Recently, LIDAR have been installed on wind turbine nacelles to yield an incoming wind speed measurement.1 A feed-forward controller uses the incoming LIDAR signal to update the pitch rate for incoming wind gusts, reducing tower and blade fatigue and generator speed variations. This potentially results in decreased structural mass, increased turbine life, and increased annual energy production (AEP).

The potential for load reduction and AEP increase are motivating Alstom to investigate LIDAR use in feed-forward controller operation. Since wind energy is competitive with conventional power sources, any reduction in the cost of energy is highly desirable. Some questions remain unanswered regarding LIDAR feed-forward control implementation, particularly for large turbines. The overall benefit may be lower than anticipated due to turbine scale. Also, safety is a concern, as incorrect controller input has potentially dangerous results.

Therefore, a turbine-mounted LIDAR will be assessed for feed-forward control application to quantify effectiveness and decrease risk. Wind speed comparisons will be made against a neighboring meteorological mast and rotor effective wind speed to validate the LIDAR.

Setup

An ECO 110 at the National Renewable Energy Laboratory (NREL) National Wind Technology Center (NWTC) is tested. The site is located approximately eight miles south of Boulder, Colorado. Figure 1 illustrates the site layout. Prevailing winds are from the west-northwest. The ECO 110 is a 3MW, 110 meter diameter turbine. It has a 90 m hub height. Cut-in and cut-out wind speeds are 3 m/s and 25 m/s, respectively. The meteorological mast utilized is M5 on Site 4.0, located 341° and 228 m relative to the Alstom turbine. The mast booms point in the 278° direction. The met mast cup anemometer at 90 m and wind vane at 87 m are used for comparison against turbine measurements.

A ZephIR DM (dual mode) turbine mounted LIDAR was installed on the ECO 110 at the NWTC. It is capable of measuring at multiple ranges between 10 m and 300 m. The LIDAR scans continuously with a half-cone angle of 30°. A half-cone angle of 15° is also an option, but simulations indicated 30° to be more accurate for yaw misalignments. Scan diameters have historically been between 503 and 803 of the turbine diameter, where the majority of power is generated. A range of 73 m yielding an 84 m scan diameter is used. The LIDAR contains filtering to remove blade pass reflections, hard object strikes, or low backscatter returns. This ensures only high quality velocity measurements are used in the turbine controller.

NREL acquires data from the turbine controller and met mast. The LIDAR data GPS timestamp is aligned with the NREL GPS timestamp, allowing comparison between the two signals. In the future, the LIDAR will be integrated into the turbine controller, and NREL will acquire the LIDAR data directly from the controller.

Methodology

Comparisons of wind speed are made between the met tower cup anemometer, LIDAR, and wind turbine. Wind turbine nacelle cup anemometers are generally unused as a validation measurement since they operate in the turbine wake. The truest measurement of the wind speed the wind turbine is experiencing is calculated based on the turbine operational values. This wind speed is known as the rotor effective wind speed, 0.

The rotor effective wind speed is calculated through a torque balance:

Q+ = (Q, , 0)

where is the rotor inertia, Q is the rotor acceleration, is the measured torque, and is the aerodynamic torque which is a function of rotor speed Q, pitch , and rotor effective wind speed 0. The aerodynamic torque is equal to

=12 3 (,) 02

where is the density of air, is the blade radius, and is the power coefficient which is a function of tip speed ratio and pitch . The tip speed ratio is defined as

$=Q \quad 0.$

Rotor inertia, rotor speed, shaft torque, and power coefficients are all known or measured quantities. The remaining unknown is 0. However, the power coefficients are dependent upon tip speed ratio, so no explicit solution can be found. A three-dimensional lookup table may be used to solve the equation. Additional information is found in Schlipf et al.2

The LIDAR calculates a horizontal wind speed, containing u and v horizontal velocity components. Yaw is also calculated relative to the LIDAR forward direction. However, 0 yields the wind speed normal to the rotor plane. Therefore, the LIDAR horizontal wind speed is yaw-corrected to be an equivalent measurement to 0.

Lastly, the LIDAR measurement leads the rotor effective wind speed, making comparison more difficult. The LIDAR phase shift is compensated using Taylor's frozen turbulence hypothesis, which assumes eddies convect at the mean wind speed.3 Therefore, the time delay would be the measurement range divided by the mean wind speed. A correction for induction can be included, as specified in Dunne et al.4

Results and Discussion of LIDAR Validation

The LIDAR is first compared to the met mast data. Figure 3 shows a time series comparison of the met mast cup anemometer at 90 m, the nacelle cup anemometer, and the LIDAR. All three signals at times correspond. However, periods of gusts around 977 min and 990 min indicate the met tower does not always correlate well with the LIDAR. The met tower is measuring a different wind field due to being 228 m away and a westerly wind direction, see Figure 1. However, the met tower yields the traditional true wind speed measurement. Therefore, 10 min averages are used to remove variations due to gusts and still be able to make good comparisons against the met tower. Figure 4 shows the 10 min averaged met wind speed in 1 m/s bins with the LIDAR wind speed average and standard deviation shown. Data is lacking at the higher wind speeds. Overall, there is excellent correlation between the two, with an rms error of 0.8 m/s.

Figure 3. Comparison of met tower cup, nacelle cup, and LIDAR anemometers.

Figure 4. Comparison of LIDAR and met tower binned 10 minute averages.

Though averages compare well, a time series comparison is also needed. The rotor effective wind speed offers a true wind speed for the LIDAR to compare against. An extended Kalman filter (EKF) is used to estimate 0. The LIDAR signal is shifted assuming Taylor's frozen hypothesis and yaw corrected. As shown in Figure 5, the estimator and LIDAR compare very well. However, at some points the LIDAR signal diverges from the estimator. A scatter plot of the time series data is shown in Figure 6. For the available time series, the overall rms error is 0.77 m/s.

Conclusions

The LIDAR system has been shown to accurately measure the incoming wind speed. First, 10 minute averages measured by a nearby met tower and the LIDAR have a 0.8 m/s rms error. Comparisons of the time shifted and yaw corrected 1 Hz time series show high correlation. The overall rms error for these is 0.77 m/s. The averaged rms is larger since the met mast is not a true comparison of the LIDAR measurement.

Acknowledgements

This work was completed under DOE contract number DE-EE0005494. The National Renewable Energy Laboratory assisted with development, acquisition, and processing of data. A special thanks to Andrew Scholbrock, Na Wang, Alan Wright, and Jason Roadman for their expertise. ZephIR also worked closely with Alstom Power ensuring high data quality and ideal system settings for our needs.

79

Sustainability of the Wind Turbine Blade Manufacturing Process: A Bio-Based Alternative

RAMIREZ, Katerin [1]; TURCOTTE, David [2]

[1] University of Massachusetts Lowell

[2] Center for Wind Energy, University of Massachusetts Lowell

Corresponding Author: ccdupont@vt.edu

Globally, more than 23,000 wind turbines were manufactured in 2011 and there were 225,000 operational wind turbines by the end of 2012 . United States' installed wind capacity will need to increase from 11.6GW to 300 GW to achieve the 203 wind production goal by 2030 . To meet the increasing demand, not only more blades are being manufactured, but also longer blades of up to 100 meters long are being produced . The current stock of blades and the manufacturing process use petroleum based thermoset composites as the primary materials. The anticipated influx in disposal and manufacturing leads to health and environmental concern, given that the industry does not manufacture blades in a sustainable manner and has no practical way to recycle these blades.

The main objective of this research project is to create an energy pathway for the sustainability of wind energy. In particular, this research is trying to develop a bio-based epoxy system for the wind turbine blade manufacturing process, in which the toughness, stiffness, durability and costs are comparable with petroleum based epoxy systems. The bio-derived thermoset will allow the industry to substitute a fossil fuel for vegetable oil, a more readily available feedstock, in the blade manufacturing process. In addition to the bio-based system, we want to realize the property of reworkability in both conventional and bio-based epoxies. The property of reworkability means that we could be able to thermally reprocess any anhydride-cured epoxy system with the addition of a special catalyst . It should allow for an effective recycling at the end of the blades' life cycle, presumably without the negative economic, health and environmental consequences that current disposal methods for thermoset composite impose.

Overall, the expectation is to produce a high performance bio-based reworkable system which should enable manufacturing of blades that would be easily repaired, reworked or ground up for reuse with another purpose. The combination of these complementary technologies should improve sustainability both at the beginning and the end of the life cycle of a typical wind turbine blade.

Approach to evaluation

To evaluate the environmental, health and economic implications of replacing the petroleum based epoxy with a bio based epoxy, we use two different methodologies. The first one is a Life Cycle Cost Analysis (LCCA) to compare conventional and bio-based manufactured blades. The aim of the LCCA is to compare different alternatives in the manufacturing process and determine which one is the least costly while maintaining the same performance. We expect the bio-based manufacturing process to be very similar in terms of blade performance, but to differ in terms of the cost over the life cycle of the blades. The present value of all recurring costs and residual value of the blade at the moment of being disposed are calculated in order to determine the best long term manufacturing process.

The second methodology is a Toxic Use Reduction (TUR) analysis. We want to analyze the environmental, health and economic consequences of changes in the manufacturing process of the bla

78

Co-location of Wind & Solar Power Plants and their Integration onto the US Power Grid

Dr. PATTISON, Chris [1]; Dr. SWIFT, Andrew [1]

[1] National Wind Institute, Texas Tech University

Corresponding Author: devenport@vt.edu

A number of research and development groups and several renewable project operators have examined combining wind power production with on-site solar power production. Past research has been devoted to small, off-grid applications only. In the absence of actually building a utility-scale project, short time scale (5 minutes) estimates of combined power production are difficult to simulate due to the lack of hub-height wind data combined with on-site solar insolation data available in similar time scales. This presentation will present hub-height, high-fidelity, wind data from the Texas Tech University's 200-meter meteorological tower combined with a co-located solar pyranometer to estimate short-term (5-minute) power production data. Recent reduced costs associated with solar-PV may make this option more attractive in the future. This analysis addresses fixed-plate, single- and dual-axis PV arrays.

This presentation also includes an plant-level and grid-level economic analysis of a wind-only, solar-only, and combined wind-solar power plant. Over the past few years, renewable energy has entered the electrical grid at an exponential rate. To reduce the uncertainties for the grid operator and wind power plants owner/operators, "firm" production has a direct impact on the power purchase agreements (PPA's). Since wind power is traditionally best at night and solar power is only during the day, by combining their synergies, uncertainty is reduced and higher PPA's are possible. This analysis will present economic estimates of the ability of plant operators to secure higher purchase prices for power by raising the "firm" production level and reducing risk.